IMPROVING LIGAMENT TISSUE SCAFFOLD WITH THE USE OF GENIPIN AND GOLD NANOPARTICLES

A Dissertation Presented to the

Faculty of the Graduate School

at the University of Missouri

In Partial Fulfilment

Of the Requirements for the Degree

Doctor of Philosophy

by

MITCH A. BELLRICHARD

Dr. Sheila A. Grant, Dissertation Supervisor

May 2020

The undersigned, appointed by the dean of the Graduate School, have examined the dissertation entitled

IMPROVING LIGAMENT TISSUE SCAFFOLD WITH THE USE OF GENIPIN AND GOLD NANOPARTICLES

presented by Mitch A. Bellrichard,

a candidate for the degree of Doctor of Philosophy,

and hereby certify that, in their opinion, it is worthy of acceptance

---

Dr. Sheila Grant

Department of Biomedical, Biological, and Chemical Engineering

---

Dr. Craig Franklin

Department of Veterinary Pathobiology

Dr. Derek Fox

Department of Veterinary Medicine & Surgery

Dr. Raghuraman Kannan

Department of Radiology

Dr. Ferris Pfeiffer

Department of Biomedical, Biological, and Chemical Engineering

DEDICATIONS

To Carmelo and Twinkie. You two provided great comfort during long hours of study. Your contributions cannot be overstated.

ACKNOWLEDGEMENTS

First, I would like to thank my advisor, Dr. Sheila Grant. I entered her lab knowing little to nothing about bioengineering, but her mentorship and guidance gave the me the skills and confidence I needed to succeed. I need to thank Dr. Craig Franklin for overseeing an excellent residency program that allowed me to explore my research interests and for his support on this project. I'd like to thank Dr. Raghuraman Kannan for the exceptional graduate certificate he created and his knowledge of nanoparticles for this project. Additional thanks to Dr. Derek Fox for providing essential input on cell studies and current medical practices, and Dr. Ferris Pfeiffer for his extensive knowledge of biomechanics. Everyone on my committee has been incredibly helpful and available with their time.

I also need to thank the rest of the Grant lab. Dave Grant was always there to discuss new ideas and provided hours of guidance on the equipment in the lab. Chris Glover you were always willing to help teach me new techniques and answered all my questions despite how they must have seemed. Toni Cusack you were always happy to let me talk through my difficulties and made the office much more enjoyable. Janae Bradley you were a great resource for conducting cell studies and Colten Snider you provided help every step of the way if not for you the lab would have been a bleak, lonely place.

I would also like to acknowledge all the contribution made by the Comparative Medicine Program. Dr. Scott Korte your advice has always been of great help to me. Dr. Jeff Henegar you provided great insight into how to operate in the research field. Sherrie Neff and Justin Wilson, you were always happy to sacrifice your time to help us collect tissue. I can't overstate the help I've received from the other residents in the program. You have all helped me along in more ways than I can count. The Comparative Medicine Program not only helped educate me, it pushed to explore interests I didn't even know I had. The contributions of the CMP to my career path cannot be overstated.

Funding for the project comes from University of Missouri Life Sciences Mission, and the MU-Coulter Translational Partnership grant.

I want to thank my collaborators. This work couldn't have been done without John Brockman and his staff and the research reactor quantifying the gold. I'd also like to thank Deanna Grant and Dave Stalla at the SEM core. Their advice and assistance is the reason we have such great images. Dr. Keiichi Kuroki provided valuable help in analyzing the histology from our in vivo study. Thanks to all those at Sinclair Research for the care they provided to our sheep.

Finally, I'd like to thank my family and friends. My parents for instilling in me a strong belief in education and an appreciation for the

power of perseverance. My siblings, Brian and Steph, for their words of encouragement and never doubting me. I also want to thank my wife. Holly you have provided constant support and backing and were always willing to pick up the load when I was working long. I could not have done it without you. Additionally, I want to thank all the friends and family who I wasn't able to mention. All of you who have taken an interest in my academic and career goals and provided words of support, you are appreciated. Lastly, I want to thank the sheep.

Table of Contents

ACKNOWLEDGEMENTS.....ii

LIST OF FIGURES.....ix

LIST OF TABLES.....xi

ABSTRACT.....xii

Chapter

1. LITERATURE REVIEW.....1

1.1 ACL Reconstruction.....1
1.1.1 Normal ACL Structure.....1
1.1.2 Injury Incidence.....2
1.1.3 Current Treatments.....3
1.1.4 Recovery.....4

1.2 Gold Nanoparticles.....9
1.2.1 Benefits to Ligament Scaffolds.....9

1.3 Genipin.....12
1.3.1 Crosslinking.....13
1.3.2 Inflammation.....15

1.4 Conclusions.....16

1.5 References.....17

2. INTRODUCTION TO RESEARCH.....29

2.1 Significance of Research.....29

2.2 Research Objectives.....30

2.3 References.....33

3. PRELIMINARY CHARACTERIZATION STUDIES.....34

3.1 Introduction.....34

3.2 Materials and Methods.....35
3.2.1 Tissue Harvest and Decellularization.....35
3.2.1.1 Carotid.....35
3.2.1.2 Diaphragm.....36
3.2.2 Gold Conjugation.....37
3.2.3 Sterilization.....38
3.2.4 Neutron Activation Analysis.....39
3.2.5 Carotid Gold Attachment.....39
3.2.6 Cell Culture.....40
3.2.7 Biocompatibility of AuNP Carotid Tissue 40
3.2.8 Genipin Concentration.....41
3.2.8 Scanning Electron Microscopy.....41
3.2.10 Statistical Analysis.....42

3.3 Results.....42
3.3 Sterilization Methods.....42
3.3.2 Carotid Gold Attachment.....44
3.3.3 Biocompatibility of AuNP Carotid Tissue.....45
3.3.4 Genipin Concentration.....46
3.3.5 Scanning Electron Microscopy.....47

3.4 Discussion.....51

3.5 References.....55

4. GENIPIN ATTACHMENT OF CONJUGATED GOLD NANOPARTICLES ATTACHMENT TO LIGAMENT SCAFFOLDS.....57

4.1 Abstract.....57

4.2 Introduction.....58

4.3 Materials and Methods.....61
4.3.1 Tissue Harvest and Decellularization.....61
4.3.2 Genipin, gold nanoparticles and the crosslinking procedure.....62
4.3.3 Experimental groups.....63
4.3.4 Neutron Activation Analysis.....64
4.3.5 Modulated Differential Scanning Calorimetry.....65
4.3.6 Cell Culture.....65
4.3.7 Cell Viability.....66

4.3.8 dsDNA assay.....67
4.3.9 Scanning electron microscopy.....68
4.3.10 Statistical Analysis.....68

4.4 Results.....68
4.4.1 Neutron Activation Analysis.....68
4.4.2 Modulated Differential Scanning Calorimetry.....70
4.4.3 Cell Viability.....71
4.4.4 dsDNA assay.....72
4.4.5 Scanning electron microscopy.....73

4.5 Discussion.....76

4.6 Conclusions.....81

4.7 Acknowledgments.....81

4.8 References.....82

5. GENIPIN ATTACHMENT OF GOLD NANOPARTICLES TO AUTOGRAFT TISSUE.....86

5.1 Abstract.....86

5.2 Introduction.....87

5.3 Materials and Methods.....89
5.3.1 Tissue Harvest and Decellularization.....89
5.3.2 Conjugation of Gold.....90
5.3.3 Experimental Groups.....91
5.3.4 Histology.....92
5.3.5 Scanning Electron Microscopy.....92
5.3.6 Neutron Activation Analysis.....92
5.3.7 Statistical Analysis.....93

5.4 Results.....93
5.4.1 Histology.....93
5.4.2 Scanning Electron Microscopy.....97
5.4.3 Neutron Activation Analysis.....101

5.5 Discussion.....102

5.6 Conclusion.....104

5.7 References.....106

6. THE USE OF GOLD NANOPARTICLES IN IMPROVING ACL GRAFT PERFORMANCE IN AN OVINE MODEL.....109

6.1 Abstract.....109

6.2 Introduction.....110

6.3 Materials and Methods.....113
6.3.1 Experimental Design.....113
6.3.2 Graft Preparation.....114
6.3.3 Neutron Activation Analysis.....114
6.3.4 Cell Culture.....115
6.3.5 Reactive Oxygen Species Assay.....115
6.3.6 Animal model.....117
6.3.7 Cytology.....118
6.3.8 Histopathology.....118
6.3.8.1 Intraarticular Graft.....118
6.3.8.2 Bone Tunnel Pathology.....120
6.3.9 Statistical Analysis.....123

6.4 Results.....123
6.4.1 Neutron Activation Analysis.....124
6.4.2 Reactive Oxygen Species.....124
6.4.3 Cytology.....125
6.4.4 Intraarticular Histology.....126
6.4.5 Bone Tunnel Histology.....128
6.4.6 Inflammation.....130

6.5 Discussion.....133

6.6 Conclusion.....136

6.7 References.....137

7. FUTURE WORK.....141

7.1 Future Studies.....141

7.2 References.....145

VITA.....147

List of Figures

Figure

3.1 Neutron Activation Analysis results for peracetic acid sterilization……43

3.2 Neutron Activation Analysis results for ethanol sterilization…..……44

3.3: Neutron Activation Analysis results for carotid scaffold……...45

3.4 Cell proliferation reagent WST-1 assay results showing percent viability relative to the control, untreated carotid scaffolds……...46

3.5 Neutron Activation Analysis results for variable genipin concentration…….……47

3.6 Scanning electron microscopy images of gold nanoparticles conjugated with genipin to decellularized diaphragm tendon……49

3.7 Scanning electron microscopy images of genipin conjugated decellularized diaphragm tendon……...50

4.1 Results of modulated differential scanning calorimetry in which the mean denaturation temperature of each tissue is shown…….…70

4.2 Cell proliferation reagent WST-1 assay results showing percent viability relative to the control, untreated tendon scaffolds……71

4.3 DNA content on tendon scaffolds plated with L929 mouse fibroblasts for 1 to 10 days……..……..73

4.4 Scanning electron microscopy images taken 1 and 3 days after fibroblasts were plated on the of the scaffold……..74

5.1 Histologic images of intact autograft scaffolds conjugated with gold nanoparticles and genipin, H&E staining at 100x……95

5.2 Histologic images of intact autograft scaffolds conjugated with gold nanoparticles without the use of genipin, H&E staining at 100x……..96

5.3 Scanning electron micrograph imaging 20 nm AuNP crosslinked autograft scaffolds using genipin……..……98

5.4 Scanning electron micrograph imaging 20 nm AuNP crosslinked autograft scaffolds without the use of genipin……100

5.5 Neutron activation analysis data comparing the concentration of gold attached to decellularized tissue versus intact tissue with and without the use of genipin……..102

6.1 The ACL reconstruction with human gracilis tendon in a sheep..118

6.2 Reactive oxygen species assay showing DCF fluorescence concentrations for each of the experimental ACL groups…….125

6.3 The number of synovial lining cells present in a 100 cell differential count performed on a cytocentrifuge concentrated slide preparation of synovial fluid from both the intact and surgically repaired stifle 8 weeks after surgery……..126

6.4 Histological score of the intraarticular graft……..127

6.5 Tendon-bone tunnel healing score for the tibia, femur, and a summation of them both……..129

6.6 Inflammation scores for the bone tunnel and intraarticular graft ……131

6.7 Representative histological findings of the bone tunnel portion of the graft at eight weeks……132

6.8 8 Representative histological findings of the intraarticular graft at eight weeks……133

List of Tables

Table

4.1 Neutron Activation Analysis results for genipin conjugated tendon tissue……69

6.1 Grading scale for histological evaluation of the intra-articular graft per high power field (×100)……120

6.2 TBTH Scoring for evaluation of tendon graft to bone tunnel healing in ACL reconstruction……122

6.3 Other histologic assessments evaluated but not included in the TBTH score for the bone tunnel portion of the graft……123

6.4 Neutron Activation Analysis Results for ACL Graft……..124

6.5 Average histological score of the intraarticular grafts as evaluated by two blinded pathologists……...128

6.6 Average TBTH score of the bone tunnel grafts as evaluated by two blinded pathologists……129

6.7 Average score for other assessments not included in the TBTH score for the bone tunnel portion of the graft as evaluated by two blinded pathologists……..130

IMPROVING LIGAMENT TISSUE SCAFFOLD WITH THE USE OF GENIPIN AND GOLD NANOPARTICLES

Mitchell A. Bellrichard

Dr. Sheila Grant, Dissertation Supervisor

ABSTRACT

Decellularized tissue is used for a wide array of tissue injuries with tendon and ligament repair being among the most common. However, despite their frequent use there is concern over the lengthy inflammatory period and slow healing associated with allografts. Gold nanoparticles (AuNPs) have been shown to improve wound healing by decreasing inflammation and promoting cellularity and biological incorporation. The focus of this dissertation was testing the effects of AuNPs on ligament repair and assessing the use of genipin as a novel method of attaching the particles. In vitro studies were conducted to examine the ability of genipin to attach AuNPs to both unprocessed tissue and a decellularized tissue scaffold. Cell studies were conducted to observe the biocompatibility of the composite tissue. The results demonstrated successful attachment of the AuNPs and successful cell attachment and proliferation. An in vivo study was conducted using sheep to observe the effects of AuNPs on ACL repair. The experimental grafts had better histological scores and decreased inflammation in comparison to the controls.

Chapter 1

LITERATURE REVIEW

1.1 ACL Reconstruction

1.1.1 Normal ACL Structure

The anterior cruciate ligament (ACL) is a cord-like structure of dense connective tissues that runs from posteromedial aspect of the lateral femoral condyle to the anteromedial aspect of the tibia between the condyles [1, 2]. Its primary purpose is to control anterior translation of the tibia. The ACL also contributes to the restraint of tibial rotation and varus or valgus stress [3]. To model the ACL, most researchers present the ACL as two bundles. The first is the anteromedial bundle which is tight in flexion, and the second is the posterolateral bundle and it's tight in extension [1]. The ACL is primarily made up of type I collagen. This is the major collagen of ligaments and tendons and it helps provide the tensile strength to the ligament [4]. There is also lesser amounts of collagen types II-IV primarily at the distal and proximal ends [5]. In addition to collagen, there is a matrix made of proteins, glycosaminoglycans, glycoproteins, and elastic systems. These components have multiple functional

interactions to allow the ligament to withstand stresses from varying angles and varying tensile strains [5].

Similar to other soft connective tissues the ACL is relatively hypocellular. This gets truer the further from the ends you go. The cells at the middle of the ACL are fusiform and spindle shaped fibroblasts. The distribution of blood vessels within the substance of the ligament is similarly non-homogeneous. The blood supply of the cruciate ligaments is provided by the middle genicular artery, but he proximal portion of the ACL is better endowed with blood vessels than distal [6]. The lack of blood supply and low cell count are believed to play a role in the poor healing potential of the ACL [7].

1.1.2 Injury Incidence

ACL tears are an exceedingly common debilitating injury among competitive and recreational athletes. In the United States alone there are between 100,000 and 200,000 ACL ruptures every year [8, 9]. At West Point, where all students are required to participate in sports, they found an overall 4-year incidence proportion of 3.24 per 100 for men and 3.51 per 100 for women [10]. Numerous other studies have confirmed women have a greater likelihood of ACL tear compared to men participating in the same sports [11-14]. This increased risk for women is incompletely understood, but scientists have suggested

several theories including differences in leg alignment, hormonal factors, neuromuscular control, and knee width [15-18].

The majority of ACL tears are the result of low-energy, noncontact injuries. This is most often the result of sudden movements or a quick, sharp turn [19]. The other 30% of ACL injuries are contact-related ACL injuries. These usually occur from a direct blow causing hyperextension or valgus deformation of the knee. In the United States, this is most commonly seen in American football when a player's foot is planted and an opponent strikes him on the lateral aspect of the planted leg [20].

1.1.3 Current Treatments

The first question a physician must answer when treating an ACL tear is whether or not to pursue surgery. Factors that must be considered include the patients activity level, the presence of additional injuries, and instability of the knee [21]. Many less active patients with partial tears and no symptoms of instability can restore their knee function without surgery using physical therapy and rehabilitation. However for patients who participate in high demand sports or occupations or have suffered a complete ACL rupture, ACL reconstruction is considered ideal treatment [22, 23].

Extensive research has been done in an attempt to achieve the best patient outcomes for ACL surgery. Early surgeons attempted suture the two ends of the torn ligament together [24, 25]. This method had an almost 100% failure rate so it was abandoned for the currently used ACL reconstruction [26, 27]. ACL reconstruction is generally performed with arthroscopy using a graft to replace the ruptured ACL. Bone tunnels are drilled in the tibia and femur and the graft material is pulled through and secured using screw, pins or buttons [28].

Graft choice remains one of the largest sources of debate concerning ACL reconstruction. The three most common grafts are the patellar tendon autograft, the hamstring tendon autograft, and the allograft. Patellar tendon grafts are the most common graft choice because they include a portion of bone at either end which gives it the advantage of allowing bone-to-bone healing within the bone tunnel [29]. However all three have their own advantages and disadvantages with no particular graft clearly demonstrating superior functional outcomes [30].

1.1.4 Recovery

Both allograft and autograft tissue undergo a similar healing process when they’re implanted. The graft undergoes a sequence of

reactions starting with necrosis, cellular repopulation, revascularization, and collagen remodeling [31]. The early phase of healing last approximately 4 weeks and it is marked by increasing graft necrosis and relative hypocellularity. As the graft breaks down it leads to the release of chemokines and cytokines which trigger a cascade of growth factors resulting in cell migration [32, 33]. By week 2, we begin to see an influx of fibroblasts with cellular proliferation reaching its peek from weeks 4 to 10 [34]. At this point cell numbers substantially surpasses that of the intact ACL [35]. In both allografts and autografts any cells that were attached to graft originally die and are replaced with cells from the synovial fluid or bone marrow elements originating from drilling maneuvers [36]. The cellular proliferation phase is also the phase where the graft has the weakest mechanical strength. This is the result of splitting and defragmentation of collagen bundles that naturally occurs before the fibroblasts can infiltrate and begin laying down collagen and applying isometric tension [37, 38].

Revascularization of the tissue begins after about 4 weeks from the operation [39, 40]. The vessels that populate the ACL graft originate predominately from the infrapatellar fat pad distally and from the posterior synovial tissues proximally [31, 41]. The vessel growth begins at the outer edge of the graft and moves toward center after

approximately 12 weeks. The vascular density returns to values of the intact ACL after approximately 6 months [42, 43]. This is about the same time that cell population returns to the values seen in intact ACLs [40, 44].

The final stage of ACL healing is ligamentization. Ligamentization is the process of molding and reshaping the graft to the morphology and mechanical strength of the intact ACL. At this stage collagen fibers regain their organization into fascicles and regain their previous crimp pattern [35, 44, 45]. However, the collagen fibers never return to their exact intact state. Intact tendons and ligaments have bimodal distribution of fibril sizes but this small and large size model is replaced with a unimodal pattern of only small collagen fibers in reconstructed ACLs [46]. Additionally, the data shows the time-zero mechanical strength of allografts and autografts is never fully regained at the completion of the remodeling process [33, 34, 47]. This may be the results the of increased collagen type III present in the reconstructed ACLs [48]. Type III collagen is normally found in scar tissue and has lower mechanical strength than type I collagen.

The majority of ACL reconstructions performed use autograft tissue to replace the torn ACL [49]. The biggest concern with autograft involves the harvest procedure. The tendon harvest is associated with significant donor-site morbidities. These morbidities include pain,

patellar fractures, patella tendonitis, numbness from damage to the saphenous nerve, and impairment of function for the quadriceps muscle [50, 51]. These problems occur in 40% to 60% of patients who undergo the ACL reconstruction using a patellar autograft [52]. The other major disadvantage of autograft surgery is the cost. On average, autograft surgery costs over 1000 dollars more than ACL reconstruction using an allograft. The cause of this is allografts require less surgery time and patients are less likely to stay overnight at the hospital [53].

Allograft surgery uses cadaver tissue to replace the torn ACL. The graft is typically taken from the Achilles or patellar tendon. However, the quadriceps, hamstring, and tibialis tendons are also used [30]. The obvious advantage of this method is it doesn't require the harvest procedure necessary for autografts. However, the use of allografts remains controversial. This is because several animal studies have shown allografts to heal at a slower rate with a prolonged inflammatory period and slower revascularization [31, 35, 54, 55]. Several human studies have backed up these results. Muramatsu et al.[56] used MRI to demonstrate that allografts have a slower reincorporation rate than autografts, and Barrett et al.[57] found that ACL allografts fail 2.6 to 4.2 times more often than autografts in young, high activity patients. Perhaps due to their slower healing,

allografts also lose more of their time zero mechanical strength than autografts [35]. Despite these studies, several authors have reported equivalent clinical outcomes when using autograft or allograft for ACL reconstructions [58, 59].

Research has shown that regardless of the treatment, patients who tear their ACL have approximately 4 times greater likelihood of developing osteoarthritis in the injured knee than in their healthy knee [60]. The risk for osteoarthritis appears to be multifactorial. Joint biomechanics, severity of initial injury, injury to other joint tissues, and patient activity after surgery all play a role [61]. Excess inflammation appears to also play a role in the development of osteoarthritis post ACL injury. When the ACL tears, it sets off a vigorous acute inflammatory cascade [62]. Animal models have shown this inflammatory response is the sustained at low levels for weeks after the injury took place [63]. Heard et al.[64] demonstrated that this inflammatory cascade can lead to cartilage degeneration in as little as two weeks' time. It is also known that if anti-inflammatory compounds are given intraarticularly the presence of the inflammatory markers is reduced and less cartilage degeneration is present [65]. We believe gold nanoparticles can be that anti-inflammatory compound.

1.2 Gold nanoparticles

People have experimented with the medicinal properties of gold colloids for centuries [66]. Today gold nanoparticles (AuNPs) are made in different sizes, shapes, and structures, depending on the application and they are used in a huge array of biomedical applications including cancer treatments, imaging, gene therapy, and drug delivery [67, 68]. Their low cytotoxicity, easily functionalized surface, a high capacity to target cells, and a tunable optical absorption peak have made them exceedingly attractive for new potential treatments [69-71]. Additionally, AuNPs also have many traits that make them exceedingly useful in modification of tissue scaffolds.

1.2.1 Benefits to Ligament Scaffolds

AuNPs have previously been used to support cell attachment and proliferation. Due to their small size, nanoparticles have large surface area compared to their volume and, this leads to increased surface energy which promotes the adsorption of proteins needed for cell attachment [72]. Hsu et al. [73] found the addition of AuNP modified the surface structure of their synthetic scaffold and this in turn lead to increase cellular attachment more cell growth. This increased cell attachment has been seen in numerous cell types including fibroblasts, keratinocytes, hepatocytes, and mesenchymal cells [74-77]. This

effect appears to be dose dependent however. Lu et al.[74] found AuNPs enhances the proliferation of keratinocytes at a low concentration but limited growth at high concentrations.

Although AuNPs have been found to promote attachment of many cell types, they appear to have the opposite effect on bacteria. While Hsu et al. [73] found AuNP supported cell growth on their scaffold, they also found it decreased bacterial adhesion. Other researchers have found similar results. Badwaik et al.[78] found AuNPs to both bacteriostatic and bactericidal against both Gram-negative and Gram-positive bacteria. The bactericidal properties come from AuNPs' ability to disrupt the bacterial cell membrane and cause a depletion of the cytoplasmic content. This is similar to the results found by Ahmad et al.[79] which showed AuNPs to be effective growth inhibitors against *Staphylococcus* aureus and *Escherichia coli*.

One concern with physicians have with tissue grafts is they can degrade too fast causing them to lose strength and potentially tear [38]. AuNPs can ameliorate this concern by improving graft stability and delaying breakdown. This is because the attachment of nanoparticles blocks collagenase binding sites on collagen molecules which is shown to delay enzymatic degradation [80, 81]. Similarly, Akturk et al.[82] showed that integrating AuNPs into a cross-linked

collagen scaffold enhanced its stability against enzymatic degradation and increased the tensile strength.

AuNPs can also help heal the bone tunnel portion of the ACL graft. The bone tunnel portion of an ACL graft heals through mineralization of the graft material. AuNPs promote osteogenic differentiation of mesenchymal stem cells as well as inhibiting the stem cells from undergoing adipogenic differentiation [83]. They do this by binding with proteins within the cytoplasm and causing mechanical stress to the cell. In response the cell activates p38 mitogen-activated protein kinase signaling pathway which regulates expression of the osteogenesis [84]. This effect is largely dependent on the size and shape of the particle. Ko et al.[85] found 30 nm and 50 nm AuNPs were preferentially up taken into the cells compared to 15 nm, 75 nm, and 100 nm particles. 30 nm and 50 nm AuNPs were then the most effective at promoting osteogenic differentiation. Other researchers later wrote that 20 nm AuNPs had a greater osteogenic effect on osteoblasts of 40 nm AuNPs [86]. The overall consensus appears to be spherical particles between 20-50 nm are ideal for osteogenesis [83, 85, 87].

Perhaps the most important of AuNPs potential benefits for tissue scaffolds is their anti-inflammatory properties. In vivo studies have shown intraarticular application of AuNPs can decrease

inflammation and inhibit arthritis development [88, 89]. The exact mechanism for AuNPs anti-inflammatory ability is incompletely understood but it appears to be multifactored. One of the mechanisms is AuNPs antioxidant capability. Researcher have found AuNPs inhibit the formation of reactive oxygen species and scavenge free radicals [90, 91]. The other major mechanism for AuNPs anti-inflammatory properties is their ability to inhibit the expression of NF-κB. AuNPs block NF-κB activation by interacting with cys-179 of IKK-β. This in turn impedes the production of pro-inflammatory cytokines, such as TNF-α and IL-1β [92].

With all the promise of AuNPs have to tissue engineering, the next important question is how best to apply them. Genipin has the potential to rapidly and safely attach AuNPs to a tissue scaffold.

1.3 Genipin

Genipin is an aglycone derived from geniposide a natural compound found in the fruit of *Gardenia jasminoides* [93]. The gardenia is an evergreen flowering plant found natively throughout much of the Asian continent [94]. The fruit of the *Gardenia jasminoides* has been used in traditional Asian medicine for generations to in treat inflammation, headache, edema, fever, hepatic disorders, and hypertension [95]. It has now come to the attention of

western medicine and is being investigated as a potential treatment for a huge variety of ailments including diabetes, depression, liver disease, and several types cancer [96-99].

1.3.1 Crosslinking

In 1988, Fujikawa et al.[100] discovered the formation of dimers of genipin in the presence of glycine. This discovery resulted in genipin being studied as a potential crosslinking agent for proteins. Genipin spontaneously forms covalent bonds with primary amines such those found in proteins, gelatin, chitosan, etc [101]. Crosslinks are formed via two separate reactions involving different sites on the genipin molecule. The first reaction begins with an initial nucleophilic attack of the genipin C3 carbon atom from a primary amine group to form an intermediate aldehyde group. This opens the dihydropyran ring. This is then followed by attack on the resulting aldehyde group by the secondary amine formed in the first step of the reaction. This reaction occurs this as soon as the genipin and comes into contact with an amine group. The second, slower, reaction is a SN2 nucleophilic substitution reaction that involves the replacement of the ester group on the genipin molecule by a secondary amide linkage [102].

One of the other outcomes of the crosslinking reaction is the formation of a blue dye. Genipin becomes blue when is reacts with

amino acids. This reaction is incompletely understood, but current evidence suggests the blue dye is a result of oxygen radical-induced polymerization of genipin followed by dehydrogenation of intermediate compounds [103, 104]. This reaction has resulted in genipin being used as a dye, and it is useful for providing visual evidence of the crosslinking reaction occurring [105].

Genipin's biocompatibility makes it a uniquely useful crosslinking agent. The most common crosslinking agent in the clinic is glutaraldehyde [106]. Glutaraldehyde however has the recognized disadvantage of being cytotoxic [107]. The cytotoxicity can cause damage to the host and lead to problems like ectopic calcification and a clastogenic response in nearby cells [108, 109]. Genipin has no such cytotoxicity. Cell studies have shown that genipin is approximately 10,000 times less cytotoxic than glutaraldehyde and the proliferative capacity of cells after exposure to genipin was approximately 5000 times greater than cells exposed to glutaraldehyde [110]. Another well-known alternative crosslinker is carbodiimides. Carbodiimides are zero length crosslinkers that form connections between the peptide chains. Unfortunately, the crosslinking reaction forms several toxic byproducts, requiring extensive washing [111]. In addition, the carbodiimides only react for a limited period of time decreasing the control of the reaction and hurting its potential use [112].

1.3.2 Inflammation

One of the problems with decellularized tissue grafts is the intrinsic immunogenicity of a protein matrix [113]. Crosslinking strengthen the matrix and stabilizes it against degradation. Perhaps the most important thing crosslinking does though is alter the intrinsic immunogenicity of the matrix. Wang et al. [114] found crosslinking with genipin inhibited the proliferation of CD3 and CD4 lymphocytes and cytokines secretion by helper T cells. This masking of immunogenic epitopes reduced the inflammatory response in a liver model. However, that is not the only way genipin reduces inflammation.

Genipin anti-inflammatory properties have demonstrated over and over both in vitro studies and in animal models. Koo et al. [95] demonstrated genipin inhibited the acute inflammatory response in carrageenan-induced rat paw edema, carrageenan-induced rat air pouch edema, and croton oil-induced mouse ear edema models. Despite this, the exact mechanism for genipin's anti-inflammatory properties is incompletely understood and appears to be multifactored. Nitric oxide synthase (NOS) and NF-κB appear be potent targets of genipin. It has been demonstrated in numerous different cell types that genipin will inhibit the expression of inducible NOS and the production of nitric oxide when they're stimulated by

lipopolysaccharide [95, 115-117]. Genipin can also reduce inflammation by inhibiting inflammasome activation, by preventing autophagy in macrophages [118]. Wang et al. [119] revealed genipin's ability to inhibit exocytosis. Lastly there is evidence that genipin also interferes with toll-like receptor signaling during sepsis [120]. This protects the animal from hyperinflammatory responses and tissue injury that occur during sepsis.

1.4 Conclusions

Gold and genipin both have been studied as potential treatment for disease for hundreds of years. However, no one has yet attempted to combine the two to provide a synergistic approach. The capabilities of both AuNPs and genipin fit perfectly to tackle the unique problems that occur during ACL reconstruction. However, more research is need to develop protocols to combine AuNPs and genipin in way that is clinically useful and to test the results to ensure the benefits to the patients.

1.5 References

1. Girgis, F.G., J.L. Marshall, and A. Monajem, *The cruciate ligaments of the knee joint. Anatomical, functional and experimental analysis.* Clinical orthopaedics and related research, 1975(106): p. 216-231.

2. Reiman, P. and D. Jackson, *Anatomy of the anterior cruciate ligament.* The anterior cruciate deficient knee. Mosby, St. Louis, MO, 1987: p. 17-26.

3. Markolf, K.L., J.S. Mensch, and H.C. Amstutz, *Stiffness and laxity of the knee--the contributions of the supporting structures. A quantitative in vitro study.* JBJS, 1976. **58**(5): p. 583-594.

4. Amiel, D., *Ligament structure, chemistry, and physiology.* Knee ligaments: Structure, function and repair, 1989: p. 34-45.

5. Duthon, V., et al., *Anatomy of the anterior cruciate ligament.* Knee surgery, sports traumatology, arthroscopy, 2006. **14**(3): p. 204-213.

6. Scapinelli, R., *Vascular anatomy of the human cruciate ligaments and surrounding structures.* Clinical Anatomy: The Official Journal of the American Association of Clinical Anatomists and the British Association of Clinical Anatomists, 1997. **10**(3): p. 151-162.

7. Rodeo, S.A., et al., *Tendon-healing in a bone tunnel. A biomechanical and histological study in the dog.* The Journal of bone and joint surgery. American volume, 1993. **75**(12): p. 1795-1803.

8. Miyasaka, K., *The incidence of knee ligament injuries in the general population.* Am J Knee Surg, 1991. **1**: p. 43-48.

9. Sanders, T.L., et al., *Incidence of anterior cruciate ligament tears and reconstruction: a 21-year population-based study.* The American journal of sports medicine, 2016. **44**(6): p. 1502-1507.

10. Mountcastle, S.B., et al., *Gender differences in anterior cruciate ligament injury vary with activity: epidemiology of anterior cruciate ligament injuries in a young, athletic population.* The

American journal of sports medicine, 2007. **35**(10): p. 1635-1642.

11. Agel, J., E.A. Arendt, and B. Bershadsky, *Anterior cruciate ligament injury in national collegiate athletic association basketball and soccer: a 13-year review.* The American journal of sports medicine, 2005. **33**(4): p. 524-531.

12. Bjordal, J.M., et al., *Epidemiology of anterior cruciate ligament injuries in soccer.* The American Journal of Sports Medicine, 1997. **25**(3): p. 341-345.

13. Hewett, T.E., G.D. Myer, and K.R. Ford, *Anterior cruciate ligament injuries in female athletes: Part 1, mechanisms and risk factors.* The American journal of sports medicine, 2006. **34**(2): p. 299-311.

14. Piasecki, D.P., et al., *Intraarticular injuries associated with anterior cruciate ligament tear: findings at ligament reconstruction in high school and recreational athletes: an analysis of sex-based differences.* The American journal of sports medicine, 2003. **31**(4): p. 601-605.

15. Pantano, K.J., et al., *Differences in peak knee valgus angles between individuals with high and low Q-angles during a single limb squat.* Clinical Biomechanics, 2005. **20**(9): p. 966-972.

16. LaPrade, R.F. and Q.M. Burnett, *Femoral intercondylar notch stenosis and correlation to anterior cruciate ligament injuries: a prospective study.* The American Journal of Sports Medicine, 1994. **22**(2): p. 198-203.

17. Wojtys, E.M., et al., *The effect of the menstrual cycle on anterior cruciate ligament injuries in women as determined by hormone levels.* The American journal of sports medicine, 2002. **30**(2): p. 182-188.

18. Zazulak, B.T., et al., *Deficits in neuromuscular control of the trunk predict knee injury risk: prospective biomechanical-epidemiologic study.* The American journal of sports medicine, 2007. **35**(7): p. 1123-1130.

19. Boden, B.P., et al., *Mechanisms of anterior cruciate ligament injury.* Orthopedics, 2000. **23**(6): p. 573-578.

20. Callaghan, J.J., *The adult knee*. Vol. 1. 2003: Lippincott Williams & Wilkins.

21. Buss, D.D., et al., *Nonoperative treatment of acute anterior cruciate ligament injuries in a selected group of patients.* The American journal of sports medicine, 1995. **23**(2): p. 160-165.

22. Delay, B.S., et al., *Current practices and opinions in ACL reconstruction and rehabilitation: results of a survey of the American Orthopaedic Society for Sports Medicine.* The American journal of knee surgery, 2001. **14**(2): p. 85-91.

23. Giove, T.P., et al., *Non-operative treatment of the torn anterior cruciate ligament.* The Journal of bone and joint surgery. American volume, 1983. **65**(2): p. 184-192.

24. O'DONOGHUE, D.H., et al., *Repair of the anterior cruciate ligament in dogs.* JBJS, 1966. **48**(3): p. 503-519.

25. Robson, A.M., *VI. Ruptured crucial ligaments and their repair by operation.* Annals of surgery, 1903. **37**(5): p. 716.

26. Kaplan, N., T.L. Wickiewicz, and R.F. Warren, *Primary surgical treatment of anterior cruciate ligament ruptures: a long-term follow-up study.* The American journal of sports medicine, 1990. **18**(4): p. 354-358.

27. Strand, T., et al., *Long-term follow-up after primary repair of the anterior cruciate ligament: clinical and radiological evaluation 15–23 years postoperatively.* Archives of orthopaedic and trauma surgery, 2005. **125**(4): p. 217-221.

28. Kiapour, A. and M. Murray, *Basic science of anterior cruciate ligament injury and repair.* Bone & joint research, 2014. **3**(2): p. 20-31.

29. West, R.V. and C.D. Harner, *Graft selection in anterior cruciate ligament reconstruction.* JAAOS-Journal of the American Academy of Orthopaedic Surgeons, 2005. **13**(3): p. 197-207.

30. Foster, T.E., et al., *Does the graft source really matter in the outcome of patients undergoing anterior cruciate ligament reconstruction? An evaluation of autograft versus allograft reconstruction results: a systematic review.* The American journal of sports medicine, 2010. **38**(1): p. 189-199.

31. Jackson, D.W., J. Corsetti, and T.M. Simon, *Biologic incorporation of allograft anterior cruciate ligament replacements.* Clinical orthopaedics and related research, 1996. **324**: p. 126-133.

32. Kuroda, R., et al., *Localization of growth factors in the reconstructed anterior cruciate ligament: immunohistological study in dogs.* Knee Surgery, Sports Traumatology, Arthroscopy, 2000. **8**(2): p. 120-126.

33. Scheffler, S., F. Unterhauser, and A. Weiler, *Graft remodeling and ligamentization after cruciate ligament reconstruction.* Knee surgery, sports traumatology, arthroscopy, 2008. **16**(9): p. 834-842.

34. Bosch, U. and W.J. Kasperczyk, *Healing of the patellar tendon autograft after posterior cruciate ligament reconstruction—a process of ligamentization? An experimental study in a sheep model.* The American journal of sports medicine, 1992. **20**(5): p. 558-566.

35. Jackson, D.W., et al., *A comparison of patellar tendon autograft and allograft used for anterior cruciate ligament reconstruction in the goat model.* The American Journal of Sports Medicine, 1993. **21**(2): p. 176-185.

36. Yoshikawa, T., et al., *Effects of local administration of vascular endothelial growth factor on mechanical characteristics of the semitendinosus tendon graft after anterior cruciate ligament reconstruction in sheep.* The American journal of sports medicine, 2006. **34**(12): p. 1918-1925.

37. Murray, M.M., et al., *Histological changes in the human anterior cruciate ligament after rupture.* JBJS, 2000. **82**(10): p. 1387.

38. Goradia, V.K., et al., *Natural history of a hamstring tendon autograft used for anterior cruciate ligament reconstruction in a sheep model.* The American Journal of Sports Medicine, 2000. **28**(1): p. 40-46.

39. Arnoczky, S.P., G. Tarvin, and J. Marshall, *Anterior cruciate ligament replacement using patellar tendon. An evaluation of graft revascularization in the dog.* The Journal of bone and joint surgery. American volume, 1982. **64**(2): p. 217-224.

40. Clancy Jr, W.G., et al., *Anterior and posterior cruciate ligament reconstruction in rhesus monkeys.* JBJS, 1981. **63**(8): p. 1270-1284.

41. Nikolaou, P.K., et al., *Anterior cruciate ligament allograft transplantation: long-term function, histology, revascularization, and operative technique.* The American journal of sports medicine, 1986. **14**(5): p. 348-360.

42. Unterhauser, F.N., et al., *Endoligamentous revascularization of an anterior cruciate ligament graft.* Clinical Orthopaedics and Related Research®, 2003. **414**: p. 276-288.

43. Weiler, A., et al., *Biomechanical properties and vascularity of an anterior cruciate ligament graft can be predicted by contrast-enhanced magnetic resonance imaging: a two-year study in sheep.* The American journal of sports medicine, 2001. **29**(6): p. 751-761.

44. Scheffler, S., et al., *The biological healing and restoration of the mechanical properties of free soft-tissue allografts lag behind autologous ACL reconstruction in the sheep model.* Trans Orthop Res, 2005. **51**: p. 0236.

45. Weiler, A., et al., *α-Smooth muscle actin is expressed by fibroblastic cells of the ovine anterior cruciate ligament and its free tendon graft during remodeling.* Journal of orthopaedic research, 2002. **20**(2): p. 310-317.

46. Oakes, B.W., *Collagen ultrastructure in the normal ACL and in ACL graft.* The anterior cruciate ligament. Current and future concepts, 1993: p. 209-217.

47. Goradia, V.K., et al., *Tendon-to-bone healing of a semitendinosus tendon autograft used for ACL reconstruction in a sheep model.* The American journal of knee surgery, 2000. **13**(3): p. 143-151.

48. Ng, G.Y., et al., *Long-term study of the biochemistry and biomechanics of anterior cruciate ligament-patellar tendon autografts in goats.* Journal of orthopaedic research, 1996. **14**(6): p. 851-856.

49. Medicine, A.O.S.f.S., *Allografts for ACL reconstruction survey report*. 2014.

50. Peterson, R.K., W.R. Shelton, and A.L. Bomboy, *Allograft versus autograft patellar tendon anterior cruciate ligament reconstruction: a 5-year follow-up.* Arthroscopy: the journal of arthroscopic & related surgery, 2001. **17**(1): p. 9-13.

51. Kartus, J., T. Movin, and J. Karlsson, *Donor-site morbidity and anterior knee problems after anterior cruciate ligament reconstruction using autografts.* Arthroscopy: The Journal of Arthroscopic & Related Surgery, 2001. **17**(9): p. 971-980.

52. Sachs, R.A., et al., *Patellofemoral problems after anterior cruciate ligament reconstruction.* The American journal of sports medicine, 1989. **17**(6): p. 760-765.

53. Cole, D.W., et al., *Cost comparison of anterior cruciate ligament reconstruction: autograft versus allograft.* Arthroscopy: The Journal of Arthroscopic & Related Surgery, 2005. **21**(7): p. 786-790.

54. Scheffler, S.U., et al., *Fresh-frozen free-tendon allografts versus autografts in anterior cruciate ligament reconstruction: delayed remodeling and inferior mechanical function during long-term healing in sheep.* Arthroscopy: The Journal of Arthroscopic & Related Surgery, 2008. **24**(4): p. 448-458.

55. Kirkpatrick, J., et al., *Cryopreserved anterior cruciate ligament allografts in a canine model.* Journal of the Southern Orthopaedic Association, 1996. **5**(1): p. 20-29.

56. Muramatsu, K., Y. Hachiya, and H. Izawa, *Serial Evaluation of Human Anterior Cruciate Ligament Grafts by Contrast-Enhanced Magnetic Resonance Imaging: Comparison of Allografts and Autografts.* Arthroscopy: The Journal of Arthroscopic & Related Surgery, 2008. **24**(9): p. 1038-1044.

57. Barrett, G.R., et al., *Allograft anterior cruciate ligament reconstruction in the young, active patient: Tegner activity level and failure rate.* Arthroscopy: The Journal of Arthroscopic & Related Surgery, 2010. **26**(12): p. 1593-1601.

58. Mariscalco, M.W., et al., *Use of irradiated and non-irradiated allograft tissue in anterior cruciate ligament reconstruction surgery: a critical analysis review.* JBJS reviews, 2014. **2**(2).

59. Zeng, C., et al., *Autograft versus allograft in anterior cruciate ligament reconstruction: a meta-analysis of randomized*

controlled trials and systematic review of overlapping systematic reviews. Arthroscopy: The Journal of Arthroscopic & Related Surgery, 2016. **32**(1): p. 153-163. e18.

60. Ajuied, A., et al., *Anterior cruciate ligament injury and radiologic progression of knee osteoarthritis: a systematic review and meta-analysis.* The American journal of sports medicine, 2014. **42**(9): p. 2242-2252.

61. Lohmander, L.S., et al., *The long-term consequence of anterior cruciate ligament and meniscus injuries: osteoarthritis.* The American journal of sports medicine, 2007. **35**(10): p. 1756-1769.

62. Swärd, P., et al., *Cartilage and bone markers and inflammatory cytokines are increased in synovial fluid in the acute phase of knee injury (hemarthrosis)–a cross-sectional analysis.* Osteoarthritis and cartilage, 2012. **20**(11): p. 1302-1308.

63. Loeser, R.F., et al., *Disease progression and phasic changes in gene expression in a mouse model of osteoarthritis.* PloS one, 2013. **8**(1): p. e54633.

64. Heard, B., et al., *Changes of early post-traumatic osteoarthritis in an ovine model of simulated ACL reconstruction are associated with transient acute post-injury synovial inflammation and tissue catabolism.* Osteoarthritis and cartilage, 2013. **21**(12): p. 1942-1949.

65. Huebner, K.D., N.G. Shrive, and C.B. Frank, *Dexamethasone inhibits inflammation and cartilage damage in a new model of post-traumatic osteoarthritis.* Journal of orthopaedic research, 2014. **32**(4): p. 566-572.

66. Daniel, M.-C. and D. Astruc, *Gold nanoparticles: assembly, supramolecular chemistry, quantum-size-related properties, and applications toward biology, catalysis, and nanotechnology.* Chemical reviews, 2004. **104**(1): p. 293-346.

67. Elahi, N., M. Kamali, and M.H. Baghersad, *Recent biomedical applications of gold nanoparticles: A review.* Talanta, 2018. **184**: p. 537-556.

68. Zhang, X., *Gold nanoparticles: recent advances in the biomedical applications.* Cell biochemistry and biophysics, 2015. **72**(3): p. 771-775.

69. Zhang, Y., et al., *New gold nanostructures for sensor applications: a review.* Materials, 2014. **7**(7): p. 5169-5201.

70. Vigderman, L. and E.R. Zubarev, *Therapeutic platforms based on gold nanoparticles and their covalent conjugates with drug molecules.* Advanced drug delivery reviews, 2013. **65**(5): p. 663-676.

71. Dykman, L. and N. Khlebtsov, *Gold nanoparticles in biomedical applications: recent advances and perspectives.* Chemical Society Reviews, 2012. **41**(6): p. 2256-2282.

72. Christenson, E.M., et al., *Nanobiomaterial applications in orthopedics.* Journal of Orthopaedic Research, 2007. **25**(1): p. 11-22.

73. Hsu, S.-h., C.-M. Tang, and H.-J. Tseng, *Gold nanoparticles induce surface morphological transformation in polyurethane and affect the cellular response.* Biomacromolecules, 2007. **9**(1): p. 241-248.

74. Lu, S., et al., *Concentration effect of gold nanoparticles on proliferation of keratinocytes.* Colloids and Surfaces B: Biointerfaces, 2010. **81**(2): p. 406-411.

75. Gu, H.-Y., et al., *The immobilization of hepatocytes on 24 nm-sized gold colloid for enhanced hepatocytes proliferation.* Biomaterials, 2004. **25**(17): p. 3445-3451.

76. Grant, S.A., et al., *Assessment of the biocompatibility and stability of a gold nanoparticle collagen bioscaffold.* Journal of Biomedical Materials Research Part A: An Official Journal of The Society for Biomaterials, The Japanese Society for Biomaterials, and The Australian Society for Biomaterials and the Korean Society for Biomaterials, 2014. **102**(2): p. 332-339.

77. Huang, C.-L., et al., *Cell adhesion over two distinct surfaces varied with chemical and mechanical properties.* Thin Solid Films, 2009. **517**(17): p. 5386-5389.

78. Badwaik, V.D., et al., *Size-dependent antimicrobial properties of sugar-encapsulated gold nanoparticles synthesized by a green method.* Nanoscale research letters, 2012. **7**(1): p. 623.

79. Ahmad, T., et al., *Biosynthesis, structural characterization and antimicrobial activity of gold and silver nanoparticles.* Colloids and Surfaces B: Biointerfaces, 2013. **107**: p. 227-234.

80. Kishen, A., et al., *Characterizing the collagen stabilizing effect of crosslinked chitosan nanoparticles against collagenase degradation.* Dental Materials, 2016. **32**(8): p. 968-977.

81. Grant, S.A., et al., *Assessment of the biocompatibility and stability of a gold nanoparticle collagen bioscaffold.* Journal of Biomedical Materials Research Part A, 2014. **102**(2): p. 332-339.

82. Akturk, O., et al., *Collagen/gold nanoparticle nanocomposites: a potential skin wound healing biomaterial.* Journal of biomaterials applications, 2016. **31**(2): p. 283-301.

83. Li, J., et al., *Gold nanoparticle size and shape influence on osteogenesis of mesenchymal stem cells.* Nanoscale, 2016. **8**(15): p. 7992-8007.

84. Yi, C., et al., *Gold nanoparticles promote osteogenic differentiation of mesenchymal stem cells through p38 MAPK pathway.* Acs Nano, 2010. **4**(11): p. 6439-6448.

85. Ko, W.-K., et al., *The effect of gold nanoparticle size on osteogenic differentiation of adipose-derived stem cells.* Journal of colloid and interface science, 2015. **438**: p. 68-76.

86. Zhang, D., et al., *Gold nanoparticles stimulate differentiation and mineralization of primary osteoblasts through the ERK/MAPK signaling pathway.* Materials Science and Engineering: C, 2014. **42**: p. 70-77.

87. Zhang, Y., et al., *Size-dependent effects of gold nanoparticles on osteogenic differentiation of human periodontal ligament progenitor cells.* Theranostics, 2017. **7**(5): p. 1214.

88. Leonavičienė, L., et al., *Effect of gold nanoparticles in the treatment of established collagen arthritis in rats.* Medicina, 2012. **48**(2): p. 16.

89. Tsai, C.Y., et al., *Amelioration of collagen-induced arthritis in rats by nanogold.* Arthritis & Rheumatism: Official Journal of the American College of Rheumatology, 2007. **56**(2): p. 544-554.

90. BarathManiKanth, S., et al., *Anti-oxidant effect of gold nanoparticles restrains hyperglycemic conditions in diabetic mice.* Journal of nanobiotechnology, 2010. **8**(1): p. 16.

91. Sul, O.-J., et al., *Gold nanoparticles inhibited the receptor activator of nuclear factor-κb ligand (RANKL)-induced osteoclast formation by acting as an antioxidant.* Bioscience, biotechnology, and biochemistry, 2010. **74**(11): p. 2209-2213.

92. Jeon, K.I., M.S. Byun, and D.M. Jue, *Gold compound auranofin inhibits IκB kinase (IKK) by modifying Cys-179 of IKKβ subunit.* Experimental and Molecular Medicine, 2003. **35**(2): p. 61-66.

93. Akao, T., K. KOBASHI, and M. ABURADA, *Enzymic studies on the animal and intestinal bacterial metabolism of geniposide.* Biological and pharmaceutical Bulletin, 1994. **17**(12): p. 1573-1576.

94. Phatak, R.S., *Phytochemistry, pharmacological activities and intellectual property landscape of Gardenia jasminoides Ellis: a review.* Pharmacognosy Journal, 2015. **7**(5).

95. Koo, H.-J., et al., *Anti-inflammatory evaluation of gardenia extract, geniposide and genipin.* Journal of ethnopharmacology, 2006. **103**(3): p. 496-500.

96. Guan, L., et al., *Genipin ameliorates age-related insulin resistance through inhibiting hepatic oxidative stress and mitochondrial dysfunction.* Experimental gerontology, 2013. **48**(12): p. 1387-1394.

97. Tian, J.-S., et al., *Antidepressant-like effect of genipin in mice.* Neuroscience letters, 2010. **479**(3): p. 236-239.

98. Shanmugam, M.K., et al., *Potential role of genipin in cancer therapy.* Pharmacological research, 2018. **133**: p. 195-200.

99. Kim, S.-J., et al., *Genipin protects lipopolysaccharide-induced apoptotic liver damage in D-galactosamine-sensitized mice.* European journal of pharmacology, 2010. **635**(1-3): p. 188-193.

100. Fujikawa, S., S. Nakamura, and K. Koga, *Genipin, a new type of protein crosslinking reagent from gardenia fruits.* Agricultural and Biological Chemistry, 1988. **52**(3): p. 869-870.

101. Yoo, J.S., et al., *Study on genipin: a new alternative natural crosslinking agent for fixing heterograft tissue.* The Korean journal of thoracic and cardiovascular surgery, 2011. **44**(3): p. 197.

102. Butler, M.F., Y.F. Ng, and P.D. Pudney, *Mechanism and kinetics of the crosslinking reaction between biopolymers containing primary amine groups and genipin.* Journal of Polymer Science Part A: Polymer Chemistry, 2003. **41**(24): p. 3941-3953.

103. Park, J.E., et al., *Isolation and characterization of water-soluble intermediates of blue pigments transformed from geniposide of Gardenia jasminoides.* Journal of Agricultural and Food Chemistry, 2002. **50**(22): p. 6511-6514.

104. Paik, Y.-S., et al., *Physical stability of the blue pigments formed from geniposide of gardenia fruits: effects of pH, temperature, and light.* Journal of agricultural and food chemistry, 2001. **49**(1): p. 430-432.

105. Lee, S.-W., et al., *Colorimetric determination of amino acids using genipin from Gardenia jasminoides.* Analytica chimica acta, 2003. **480**(2): p. 267-274.

106. Nimni, M.E., *Bioprosthesis derived from cross-linked and chemically modified collagenous tissues.* Cllagen Vol. 3 Biotechnology, 1988: p. 1-38.

107. Speer, D.P., et al., *Biological effects of residual glutaraldehyde in glutaraldehyde-tanned collagen biomaterials.* Journal of biomedical materials research, 1980. **14**(6): p. 753-764.

108. Schoen, F.J., et al., *Biomaterial-associated calcification: pathology, mechanisms, and strategies for prevention.* Journal of biomedical materials research, 1988. **22**(A1 Suppl): p. 11-36.

109. Tsai, C.C., et al., *In vitro evaluation of the genotoxicity of a naturally occurring crosslinking agent (genipin) for biologic tissue fixation.* Journal of biomedical materials research, 2000. **52**(1): p. 58-65.

110. Sung, H.-W., et al., *In vitro evaluation of cytotoxicity of a naturally occurring cross-linking reagent for biological tissue fixation.* Journal of Biomaterials Science, Polymer Edition, 1999. **10**(1): p. 63-78.

111. Yang, C., *Enhanced physicochemical properties of collagen by using EDC/NHS-crosslinking.* Bulletin of Materials Science, 2012. **35**(5): p. 913-918.

112. Deeken, C., et al., *Assessment of the biocompatibility of two novel, bionanocomposite scaffolds in a rodent model.* Journal of Biomedical Materials Research Part B: Applied Biomaterials, 2011. **96**(2): p. 351-359.

113. Lider, O., R. Hershkoviz, and S.G. Kachalsky, *Interactions of migrating T lymphocytes, inflammatory mediators, and the extracellular matrix.* Critical Reviews™ in Immunology, 1995. **15**(3-4).

114. Wang, Y., et al., *Genipin crosslinking reduced the immunogenicity of xenogeneic decellularized porcine whole-liver matrices through regulation of immune cell proliferation and polarization.* Scientific reports, 2016. **6**: p. 24779.

115. Koo, H.-J., et al., *Antiinflammatory effects of genipin, an active principle of gardenia.* European journal of pharmacology, 2004. **495**(2-3): p. 201-208.

116. Araki, R., Y. Hiraki, and T. Yabe, *Genipin attenuates lipopolysaccharide-induced persistent changes of emotional behaviors and neural activation in the hypothalamic paraventricular nucleus and the central amygdala nucleus.* European journal of pharmacology, 2014. **741**: p. 1-7.

117. Wang, Q.-S., et al., *Dietary blue pigments derived from genipin, attenuate inflammation by inhibiting LPS-induced iNOS and COX-2 expression via the NF-κB inactivation.* PloS one, 2012. **7**(3): p. e34122.

118. Yu, S.-X., et al., *Genipin inhibits NLRP3 and NLRC4 inflammasome activation via autophagy suppression.* Scientific reports, 2015. **5**: p. 17935.

119. Wang, G.-f., et al., *Genipin inhibits endothelial exocytosis via nitric oxide in cultured human umbilical vein endothelial cells.* Acta Pharmacologica Sinica, 2009. **30**(5): p. 589.

120. Kim, T.-H., S.-J. Yoon, and S.-M. Lee, *Genipin attenuates sepsis by inhibiting Toll-like receptor signaling.* Molecular medicine, 2012. **18**(3): p. 455-465.

Chapter 2

INTRODUCTION TO RESEARCH

2.1 Significance of Research

Anterior cruciate ligament (ACL) injuries are among the most common sporting injuries in the world. There are between 100,000 and 200,000 ACL ruptures per year in the United States alone [1, 2]. The most common treatment for ACLs tears is surgical reconstruction. However, despite the now routine nature of this surgery, the issue of graft choice for remains one of debate. The most common grafts are either patellar or hamstring tendon autograft or an allograft, which is predominantly taken from an Achilles or patellar tendon [3].

Both allograft and autograft surgery have their pros and cons. Allografts are favored by some surgeons because they do not require the harvest procedure required in an autograft surgery. This decreases surgical time and reduces harvest site morbidity [4]. However, animal data has shown allografts lose a greater proportion of time-zero strength during remodeling and incorporation occurs more slowly and less completely [5, 6]. In addition, while most patients are able to return to activity, ACL injuries greatly increase the long-term risk of osteoarthritis (OA). According to one review, the risk of OA in a knee

with a surgically repaired ACL is approximately four times that of the uninjured knee from the same patients and the OA occur at the same rate regardless of the treatment [7].

The significance of this research was to develop and test a method to improve ACL grafts with the use of gold nanoparticles and genipin. We believed these compounds have the potential to decrease inflammation, accelerate ligamentization, and slow down degradation.

2.2 Research Objectives

The overarching objective of this project was to characterize and optimize the use of genipin for attaching gold nanoparticles to tissue. The initial in vitro studies explored the possibility of utilizing genipin for tendon and vascular tissue samples. The resulting data led to concentrating the research on tendon tissue with ACL repair being the primary focus due to the frequency of this surgical procedure.

The in vitro tendon work was designed to provide basic information about the ability to attach gold using genipin and the influence of gold attachment on tissue biocompatibility. Published decellularization protocols from the Grant's laboratory were leveraged to create the tendon scaffolds. Genipin was utilized to conjugate gold nanoparticles and tested at a range of timepoints. The gold levels were then measured using neutron activation analysis (NAA), and

fibroblasts were used to study cell attachment and proliferation. Two different biocompatibility studies were examined and scanning electron microscopy was used to visualize the cell attachment.

The results of the initial studies were encouraging and led to the question would the same process for allograft tissue-gold attachment also work in autograft tissue-gold attachment. Autografts are utilized in 75% of ACL reconstruction surgeries [8], so if genipin could be utilized in these cases it could impact the clinical outcomes of autografts as well as allografts utilized in ACL reconstruction. Porcine diaphragm tendons were harvested and similar gold nanoparticle conjugation were utilized. Shorter timepoints were chosen for crosslinking times due to the nature of autograft surgery. The quantity of gold was determined using NAA and the results were compared against conjugation using decellularized tissue. Histology and scanning electron microscopy were conducted to visualize the condition of the tissue and the nanoparticles

The project concluded with an animal study. This study conjugated gold nanoparticles on human gracilis tendon in order to evaluate the affect the nanoparticles would have on ACL repair. The study lasted 8 weeks in order to determine early signs of mineralization in the bone tunnel.

The results of all these studies demonstrated genipin is beneficial for attaching nanoparticles to tissue. It is able to work rapidly and is biocompatible. The gold nanoparticles also showed great potential for decreasing inflammation in the bone tunnel and the intraarticular portion of the graft.

2.3 References

1. Miyasaka, K., *The incidence of knee ligament injuries in the general population.* Am J Knee Surg, 1991. **1**: p. 43-48.

2. Sanders, T.L., et al., *Incidence of anterior cruciate ligament tears and reconstruction: a 21-year population-based study.* The American journal of sports medicine, 2016. **44**(6): p. 1502-1507.

3. Foster, T.E., et al., *Does the graft source really matter in the outcome of patients undergoing anterior cruciate ligament reconstruction? An evaluation of autograft versus allograft reconstruction results: a systematic review.* The American journal of sports medicine, 2010. **38**(1): p. 189-199.

4. Kartus, J., T. Movin, and J. Karlsson, *Donor-site morbidity and anterior knee problems after anterior cruciate ligament reconstruction using autografts.* Arthroscopy: The Journal of Arthroscopic & Related Surgery, 2001. **17**(9): p. 971-980.

5. Jackson, D.W., J. Corsetti, and T.M. Simon, *Biologic incorporation of allograft anterior cruciate ligament replacements.* Clinical orthopaedics and related research, 1996. **324**: p. 126-133.

6. Kirkpatrick, J., et al., *Cryopreserved anterior cruciate ligament allografts in a canine model.* Journal of the Southern Orthopaedic Association, 1996. **5**(1): p. 20-29.

7. Ajuied, A., et al., *Anterior cruciate ligament injury and radiologic progression of knee osteoarthritis: a systematic review and meta-analysis.* The American journal of sports medicine, 2014. **42**(9): p. 2242-2252.

8. Medicine, A.O.S.f.S., *Allografts for ACL reconstruction survey report*. 2014.

Chapter 3

PRELIMINARY CHARACTERIZATION STUDIES

3.1 Introduction

The development of novel biomaterial requires many preliminary studies that must be undertaken to ensure the material is worthy of further pursuit. This chapter contains experiments that were not necessary for publication but useful initial studies and helpful for telling the full story of the project.

At the initial phases, this project looked at the possibility of using genipin to attach gold nanoparticles (AuNPs) to both vascular and tendon tissue. Genipin will naturally crosslink any available amine groups, so its potential use is not limited to any one tissue [1, 2]. Vascular tissue was studied for its potential use in creating scaffold for repairing trauma, congenital defects, or aneurysms [3, 4].

Overtime we were forced to focus the project more on a single tissue type, but there were still many basic questions that needed answering. Do the commonly used sterilization methods have any effect on the genipin crosslinking? What effect does changing the genipin concentration have on the gold levels? Finally, it was necessary to visualize the AuNPs and their placement on the tissue. In

addition, we needed to know what effect the genipin crosslinking was having on the tissue. Scanning electron microscopy was utilized to answer these questions.

The broad hypothesis for these studies is it possible to use genipin to conjugate AuNPs onto decellularized tissue and what effect does the genipin have on the tissue. These initial studies were designed to answer many basic questions and allow us to move forward with more advanced studies.

3.2 Materials and Methods

3.2.1 Tissue Harvest and Decellularization

3.2.1.1 Carotid

Porcine carotid arteries were harvested immediately following euthanasia of swine after a laboratory exercise at the University of Missouri. Decellularization protocol was tailored from previously published protocols [5, 6]. Vessels were harvested and immediately placed into distilled water to begin the decellularization. They were then cleaned of blood and excess surrounding tissue and submerged in distilled water for 24 h at 4 °C to rupture cell membranes. The vessels were then treated with 0.025% trypsin EDTA (ATCC) diluted in Dulbecco's phosphate buffered saline (ATCC) for 24 hours at 37 °C in the environmental shaker. This was followed by the tissue being put

into a solution of 1% Triton x-100 (Sigma) and 0.1% ammonium hydroxide (Fisher) in distilled water for 72 hours at 4 °C on a rocker to remove nuclear components and lyse cell membranes and cytoplasmic proteins. To deactivate remaining trypsin, the tissue was then placed into a solution of Eagle's Minimum Essential Medium (ATCC) supplemented with 10% (v/v) horse serum and PennStrep (200 U/mL) for 24 hours at 37 °C at 125 rpm. Tissue was washed for 24 hours in distilled water at 4 °C after which the distilled water was changed to PBS for another 24 hours. 4.8 mm circular discs were cut from the decellularized tissue and stored in 70% (v/v) ethanol at 4° C.

3.2.1.2 Diaphragm

Porcine diaphragms were harvested immediately following euthanasia after a laboratory exercise at the University of Missouri. The diaphragm decellularization protocol was adapted from a previously published protocol [7]. The central tendon portion of the diaphragm was dissected from the surrounding muscle. The tissues were immersed in a tris buffer solution containing, 5 mM ethylenediaminetetraacetic acid (EDTA), 0.4 mM phenylmethylsulfonyl fluoride (PMSF), 0.2% (w/v) sodium azide and 1% (v/v) tri(n-butyl) phosphate (TnBP) (Sigma-Aldrich, St. Louis, MO) and subjected to continuous agitation on an orbital shaker at ambient temperature for 24 h. The 1% TnBP solution was removed after 24 h and exchanged

with fresh solution, and the tissues were subjected to continuous agitation for an additional 24 h. This treatment was followed by a 24 h rinse with double distilled water and another 24 h rinse with 70% (v/v) ethyl alcohol, both with continuous agitation at ambient temperature. 4.8 mm circular discs were cut from the decellularized diaphragm tendon and stored in 70% (v/v) ethanol at 4° C.

3.2.2 Gold Conjugation

Specific experimental groups are listed with their respective experiments. Due to the early nature of the experiments, the groups varied but they all had the same basic preparations.

EDC/NHS crosslinking method was based on a previously published protocol by Deeken et al. [8]. The solution consists of 2mM 1-ethyl-3-(3-dimethylaminopropyl) carbodiimide hydrochloride (EDC) and combined with 5mM N-hydroxysuccinimide (NHS) added to a 50:50 (v/v) acetone:phosphate buffered saline mixture. The EDC is first dissolved in MES (2-(N-Morpholino)ethanesulfonic acid with 0.5M NaCl. The NHS is dissolved in a small amount of dimethyl formamide. The EDC and NHS solutions are combined and immediately added to the acetone. The tissue is incubated in 0.25 mL of crosslinking solution for 15 minutes to activate carboxyl groups present on the collagen molecules. The crosslinking solution is withdrawn and 0.25 ml of PBS and 92.6 µl of 20 nm (7.0×10^{11}) functionalized nanoparticles were

added. Nanoparticles were functionalized with amine groups by adding .001 mg/ml 2-mercaptoethyamine (MEA) to the nanoparticles. The tissue is then incubated overnight and then rinsed for 48 hours in PBS at 225 rpm. EDC/NHS is a zero-length crosslinker commonly utilized to crosslinked tissue

Genipin crosslinking was conducted by immersing the decellularized tissue into 1 ml of crosslinking solution containing dissolved genipin. The genipin was dissolved using a minimal amount dimethyl sulfoxide and suspended in PBS. This was accompanied with 0.25 ml of 20 nm gold nanoparticles at a concentration of 7.0×10^{11} functionalized with 0.001 mg/ml of MEA. The samples were crosslinked for timepoints ranging from 15 minutes to 24 hours and then were rinsed repeatedly with PBS.

The 20 nm AuNP tissue control samples were created using the same methodology with the exception that the genipin crosslinking solution was replaced with PBS.

3.2.3 Sterilization

Two separate methods of sterilization were tested for both ability to sterilize and their effect on the genipin attached nanoparticles. The first method was incubating the samples for 24 hours 0.25% (v/v) neutral buffed peracetic acid followed by two 24-hour sterile PBS

rinses. This was conducted on tissue crosslinked for 24 hours and 8 hours.

The second method was immersing the samples in 90% ethanol for 24 hours under constant agitation. This method was tested on samples crosslinked for 1 hour, 4 hours, and 24 hours.

3.2.4 Neutron Activation Analysis

NAA was utilized to quantify the gold levels in the tissue scaffolds. Following crosslinking, samples were lyophilized, weighed, and packed into high density polyethylene NAA vials. At the University of Missouri Research Reactor, the samples were loaded into a rabbit system with Au comparator standards and irradiated for 120 seconds in a thermal neutron flux of 5.0×10^{13} n/cm^2/s. The ^{197}Au captures a neutron to produce the radio-isotope ^{198}Au with a 2.7 d half-life. The samples were allowed to decay for 1-7 hours and then counted for 10 minutes each using a high purity Ge detector controlled by Canberra Genie 2000 software. The detector dead-time was less than 5% for all samples.

3.2.5 Carotid Gold Attachment

Decellularized carotid was tested for the ability to attach gold nanoparticles using genipin conjugation. The samples were conjugated with functionalized nanoparticles for 15 or 30 minutes with 5 mM

genipin or PBS. EDC/NHS crosslinking was used as a positive control. The samples were analyzed by NAA.

3.2.6 Cell Culture

L-929 murine fibroblast cells (ATCC- Manassas, VA) were cultured in EMEM supplemented with 10% (v/v) horse serum and 200 U/ml penicillin-streptomycin solution in an incubator at 37 °C and 5% CO^2.

3.2.7 Biocompatibility of Gold Nanoparticle Carotid Tissue

Cell proliferation reagent WST-1 (Roche Diagnostics Corporation, Indianapolis, IN) was used to evaluate the biocompatibility of the scaffolds. The WST-1 assay works via the use of tetrazolium salts. The salts are added to wells containing cells and the tissue discs. The tetrazolium salts are then cleaved to formazan by mitochondrial dehydrogenase activity. This correlates to the number of metabolically active cells. The resulting formazan can be quantified using UV–Vis absorbance measurements. A total of 5 carotid scaffolds (N=5) from 6 treatment types (untreated, 5 minutes genipin and AuNPs, 15 minutes genipin only, 15 minutes genipin and AuNPs, 30 minutes genipin AuNPs, EDC/NHS) were seeded with L929 mouse connective tissue fibroblasts and incubated for 3 days with half of the media in each well replaced every 48 hours. WST-1 reagent was added to each well and

the plates incubated at 37°C for 4 h. After gentle mixing, 100 µL was removed from each well and absorbance readings were acquired using a Tecan Safire II plate reader. The resulting values were then normalized by the average absorbance of the decellularized group. Culture medium with the WST-1 reagent and no cells served as the blank.

3.2.8 Genipin Concentration

Decellularized diaphragm was used to investigate the effect modifying the genipin concentration would have on conjugation of nanoparticles. The tissue punches were conjugated with nanoparticles for 15 minutes, 30 minutes, and 1 hour. The genipin concentrations tested were 3 mM, 5 mM, 10 mM and 0 genipin. Following conjugation, the tissue was rinsed with PBS and gold concentration was measured using NAA.

3.2.8 Scanning Electron Microscopy

SEM was utilized to visualize the attachment of the nanoparticles on the tendon scaffold and observe the overall microstructure. Samples were conjugated with 3 mM genipin for 15 minutes or 24 hours.

The scaffolds were then prepared by fixation in 0.1M cacodylate buffer containing 2% glutaraldehyde and 2% paraformaldehyde. The

samples were either critically point dried to view fine architecture or view intact to better examine the big picture architecture. Scaffold were examined using a FEI Quanta 600F Environmental SEM.

3.2.10 Statistical Analysis

GraphPad Prism 8.0.1 (GraphPad Software, San Diego, CA) was used to analyze experimental data. The Student's t test was used to analyze gold levels between samples with and without genipin. One-way analysis of variance was conducted followed by a Tukey-Kramer post-test to determine significant differences between means of the experimental groups. The results were considered statistically significant where P was less than 0.05.

3.3 Results

3.3.1 Sterilization Methods

Both sterilization methods were successful at removing bacterial contaminants. However, the peracetic acid sterilization also removed a significant amount of the AuNPs. The removal of the genipin was evident because the scaffolds had lost blue coloration that results from genipin following sterilization. The sterilization with alcohol did not affect the blue coloration brought on by the genipin and the difference in AuNPs was far less. Only the 24 hour conjugation time showed a

statistical difference with significantly less gold on the sterilized sample than on the unwashed scaffold.

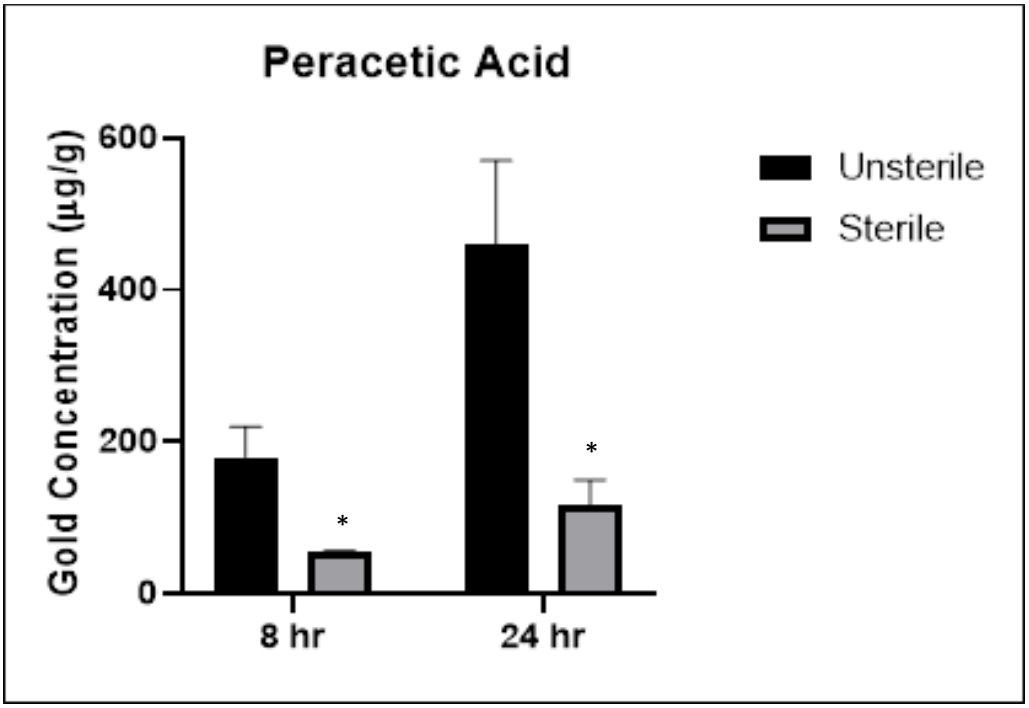

Figure 3.1: Neutron Activation Analysis results for peracetic acid sterilization. Concentration of gold (µg/g) on lyophilized tissue crosslinked with genipin and 20 nm AuNPs for 8 or 24 hrs. Samples were either rinsed with PBS or underwent the sterilization procedure using peracetic acid. * indicates significantly different from unsterilized samples ($p < 0.05$). Error bar displays standard error of the mean.

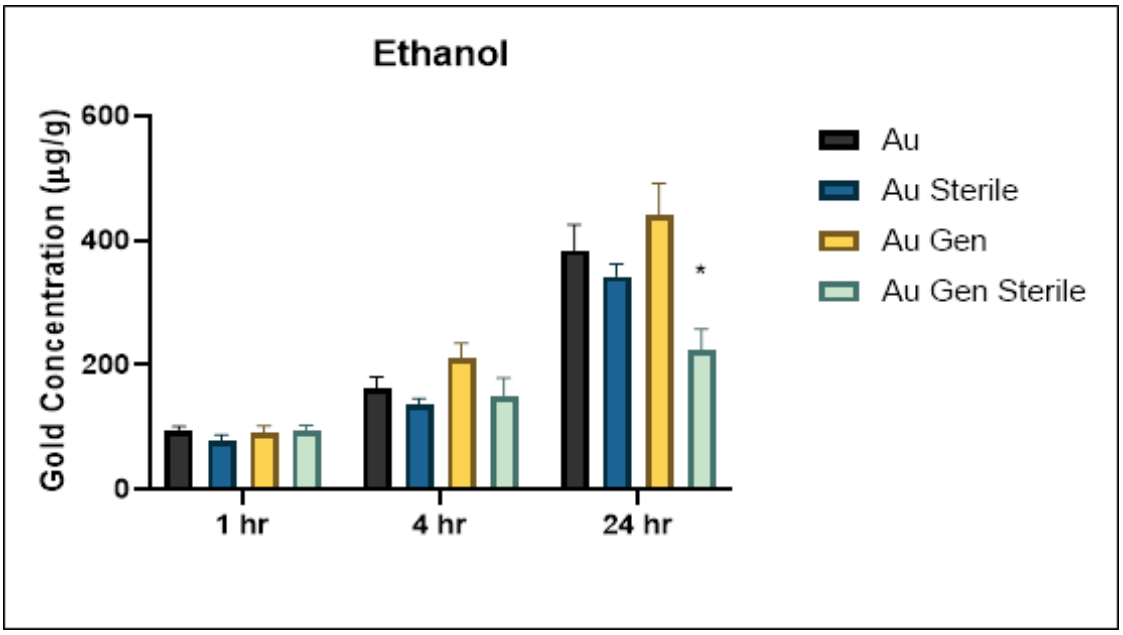

Figure 3.2: Neutron Activation Analysis results for ethanol sterilization. Concentration of gold (µg/g) on lyophilized tissue crosslinked with or without genipin and 20 nm AuNPs for 1, 4 or 24 hrs. Samples were either rinsed with PBS or underwent the sterilization procedure using 90% ethanol. * indicates significantly different from unsterilized samples ($p < 0.05$). Error bar displays standard error of the mean.

3.3.2 Carotid Gold Attachment

The gold nanoparticles were able to successfully attach to carotid tissue. The addition of the genipin did not increase the level of gold attached. At both timepoints, the genipin crosslinked samples had less gold than the samples conjugation with functionalized AuNPs alone, although this was not statistically significant. The genipin crosslinking

had significantly less gold than the scaffolds conjugated using the EDC/NHS.

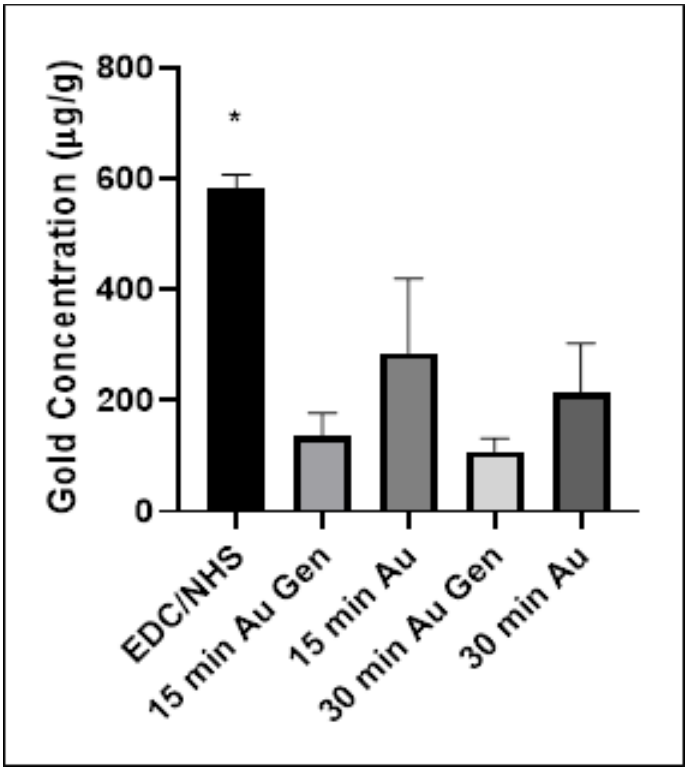

Figure 3.3: Neutron Activation Analysis results for carotid scaffold. concentration of gold (µg/g) on lyophilized decellularized carotid tissue. Samples were crosslinked with or without genipin for 15 or 30 minutes. EDC/NHS crosslinking was used as a positive control. * indicates significantly different from all other samples ($p < 0.05$). Error bar displays standard error of the mean.

3.3.3 Biocompatibility of Gold Nanoparticle Carotid Tissue

The addition of the AuNPs and genipin did not affect the cell viability of the carotid scaffolds. There were no significant differences

between any of the groups, although the samples crosslinked genipin and gold for 15 minutes had the highest cell viability at approximately 150% cell numbers when compared to uncrosslinked scaffold.

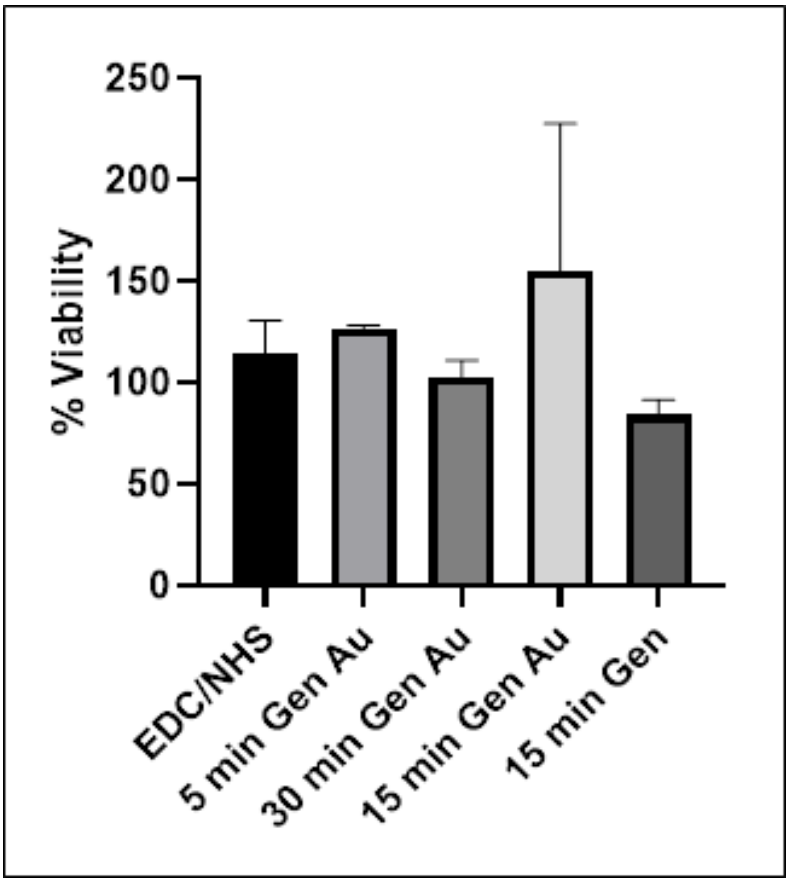

Figure 3.4: Cell proliferation reagent WST-1 assay results showing percent viability relative to the control, untreated tissue carotid scaffolds. Cell were grown on the scaffold for 3 days. Error bar displays standard error of the mean.

3.3.4 Genipin Concentration

There were no significant differences seen between the gold concentrations for any of the scaffolds. The concentration of genipin did not affect the gold levels for any of the timepoints tested. There gold levels were not changed when genipin wasn't used at all.

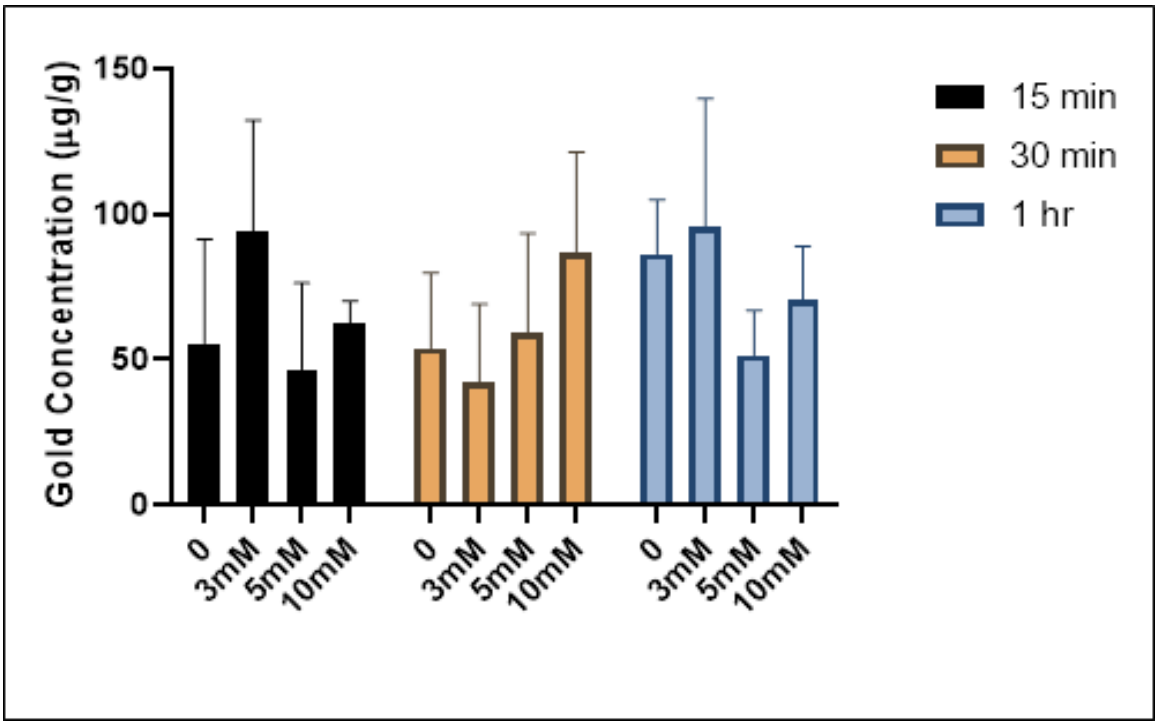

Figure 3.5: Neutron Activation Analysis results for variable genipin concentration. Concentration of gold (µg/g) on lyophilized tendon tissue crosslinked for 15 minutes, 30 minutes, or 1 hour with varying genipin concentrations. Error bar displays standard error of the mean.

3.3.5 Scanning Electron Microscopy

The SEM images clearly displayed the presence of the AuNPs on the tissue scaffold at all time points. However, it is also clear that with

the longer timepoints the AuNPs are clumping together instead of being evenly spread across the tissue fibers. This is clearly visible in Figure 3.6. Image B shows the AuNPs spread across the fiber in an uniformly while the nanoparticle in image E are grouped together.

There were also differences in the tissue architecture. Figure 3.7 displays the surface of structure of tissue scaffold. Image A and B show the tissue crosslinked for 15 minutes and there are clearly more ridges and clefts on the surface of the scaffold when compared to Images C and D which were crosslinked for 24 hours. The crosslinking evidently closed off many the openings when the reaction is allowed to occur for an extended period of time.

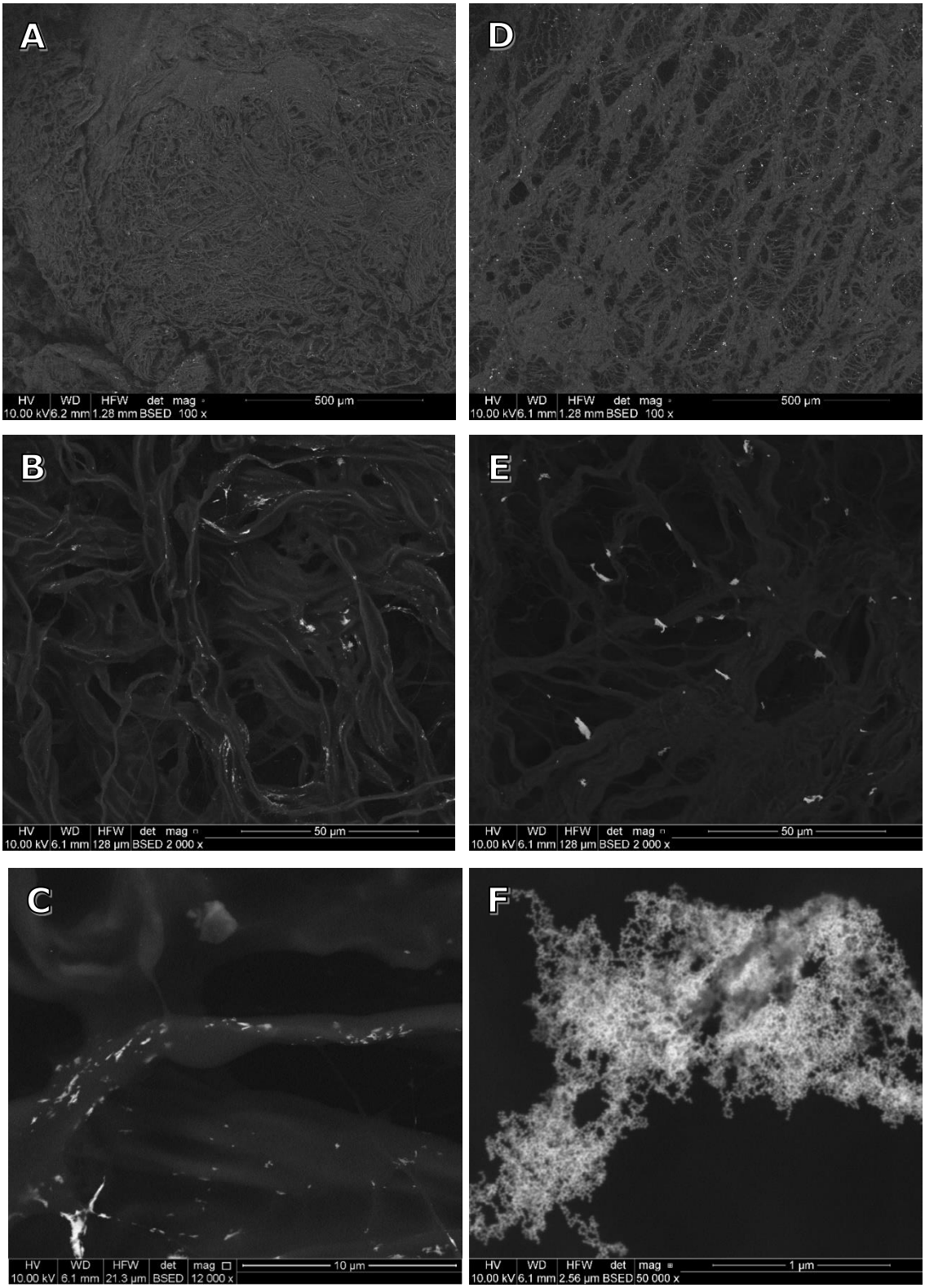
A
HV WD HFW det mag
10.00 kV 6.2 mm 1.28 mm BSED 100 x
500 µm
D
HV WD HFW det mag
10.00 kV 6.1 mm 1.28 mm BSED 100 x
500 µm
B
HV WD HFW det mag
10.00 kV 6.1 mm 128 µm BSED 2 000 x
50 µm
E
HV WD HFW det mag
10.00 kV 6.1 mm 128 µm BSED 2 000 x
50 µm
C
HV WD HFW det mag
10.00 kV 6.1 mm 21.3 µm BSED 12 000 x
10 µm
F
HV WD HFW det mag
10.00 kV 6.1 mm 2.56 µm BSED 50 000 x
1 µm

Figure 3.6: Scanning electron microscopy images of gold nanoparticles conjugated with genipin to decellularized diaphragm tendon. A, B, and C were crosslinked for 15 minutes. D, E, and F were crosslinked for 24 hours.

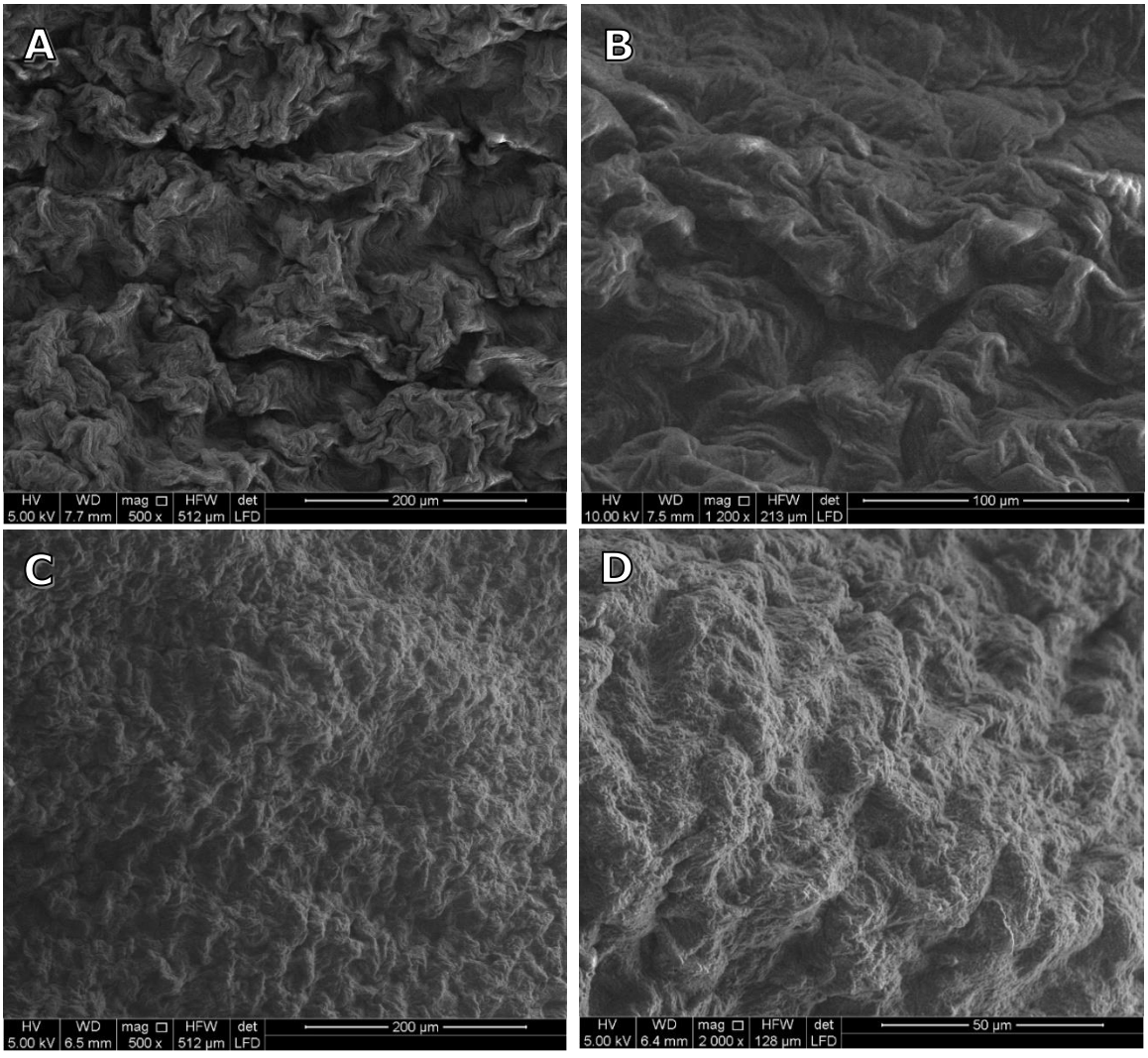

Figure 3.7: Scanning electron microscopy images of genipin conjugated decellularized diaphragm tendon. A and B were crosslinked for 15 minutes. C and D were crosslinked for 24 hours.

3.4 Discussion

These preliminary studies were performed using porcine carotid and diaphragm tendon to test the ability of AuNPs to attach to the tissue using genipin. Our lab has previously used the zero-length crosslinking method using EDC/NHS to attach nanoparticles [9-11]. While this method can sufficiently attach AuNPs, it is not without problems. EDC/NHS crosslinking produces numerous cytotoxic byproducts [12]. As a result, samples must undergo extensive washing following crosslinking. In addition, the EDC/NHS crosslinking protocols only allow for a rough estimate of the amount of attached gold because the agents only react quickly but for a limited period of time [13, 14]. Genipin was selected because it does not have the cytotoxicity issues, and its reaction begins immediately and continues as long as genipin or amine groups are present [1, 2]. These necessary studies provided the framework for all other studies moving forward.

In order to conduct the later cell studies and any in vivo analysis, its essential to find a method to sterilize the scaffold. Tissue

banks typically employ one of two methods of sterilization: ethylene oxide or gamma irradiation [15]. Those methods require large industrial equipment and are not possible for a lab setting. Our lab had previously developed a sterilization protocol peracetic acid that worked well with other crosslinking methodologies [7]. However, when this protocol was used on the genipin crosslinked samples, the scaffolds lost almost all of the blue coloration that comes with genipin crosslinking. When the gold levels were tested with and without the peracetic acid sterilization, it is clear a majority of the gold was removed by this method. A second method of sterilization was developed based on the work of Delgado et al. [16]. The samples were immersed in 90% ethanol for 24 hours under constant agitation. As seen in Figure 3.2, this had little effect on the gold levels, and the tissue retained its blue coloration. No contamination was seen in any of the subsequent cell studies using this method of sterilization.

In the early phases of this study, genipin conjugation of AuNPs was studied using both decellularized carotid and diaphragm tendon. Figure 3.3 demonstrates we were able to successfully attach AuNPs to the carotid tissue. However, the gold levels attached are far less than levels seen using the EDC/NHS crosslinking method, and this was not the case for the decellularized tendon tissue. Additionally, the samples conjugated using genipin had a lower concentration of gold than the

samples conjugated with functionalized nanoparticles alone, although the differences were not significant. When this was combined with the WST-1 assay which showed no effect from the AuNPs and genipin on cell viability, it was decided to focus our efforts on the tendon tissue.

The neutron activation analysis (Figure 3.5) was conducted to find if modifying the genipin concentration would alter the concentration of gold attached. The analysis showed no difference in gold concentration regardless of the concentration of genipin or whether or not genipin was even present. This is despite the fact that previous studies have shown faster reaction times when higher genipin concentration is present [17]. Because the concentration of genipin had no effect on gold attachment, subsequent studies used the small genipin concentrations. Figure 3.7 confirms the genipin was having an effect on the tissue though. The tissue crosslinked with genipin has a much more densely packed even surface while the uncrosslinked sample demonstrated loose undulations of tissue. The SEM images were also used to visually confirm the presence of the AuNPs. Figure 3.6 shows the presence of the gold on both the samples crosslinked for 15 minutes and 24 hours. However, the long crosslinking time did lead to the particles coming together into clumps, while the nanoparticles for the 15 minute crosslinking time are more evenly spread across the tissue fibers.

Overall these preliminary studies gave us an important basic information on the ability to attach functionalized nanoparticles to tissue as well as the effects of genipin on the tissue surface. Further in vitro and in vivo testing of these materials is available over the next several chapters of the dissertation.

3.5 References

1. Yoo, J.S., et al., *Study on genipin: a new alternative natural crosslinking agent for fixing heterograft tissue.* The Korean journal of thoracic and cardiovascular surgery, 2011. **44**(3): p. 197.

2. Sung, H.W., et al., *Feasibility study of a natural crosslinking reagent for biological tissue fixation.* Journal of Biomedical Materials Research Part A, 1998. **42**(4): p. 560-567.

3. Robinson, K.A., et al., *Extracellular matrix scaffold for cardiac repair.* Circulation, 2005. **112**(9_supplement): p. I-135-I-143.

4. Schaner, P.J., et al., *Decellularized vein as a potential scaffold for vascular tissue engineering.* Journal of vascular surgery, 2004. **40**(1): p. 146-153.

5. Williams, C., et al., *Altered structural and mechanical properties in decellularized rabbit carotid arteries.* Acta biomaterialia, 2009. **5**(4): p. 993-1005.

6. Amiel, G.E., et al., *Engineering of blood vessels from acellular collagen matrices coated with human endothelial cells.* Tissue engineering, 2006. **12**(8): p. 2355-2365.

7. Deeken, C., et al., *Assessment of the biocompatibility of two novel, bionanocomposite scaffolds in a rodent model.* Journal of Biomedical Materials Research Part B: Applied Biomaterials, 2011. **96**(2): p. 351-359.

8. Deeken, C., et al., *Method of preparing a decellularized porcine tendon using tributyl phosphate.* Journal of Biomedical Materials Research Part B: Applied Biomaterials, 2011. **96**(2): p. 199-206.

9. Grant, S.A., et al., *In vivo bone tunnel evaluation of nanoparticle-grafts using an ACL reconstruction rabbit model.* Journal of Biomedical Materials Research Part A, 2017. **105**(4): p. 1071-1082.

10. Grant, S.A., et al., *Assessment of the biocompatibility and stability of a gold nanoparticle collagen bioscaffold.* Journal of Biomedical Materials Research Part A, 2014. **102**(2): p. 332-339.

11. Ostdiek, A.M., et al., *An in vivo study of a gold nanocomposite biomaterial for vascular repair.* Biomaterials, 2015. **65**: p. 175-183.

12. Nishi, C., N. Nakajima, and Y. Ikada, *In vitro evaluation of cytotoxicity of diepoxy compounds used for biomaterial modification.* Journal of Biomedical Materials Research Part A, 1995. **29**(7): p. 829-834.

13. Deeken, C.R., et al., *Characterization of bionanocomposite scaffolds comprised of amine-functionalized gold nanoparticles and silicon carbide nanowires crosslinked to an acellular porcine tendon.* Journal of Biomedical Materials Research Part B: Applied Biomaterials, 2011. **97**(2): p. 334-344.

14. Ostdiek, A.M., et al., *Feasibility of a nanomaterial-tissue patch for vascular and cardiac reconstruction.* Journal of Biomedical Materials Research Part B: Applied Biomaterials, 2016. **104**(3): p. 449-457.

15. Vangsness Jr, C.T., et al., *Allograft transplantation in the knee: tissue regulation, procurement, processing, and sterilization.* The American journal of sports medicine, 2003. **31**(3): p. 474-481.

16. Delgado, L.M., K. Fuller, and D.I. Zeugolis, *Collagen cross-linking: biophysical, biochemical, and biological response analysis.* Tissue Engineering Part A, 2017. **23**(19-20): p. 1064-1077.

17. Butler, M.F., Y.F. Ng, and P.D. Pudney, *Mechanism and kinetics of the crosslinking reaction between biopolymers containing primary amine groups and genipin.* Journal of Polymer Science Part A: Polymer Chemistry, 2003. **41**(24): p. 3941-3953.

Chapter Four

GENIPIN ATTACHMENT OF CONJUGATED GOLD NANOPARTICLES ATTACHMENT TO LIGAMENT SCAFFOLDS

4.1 Abstract

Decellularized allograft tissue is used for a wide array of tissue injuries and repair with tendons and ligament repair being among the most common. However, despite their frequent use there is concern over the lengthy inflammatory period and slow healing associated with allografts. One promising solution has been the use of nanoparticles. There is currently no easy, fast method to achieve consistent conjugation of nanoparticles to tissue. The available conjugation methods can be time-consuming and/or may create numerous cytotoxic byproducts. Genipin, a naturally derived crosslinking agent isolated from the fruits of Gardenia jasminoides was investigated as a conjugation agent to achieve fast, consistent crosslinking without cytotoxic byproducts. The rational of utilizing genipin is that is reacts spontaneously with amino-group-containing compounds such as proteins, collagens, and gelatins and does not require extensive washing after conjugation. Porcine diaphragm tendons were decellularized and then immersed in cysteamine functionalized gold

nanoparticles and genipin for various time points. Tissue scaffolds were tested for the degree of crosslinking, gold nanoparticle concentrations, and fibroblast attachment and biocompatibility. Results demonstrated that genipin can successfully and reproducibility attached gold nanoparticles to tissue in as little as 15 minutes. The genipin had no cytotoxic effects and improved fibroblast attachment and proliferation. Genipin can be used to attach gold nanoparticles to tissue in a fast, cell safe manner.

4.2 Introduction

Tissue engineering has advanced as a promising solution for the repair of damaged or diseased tissues with the goal of creating functional scaffolds that mimics native tissue and can be colonized by the host's cells. Decellularized tissue has shown promise in this regard, and there are numerous surgical scaffolds in clinic use today utilizing both allogenic and xenogeneic decellularized tissue including, urinary bladder, small intestine, dermis, mesothelium, heart valves, and pericardium [1]. In addition, researchers are working towards the use of three-dimensional scaffolds created through whole organ decellularization as a treatment for end-stage organ failure without the risk of chronic rejection and the morbidity associated with immunosuppression [2-4]. Biologic tissue is better able to mimic the full complexity of the tissue architecture while also being a source of

signaling molecules and growth factors creating a superb environment for cellular attachment and proliferation [5, 6]. Although decellularized tissue has numerous promising characteristics, it is not without its drawbacks. These concerns include decellularization weakening mechanical properties, inherent heterogeneity, high immunogenicity, rapid biodegradation, and slow integration [7-9]. This is specifically true with ligament grafts. Decellularized ligament and tendon use is limited due to a prolonged inflammatory period, delayed graft remodeling [10]. A potential solution to some of these concerns is the utilization of gold nanoparticles.

Gold nanoparticles (AuNPs), conjugated to decellularized tissue, can mitigate some of the concerns with decellularized tissue grafts. First, AuNPs have long been utilized for their anti-inflammatory properties, which is believed to be the result of free radical scavenging [11-13]. Secondly, gold nanoparticle attachment modifies the surface structure and encourages cellular attachment and proliferation [14, 15]. The increased surface energy of AuNPs may promote attachment of proteins including those necessary for cellular attachment [16]. In addition, conjugation of the AuNPs to the tissue is believed to block collagenase attachment and thereby slowing down scaffold degradation [15]. Gold nanoparticles can also be used to direct the differentiation of stem cells into specific cell types. Yi et al.

demonstrated that AuNPs promote the osteogenic differentiation of mesenchymal stem cells by activating the p38 mitogen-activated protein kinase pathway, and Dong et al. demonstrated the addition of AuNPs promotes osteogenic differentiation of adipose-derived stem cells and results in significantly higher new bone formation in a rabbit model [17, 18].

With all the promise of nanoparticles, their attachment to tissue remains challenging. The commonly used methods have cytotoxic byproducts and require multiple washes to remove them [19, 20]. In addition, the current conjugation protocols only enable a rather rough estimate of the amount of attached gold as many of the agents only react for a limited period of time [21, 22]. There is a need to find a biocompatible, stable, crosslinking agent to facilitate the attachment of nanoparticles. Genipin is a potential solution to this problem. Genipin is a chemical compound extracted from the fruits of *Gardenia jasminoides.* It is a natural crosslinking agent, and it spontaneously reacts with amino-group-containing compounds such as proteins, collagens, and gelatins to form mono- to tetramer crosslinks, and has an exceptionally low cytotoxicity [23, 24]. Genipin also has the added benefit of acting as an anti-inflammatory agent and simultaneously reducing the immunogenicity of the scaffold [8, 25, 26].

In this study, it is hypothesized that genipin is a viable agent to conjugate gold nanoparticles to a decellularized tendon scaffold quickly and efficiently. Porcine diaphragm tendon was decellularized and exposed to solutions containing either genipin, 20 nm gold nanoparticles, or both for time points ranging from 15 minutes to 24 hours. The thermal stability of the tissue was measured using differential scanning calorimetry to evaluate the degree of crosslinking and potential damage to the tissue. Neutron activation analysis (NAA) was used to measure the amount of gold attached to each sample. WST-1 and dsDNA assay PicoGreen assay was performed to measure viability of the fibroblast cells cultured on the scaffolds, and scanning electron microscopy was performed to visualize the fibroblast attachment.

4.3 Materials and Methods

4.3.1 Tissue Harvest and Decellularization

Porcine diaphragms were harvested immediately following euthanasia after a laboratory exercise at the University of Missouri. The central tendon portion of the diaphragm was dissected from the surrounding muscle. They were then decellularized according to a previously published protocol [22]. In brief, the tissues were immersed in a solution containing 1% (v/v) tri(n-butyl) phosphate (TnBP) (Sigma-Aldrich, St. Louis, MO) in storage buffer solution and subjected

to continuous agitation on an orbital shaker at ambient temperature for 24 h. The 1% TnBP solution was removed after 24 h and exchanged with fresh solution, and the tissues were subjected to continuous agitation for an additional 24 h. This treatment was followed by a 24 h rinse with double distilled water and another 24 h rinse with 70% (v/v) ethyl alcohol, both with continuous agitation at ambient temperature. This method of decellularization was previously studied in our lab and verified to effectively remove all cell nuclei while leaving the structure and composition of the tissue intact [27]. 4.8 mm circular discs were cut from the decellularized diaphragm tendon and stored in 70% (v/v) ethanol at 4° C.

4.3.2 Genipin, gold nanoparticles and the crosslinking procedure

Genipin (Sigma-Aldrich, St. Louis, MO) crosslinking was conducted by immersing the decellularized tissue into 1 ml of solution containing 3 mM or 10 mM dissolved genipin. The genipin was dissolved using dimethyl sulfoxide and suspended in PBS. This was accompanied with 0.25 ml of 20 nm gold nanoparticles (Ted Pella, Redding, CA) at a concentration of 7.0×10^{11}. The 20 nm AuNPs were utilized due to a previous study demonstrating the efficacy of nanoparticles in this size range in reducing inflammation [28]. Nanoparticles were functionalized with amine groups by the addition of

0.001 mg/ml 2-mercaptoethyamine (MEA) to the nanoparticles. The scaffolds were crosslinked for 15 minutes, 1 hour, 4 hours, or 24 hours and then were quickly rinsed with PBS. The AuNP tissue control samples were created using the same methodology with the exception that the genipin solution was replaced with PBS.

Tissue scaffolds were sterilized following crosslinking by immersion in 90% ethanol for 24 hours at 225 rpm. This was followed by three washes in sterilized phosphate buffered saline.

4.3.3 Experimental groups

1. Untreated: porcine diaphragm tendon that underwent decellularization protocol.

2. 15 min, 1 hr, 4 hr, 8 hr, 24 hr Au Gen: decellularized tissue crosslinked with 0.25 ml of functionalized 20 nm gold nanoparticles at the stock and 1 ml of genipin at 3 mM. Crosslinking time ranged from 15 minutes to 24 hours.

3. 15 min, 1 hr, 4 hr, 8 hr, 24 hr Gen: decellularized tissue crosslinked with 0.25 ml of PBS at the stock and 1 ml of genipin at 3 mM. Crosslinking time ranged from 15 minutes to 24 hours. This group was crosslinked with genipin but without the addition of AuNPs.

4. 15 min, 1 hr, 4 hr, 8 hr, 24 hr Au: decellularized tissue crosslinked with 0.25 ml of functionalized 20 nm gold nanoparticles at the stock and 1 ml of PBS. Crosslinking time ranged from 15 minutes

to 24 hours. This group was conjugated with nanoparticles but without the addition of genipin.

5. EDC: Group 5. EDC/NHS crosslinked tissue: decellularized tissue that were crosslinked with thechemical crosslinkers 1-ethyl-3-[3-dimethylaminopropyl]carbodiimide (EDC) (Thermo Fisher Scientific, Waltham, MA) and N-hydroxysuccinimide (NHS) (Thermo Fisher Scientific, Waltham, MA) according to a previously published protocol [26] . Briefly, 2mM EDC 2-(N-Morpholino)ethanesulfonic acid buffer and combined with 5mM NHS in dimethyl formamide. These are then added to a 50:50 (v/v) acetone:phosphate buffered saline mixture. The tissue is incubated in 0.25 mL of crosslinking solution for 15 minutes. The tissue is then incubated overnight and then rinsed for 48 hours in PBS at 225 rpm. EDC/NHS is a zero-length crosslinker commonly utilized to crosslinked tissue. It was utilized as a control in the DSC studies.

4.3.4 Neutron Activation Analysis

NAA was utilized to quantify the gold levels in the tissue scaffolds. Following crosslinking, five samples of each treatment type (N=5) were lyophilized, weighed, and packed into high density polyethylene NAA vials. At the University of Missouri Research Reactor, the samples were loaded into a rabbit system with Au comparator standards and irradiated for 120 seconds in a thermal neutron flux of

$5.0x10^{13}$ n/cm^2/s. The ^{197}Au captures a neutron to produce the radio-isotope ^{198}Au with a 2.7 d half-life. The samples were allowed to decay for 1-7 hours and then counted for 10 minutes each using a high purity Ge detector controlled by Canberra Genie 2000 software. The detector dead-time was less than 5% for all samples.

4.3.5 Modulated Differential Scanning Calorimetry

Following crosslinking, five specimens (n=5) from the 7 treatment types were rinsed in DI water and placed in an aluminum pan with a hermetic lid. The treatment type were EDC/NHS, untreated, 15 minutes crosslinking with 3 mM genipin, 4 hours crosslinking with 3 mM genipin, 8 hours crosslinking with 3 mM genipin, 24 hours crosslinking with 3 mM genipin, and 24 hours crosslinking with 10 mM genipin. The 10 mM treatment type was added to verify that increasing the genipin concentration would further increase the amount of crosslinking that occurred. The reference pan consisted of an aluminum pan containing 2 μL of double distilled water and sealed with a hermetic lid. Each specimen was then subjected to modulated differential scanning calorimetry using a Q2000 DSC (TA Instruments, New Castle, DE) to raise the temperature from 5°C to 120°C at a rate of 5°C per minute with a modulation of ±0.64°C every 80 seconds. The mean denaturation temperature is reported.

4.3.6 Cell Culture

L-929 mouse fibroblast cells were obtained from ATCC (Manassas, VA). They were cultured in EMEM (ATCC, Manassas, VA) supplemented with 10% (v/v) horse serum (Sigma-Aldrich, St. Louis, MO) and 200 U mL−1 penicillin–streptomycin (Sigma-Aldrich, St. Louis, MO) solution in an incubator at 37°C and 5% CO_2. 1 ml of 3 x 10^4 cell/ml cell solution was plated on each scaffold and allowed to grow for 1, 3, 7, or 10 days with fresh media being replaced every 48 days.

4.3.7 Cell Viability

Cell proliferation reagent WST-1 (Roche Diagnostics Corporation, Indianapolis, IN) was used to evaluate the biocompatibility of the scaffolds. The WST-1 assay works via the use of tetrazolium salts. The salts are added to wells containing cells and the tissue discs. The tetrazolium salts are then cleaved to formazan by mitochondrial dehydrogenase activity. This correlates to the number of metabolically active cells. The resulting formazan is can be quantified using UV–vis absorbance measurements. A total of 5 scaffolds (N=5) from ten treatment types (untreated, 15 minutes, 1 hour, and 24 hours with 3 mM genipin and gold nanoparticles or either of the components independently) were seeded with L929 mouse connective tissue fibroblasts and incubated for 1, 3, 7, and 10 days with half of the media in each well replaced every 48 hours. WST-1 reagent was added

to each well and the plates incubated at 37°C for 4 h. After gentle mixing, 100 µL was removed from each well and absorbance readings were acquired using a Tecan Safire II plate reader. The resulting values were then calculated relative to the absorbance found on the untreated control scaffold. The data is shown as a percentage in comparison to the control. Culture medium with the WST-1 reagent and no cells served as the blank.

4.3.8 dsDNA assay

A total of 5 scaffolds (N=5) from 5 treatment types (untreated, 15 minutes gold and genipin, 1 hour gold and genipin, 24 hour gold and genipin, and 24 hour genipin only) were seeded with L929 mouse connective tissue fibroblasts and incubated for 1, 3, 7 and 10 days. Following cell culture, the discs were removed from their wells, gently rinsed, frozen at 70 °C. Samples were then lyophilized and submerged in papin digest and incubated at 60° C for 24 h. A Quant-iT PicoGreen double stranded DNA quantification assay (Thermo Fisher Scientific, Waltham, MA) was used to determine the cellularity of the scaffold. 25 µL of each papain digested sample were added to a 48-well plate. 225 µL of TE buffer (10 mM Tris-HCl, 1 mM EDTA, pH 7.5) and 250 µL of 2 µg/mL of PicoGreen reagent was added to each well and the plate was incubated for 5 min. Sample fluorescence was read at 480 nm excitation/520 nm using a Tecan Safire II plate reader. A Lambda DNA

standard curve was used to determine DNA concentrations for the experimental samples.

4.3.9 Scanning electron microscopy

SEM was utilized to visualize the attachment of the fibroblasts on the scaffold and observe the overall microstructure. The scaffolds were either uncrosslinked or crosslinked with 3 mM genipin with or without the presence of 20 nm AuNP. Scaffolds were plated with fibroblasts for 1 or 3 days and were then prepared by fixation in 0.1M cacodylate buffer containing 2% glutaraldehyde and 2% paraformaldehyde. Samples were critically point dried and examined using a FEI Quanta 600F Environmental SEM.

4.3.10 Statistical Analysis

GraphPad Prism 8.0.1 (GraphPad Software, San Diego, CA) was used to analyze experimental data. The Student's t test was used to analyze gold levels between samples with and without genipin. One-way analysis of variance was conducted followed by a Tukey-Kramer post-test to determine significant differences between means of the experimental groups. The results were considered statistically significant where P was less than 0.05.

4.4 Results

4.4.1 Neutron Activation Analysis

NAA was performed to measure the concentration of gold attached to the tissue scaffold. As shown in Table 4.1, the number of nanoparticles increased with the amount of crosslinking time with or without the use of genipin. For all time points, the scaffold with genipin had a higher concentration of gold, but the difference was only significant at the 15-minute time point.

Table 4.1 Neutron Activation Analysis results for genipin conjugated tendon tissue. Concentration of gold (μg/g) on lyophilized tissue with and without the addition of genipin. *Indicates constructs that have significantly higher concentration of AuNPs than the sample incubated for the same amount of time without genipin. Values given as ± the standard deviation.

Conjugation Time	Au	Au and Genipin
15 minutes	51	100*
1 hour	86	92
4 hours	153	190
8 hours	224	228
24 hours	373	389

4.4.2 Modulated Differential Scanning Calorimetry

Figure 4.1 displays the denaturation temperatures of the tissue scaffold with different crosslinking times and different concentrations of genipin. The denaturation temperature significantly increases with only 15 minutes of genipin crosslinking. We see another significant increase at 24 hours of crosslinking. Denaturation temperature also significantly increased with higher genipin concentrations.

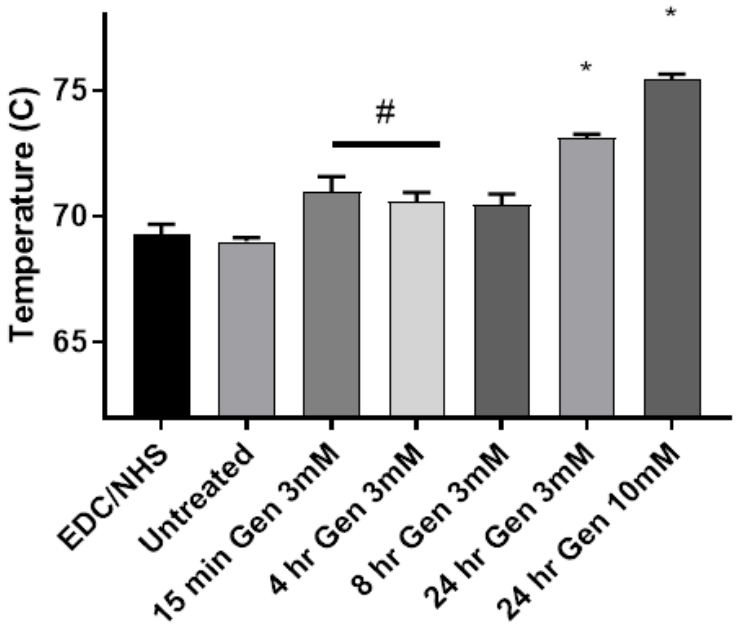

Figure 4.1 Results of modulated differential scanning calorimetry in which the mean denaturation temperature of each tissue is shown. α indicates significantly lower than 24 hr 10 mM samples, β indicates significantly lower than 24 hr 3 mM samples, and γ indicates

significantly higher than the untreated samples. Error bar displays standard error of the mean.

4.4.3 Cell Viability

Figure 4.2 shows the percent viability for each experimental group relative to decellularized untreated scaffolds (n=5). The scaffolds crosslinked with genipin for 24 hours, with or without gold nanoparticles, had significantly higher relative viability when compared to the uncrosslinked samples at day 1 and day 10. All other samples were not significantly higher than the uncrosslinked scaffolds.

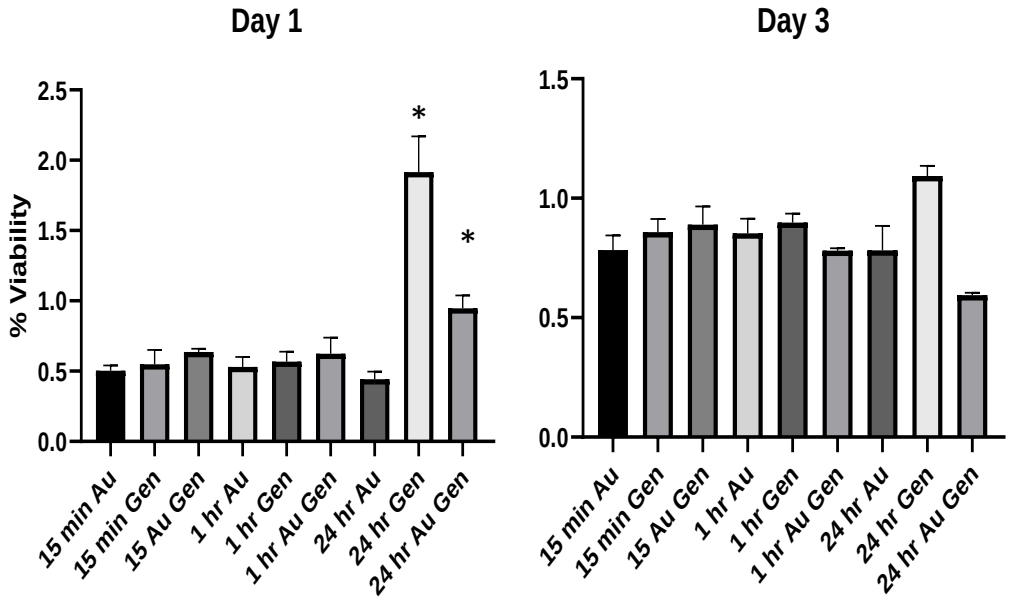

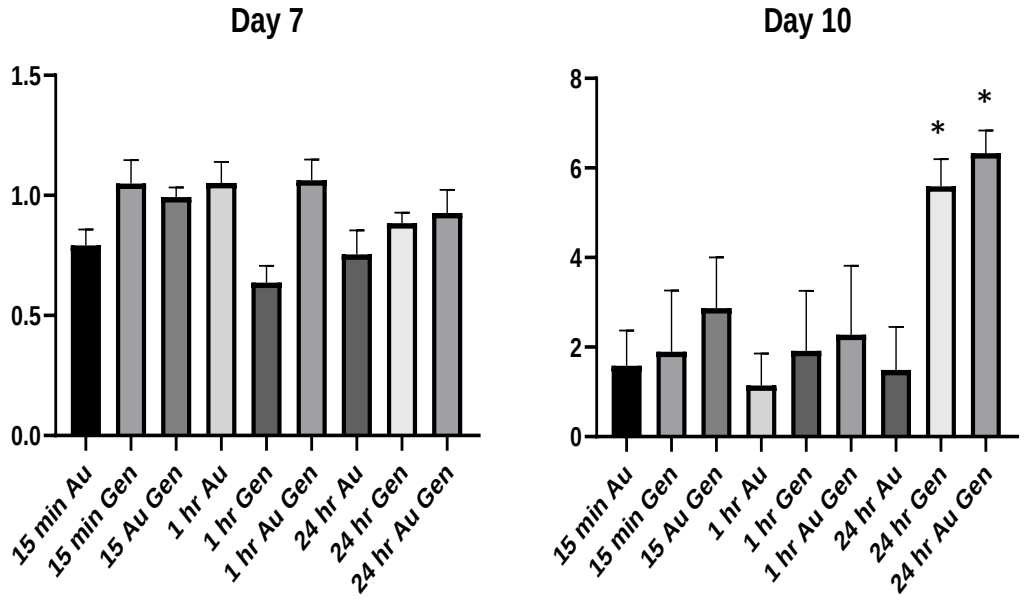

Figure 4.2: Cell proliferation reagent WST-1 assay results showing percent viability relative to the control, untreated tendon scaffolds. * indicates significantly different from untreated control ($p < 0.05$). Error bar displays standard error of the mean.

4.4.4 dsDNA assay

The PicoGreen assay used to determine dsDNA content of the cells attached to the tissue scaffold. The sample with the 24 hour genipin crosslinking with no gold nanoparticles had the highest levels of dsDNA for all time points. It was significantly higher than all other samples except the 24 hour genipin with gold at day 3 and significantly higher than the samples crosslinked for 15 minutes or 1 hour at day 1 and day 10.

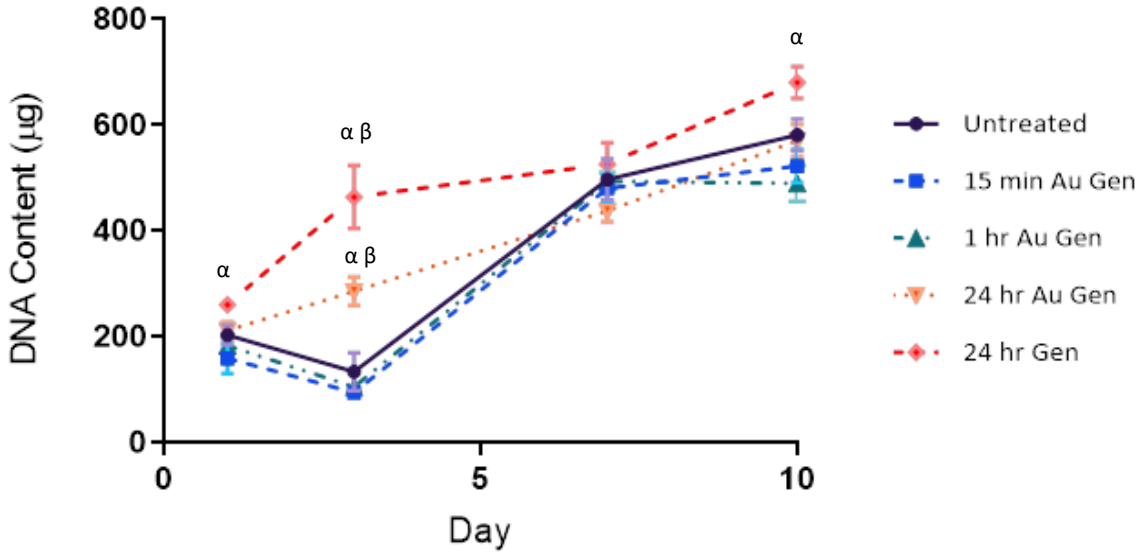

Figure 4.3: DNA content on tendon scaffolds plated with L929 mouse fibroblasts for 1 to 10 days. α indicates significantly higher DNA content than 15 min or 1-hour crosslinking samples. β indicates significantly higher DNA content than the untreated samples. ($p < 0.05$). Error bar displays standard error of the mean.

4.4.5 Scanning electron microscopy

The SEM images clearly demonstrate the presence of fibroblast cells on the scaffold. The images also show the cells plated on the scaffolds with genipin alone are flusher, and more tightly adhered to the scaffold in comparison to the more spherical cells on the uncrosslinked scaffold at both day 1 and day 3. This is especially visible at the day 3 timepoint and can be seen on images D and G versus E and I in figure 4. The fibroblasts on the genipin and AuNP scaffolds are moderately leveled but remained more spherical than the

fibroblasts attached to scaffold with genipin alone as seen in images B, F, and H.

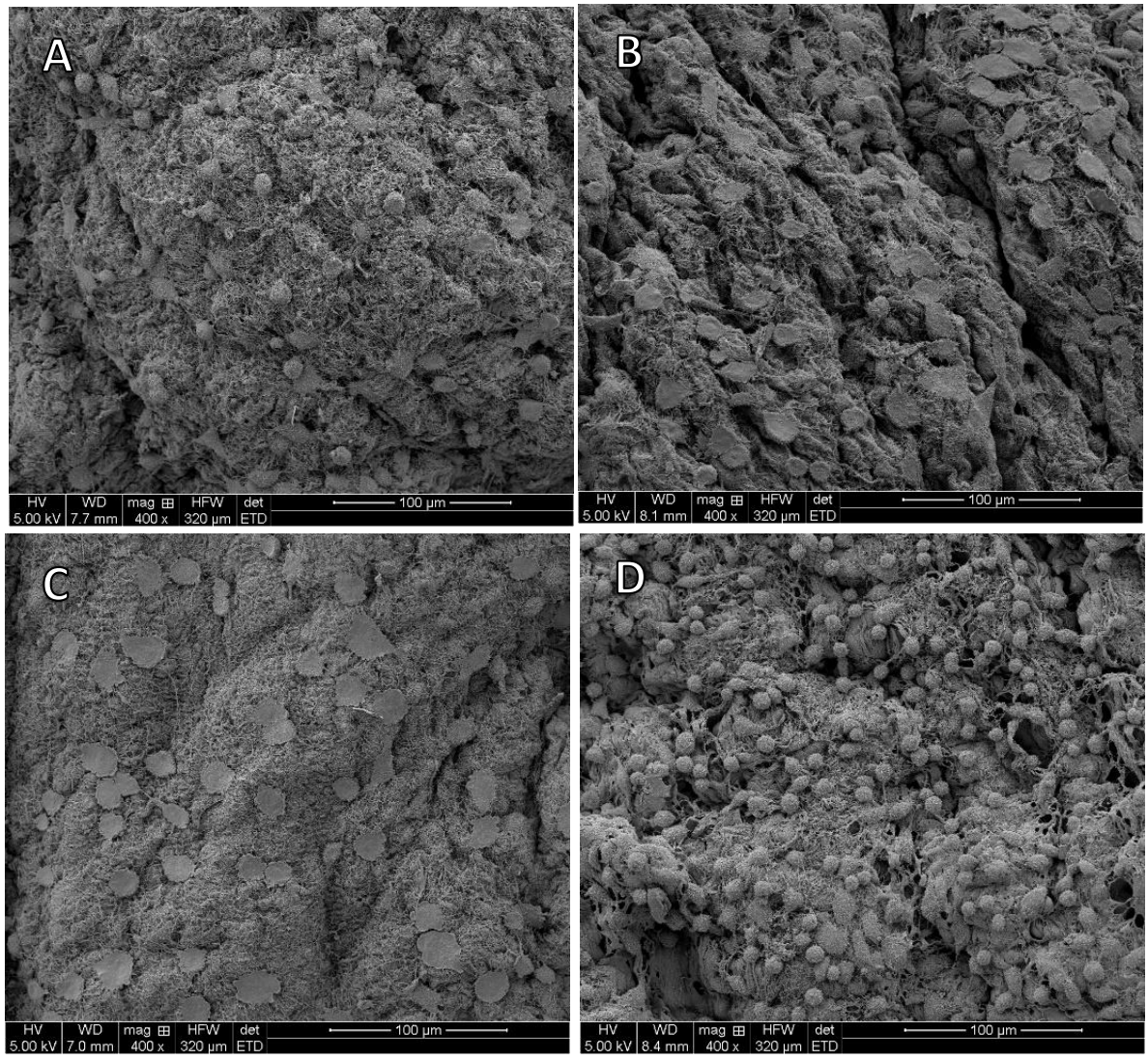

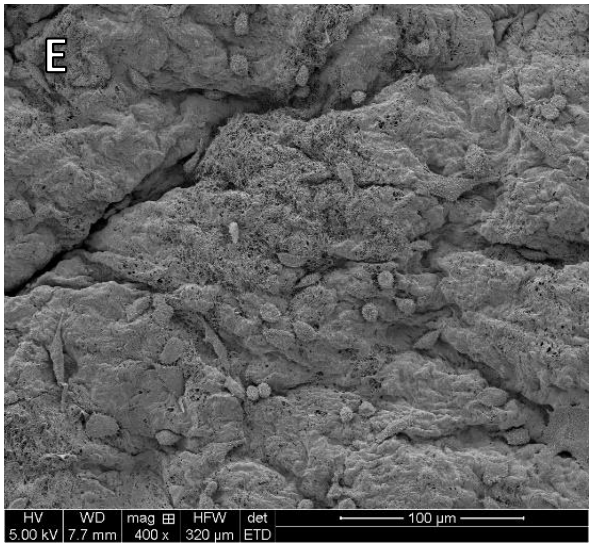
E
HV 5.00 kV
WD 7.7 mm
mag 400 x
HFW 320 µm
det ETD
100 µm

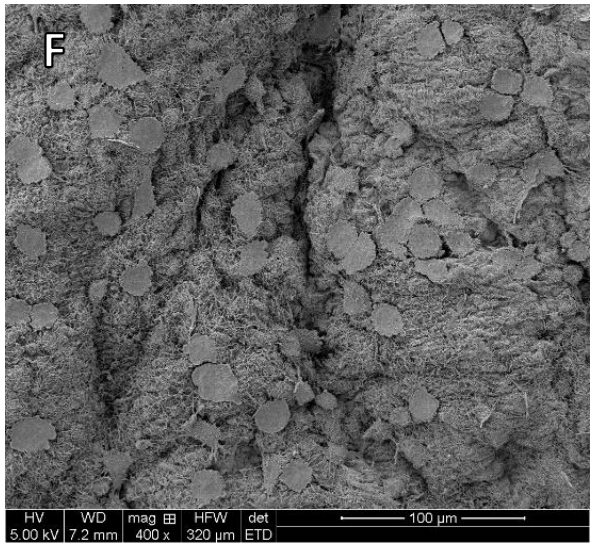
F
HV 5.00 kV
WD 7.2 mm
mag 400 x
HFW 320 µm
det ETD
100 µm

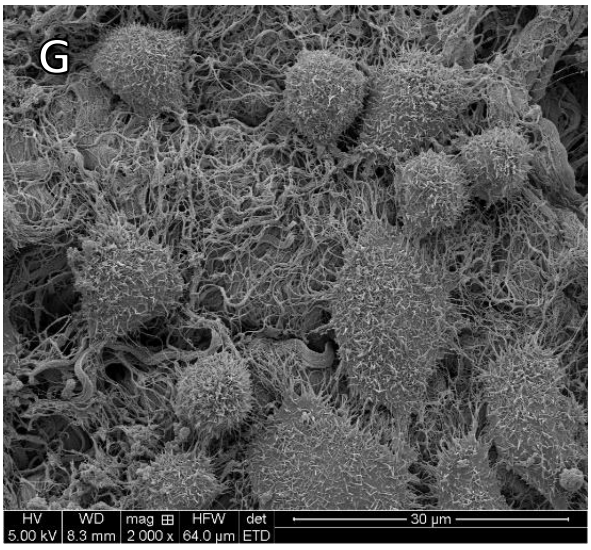
G
HV 5.00 kV
WD 8.3 mm
mag 2 000 x
HFW 64.0 µm
det ETD
30 µm

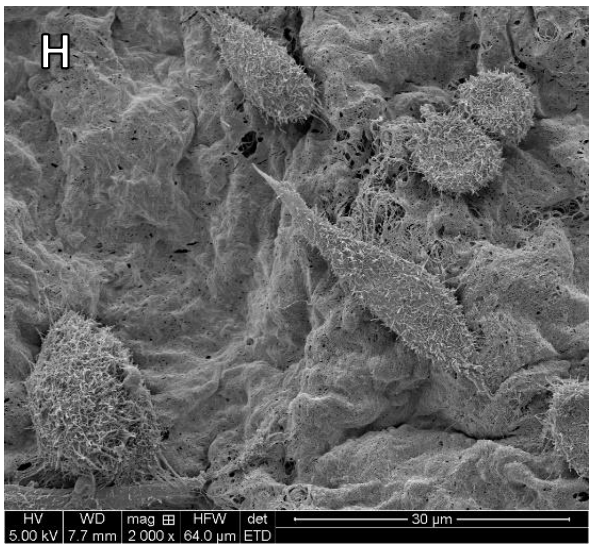
H
HV 5.00 kV
WD 7.7 mm
mag 2 000 x
HFW 64.0 µm
det ETD
30 µm

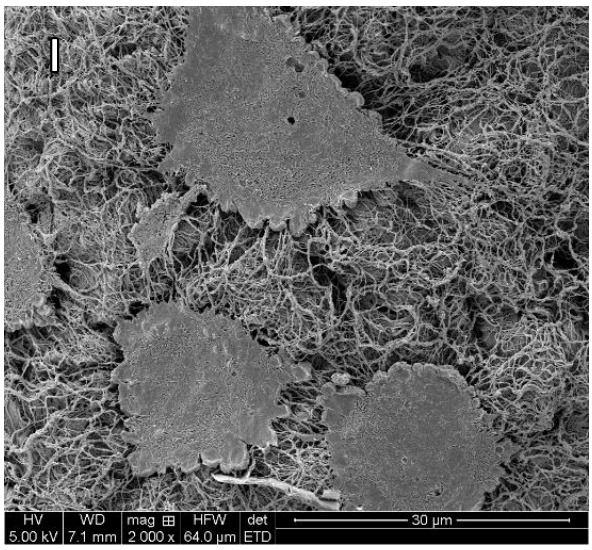
I
HV 5.00 kV
WD 7.1 mm
mag 2 000 x
HFW 64.0 µm
det ETD
30 µm

Figure 4.4: Scanning electron microscopy images taken 1 and 3 days after fibroblasts were plated on the of the scaffold. A. Uncrosslinked samples plated for 1 day. B. 24-hour crosslinking with 3 mM genipin and 20 nm gold nanoparticles plated for 1 day C. 24-hour crosslinking with 3 mM genipin plated for 1 day without nanoparticles. D and G. Uncrosslinked samples plated for 3 days. E and H. 24-hour crosslinking with 3 mM genipin and 20 nm gold nanoparticles plated for 3 days. F and I. 24-hour crosslinking with 3 mM genipin without nanoparticles plated for 3 days. Images G, H, and I feature the same treatment type as D, F, and E respectively, but with increased magnification for clarity.

4.5 Discussion

Genipin was first utilized as a crosslinker in 1988 and since then its use has been studied for a wide array of applications [29]. In materials as diverse as the trachea, pericardium, cartilage, chitosan and gelatin gels, genipin has been successfully utilized to increase the mechanical strength and reduce antigenicity [8, 30-33]. Our study correlates with others on the ability of genipin to attach functionalized AuNPs to the tissue. The results of the study demonstrated the ability of genipin to conjugate gold nanoparticles to a decellularized porcine tissue scaffold while also maintaining good biocompatibility. The gold nanoparticles, functionalized with amino groups, allowed the genipin to

covalently cross-link between the amino residues on the nanoparticles and the amino groups on the tissue. The modified cyclic form of genipin resides stably within the extracellular collagen matrix adding bridges from adjacent fibers to the functionalized AuNPs [34].

The NAA results demonstrated a correlation between the crosslinking time and the amount of AuNPs attached to the scaffold. An interesting result is noted in that there is an increase in the amount of AuNPs from 15 minutes to the 4 hour immersion times. However, there is no significant increase from the 4 hour to 8 hour time point followed by a significant increase at 24 hours. These biphasic results can be explained via the mechanism of genipin crosslinking. As explained by Butler et al., genipin crosslinking occurs via two separate reactions involving different sites on the genipin molecule. The first reaction is a nucleophilic attack of the genipin C3 carbon atom from a primary amine group which occurs almost immediately. The second slower reaction is the nucleophilic substitution of genipin's ester group to form a secondary amide [34]. The results clearly demonstrated genipin's biphasic reaction. In addition, the results also demonstrated that the functionalized AuNPs will bind to the tissue without the use of a crosslinker; however, the amount is significantly lower.

The DSC results provided additional confirmation on the binding ability of genipin. As shown in Figure 4.1, genipin demonstrated

higher denaturation temperatures with the increased crosslinking times (15 minutes vs 24 hours) and with the higher genipin concentration (3 mM vs 10 mM). The results also demonstrated the "two stage" binding ability of genipin in which the 4 hr and 8 hr crosslinking times displayed very similar denaturation temperatures. These results correlated with what other researchers reported. L. Bi et al. utilized genipin to crosslink a collagen chitosan scaffold. The results showed that the longer crosslinking times and higher genipin concentrations led to increased mechanical strength in their scaffold. However, it was also seen that when genipin concentrations reached above 1% (w/v) the mechanical strength decreased [35].

Our biocompatibility results demonstrated that genipin is not cytotoxic as confirmed by previous results [36]. To the contrary, the scaffolds with longer incubation times showed both an increase in cell numbers (Figure 4.3) and cell proliferation (Figure 4.2) when compared to untreated samples. We saw this result with or without the addition of the AuNPs meaning the genipin alone is associated with this increased cell growth. The enhanced cellular viability was demonstrated almost immediately with both biocompatibility assays showing a difference between the controls and the genipin treated scaffolds as early as 24 hours after plating the cells. This led us to believe the enhanced cellular capabilities are the results of improved

cell adhesion. To confirm this, SEM images were acquired at day 1 and day 3 after the scaffolds were plated with fibroblast cells. The cell plated on the scaffolds crosslinked with genipin alone are undoubtedly flusher to the scaffold than the other two treatment types. The treatment of genipin allows the cells to more quickly adhere and regain their spindle like appearance in comparison to the scaffolds left uncrosslinked or the scaffolds treated with genipin and gold.

Cell adhesion is a dynamic process involving interactions between cell cytoskeleton, extracellular matrix proteins, and peripheral membrane proteins. These adhesion protein complexes are crucial for the assembly of individual cells into the three-dimensional tissues and play an important role in further cell proliferation, viability, and differentiation [37]. It is well documented that physical surface properties, including stiffness, can significantly influence cell attachment. Forces generated by the cytoskeleton are applied to membrane attachment sites. This can deform materials that lack a degree of stiffness but cannot move an attachment site on a rigid surface. Consequently, cell morphology and functions hinge on substrate stiffness [38]. Gao et al. previously found that the use of genipin crosslinking increased surface roughness and stiffness on a hydrogel surface. This in turn resulted in better cell attachment, and better cell adhesion was associated with higher cell viability and

proliferation [39]. As shown in Figure 4.2, there was an abrupt increase in 10 days 24 hr Gen and 24 hr Au Gen samples. In correlation, the DSC results showed the samples immersed in the genipin solution for 24 hours had a higher degree of crosslinking. This crosslinking most likely resulted in increased scaffold stiffness, and this may have contributed to the increased cell growth at 24 hours as shown in Figure 4.2.

There is evidence that the improved cell attachment may be the result of direct genipin interactions with the cells. The switch from spherical to flattened shapes was not only demonstrated on the fibroblasts growing on the scaffolds, but this phenomenon was also witnessed in the cells attached to the well plate directly adjacent to the scaffolds crosslinked with genipin for 24 hours. This is most likely the result of leaching of genipin, or other products of the crosslinking reaction, from the scaffold to the nearby cells. The exact mechanism for this is unclear, and there were no other cases of this phenomena cited in the literature. To the contrary, Wang et al. hypothesized that genipin may impair cell adhesion as it halved the mRNA expression of essential cell adhesion protein integrin β1 in chondrocytes [40]. However, our results clearly demonstrate genipin supporting fibroblasts as they attach, spread out, and flatten both on the scaffold and neighboring to it.

4.6 Conclusions

In this study, genipin was evaluated for its ability to attach gold nanoparticles to a decellularized porcine tendon scaffold. Genipin was able to attach gold levels equivalent to previously used methods in as little as 15 minutes. We also found cysteamine conjugated gold nanoparticles will attach to decellularized tissue without the use of any other compounds. The use of genipin resulted in no signs of cytotoxicity and instead accelerated cell attachment and growth when crosslinked for 24 hours. Based on these results genipin and gold nanoparticles can be used on tendon and ligament allografts to potentially decrease inflammation, improve cellular integration, and delay degradation. Our work focused on tendon tissue, but as genipin will bind to any amine group, there is no foreseeable reason why this would not also work on any type of decellularized tissue graft with similar results.

4.7 Acknowledgments

This research was sponsored in part by the University of Missouri Enhanced Infrastructure for Biomedical Researchers Using Animal Models Grant and the University of Missouri Department of Biomedical, Biological, Chemical Engineering. The authors would like to thank Sherrie Neff and Justin Wilson for all their help.

4.8 References

1. Crapo, P.M., T.W. Gilbert, and S.F. Badylak, *An overview of tissue and whole organ decellularization processes.* Biomaterials, 2011. **32**(12): p. 3233-3243.

2. Ott, H.C., et al., *Perfusion-decellularized matrix: using nature's platform to engineer a bioartificial heart.* Nature medicine, 2008. **14**(2): p. 213.

3. Petersen, T.H., et al., *Tissue-engineered lungs for in vivo implantation.* Science, 2010. **329**(5991): p. 538-541.

4. Uygun, B.E., et al., *Organ reengineering through development of a transplantable recellularized liver graft using decellularized liver matrix.* Nature medicine, 2010. **16**(7): p. 814.

5. Londono, R. and S.F. Badylak, *Biologic Scaffolds for Regenerative Medicine: Mechanisms of In vivo Remodeling.* Annals of Biomedical Engineering, 2015. **43**(3): p. 577-592.

6. Gilbert, T.W., T.L. Sellaro, and S.F. Badylak, *Decellularization of tissues and organs.* Biomaterials, 2006. **27**(19): p. 3675-3683.

7. Whitlock, P.W., et al., *A naturally derived, cytocompatible, and architecturally optimized scaffold for tendon and ligament regeneration.* Biomaterials, 2007. **28**(29): p. 4321-4329.

8. Wang, Y., et al., *Genipin crosslinking reduced the immunogenicity of xenogeneic decellularized porcine whole-liver matrices through regulation of immune cell proliferation and polarization.* Scientific reports, 2016. **6**: p. 24779.

9. Partington, L., et al., *Biochemical changes caused by decellularization may compromise mechanical integrity of tracheal scaffolds.* Acta biomaterialia, 2013. **9**(2): p. 5251-5261.

10. Jackson, D.W., J. Corsetti, and T.M. Simon, *Biologic incorporation of allograft anterior cruciate ligament replacements.* Clinical orthopaedics and related research, 1996. **324**: p. 126-133.

11. Norton, S., *A brief history of potable gold.* Molecular interventions, 2008. **8**(3): p. 120.

12. Ionita, P., F. Spafiu, and C. Ghica, *Dual behavior of gold nanoparticles, as generators and scavengers for free radicals.* Journal of materials science, 2008. **43**(19): p. 6571-6574.

13. BarathManiKanth, S., et al., *Anti-oxidant effect of gold nanoparticles restrains hyperglycemic conditions in diabetic mice.* Journal of nanobiotechnology, 2010. **8**(1): p. 16.

14. Hsu, S.-h., C.-M. Tang, and H.-J. Tseng, *Gold nanoparticles induce surface morphological transformation in polyurethane and affect the cellular response.* Biomacromolecules, 2007. **9**(1): p. 241-248.

15. Grant, S.A., et al., *Assessment of the biocompatibility and stability of a gold nanoparticle collagen bioscaffold.* Journal of Biomedical Materials Research Part A, 2014. **102**(2): p. 332-339.

16. Christenson, E.M., et al., *Nanobiomaterial applications in orthopedics.* Journal of Orthopaedic Research, 2007. **25**(1): p. 11-22.

17. Yi, C., et al., *Gold nanoparticles promote osteogenic differentiation of mesenchymal stem cells through p38 MAPK pathway.* Acs Nano, 2010. **4**(11): p. 6439-6448.

18. Heo, D.N., et al., *Enhanced bone regeneration with a gold nanoparticle–hydrogel complex.* Journal of Materials Chemistry B, 2014. **2**(11): p. 1584-1593.

19. Yang, C., *Enhanced physicochemical properties of collagen by using EDC/NHS-crosslinking.* Bulletin of Materials Science, 2012. **35**(5): p. 913-918.

20. Nishi, C., N. Nakajima, and Y. Ikada, *In vitro evaluation of cytotoxicity of diepoxy compounds used for biomaterial modification.* Journal of Biomedical Materials Research Part A, 1995. **29**(7): p. 829-834.

21. Sperling, R.A., et al., *Biological applications of gold nanoparticles.* Chemical Society Reviews, 2008. **37**(9): p. 1896-1908.

22. Deeken, C., et al., *Assessment of the biocompatibility of two novel, bionanocomposite scaffolds in a rodent model.* Journal of

Biomedical Materials Research Part B: Applied Biomaterials, 2011. **96**(2): p. 351-359.

23. Yoo, J.S., et al., *Study on genipin: a new alternative natural crosslinking agent for fixing heterograft tissue.* The Korean journal of thoracic and cardiovascular surgery, 2011. **44**(3): p. 197.

24. Sung, H.W., et al., *Feasibility study of a natural crosslinking reagent for biological tissue fixation.* Journal of Biomedical Materials Research Part A, 1998. **42**(4): p. 560-567.

25. Koo, H.-J., et al., *Anti-inflammatory evaluation of gardenia extract, geniposide and genipin.* Journal of ethnopharmacology, 2006. **103**(3): p. 496-500.

26. Nam, K.N., et al., *Genipin inhibits the inflammatory response of rat brain microglial cells.* International immunopharmacology, 2010. **10**(4): p. 493-499.

27. Deeken, C., et al., *Method of preparing a decellularized porcine tendon using tributyl phosphate.* Journal of Biomedical Materials Research Part B: Applied Biomaterials, 2011. **96**(2): p. 199-206.

28. Leonavičienė, L., et al., *Effect of gold nanoparticles in the treatment of established collagen arthritis in rats.* Medicina, 2012. **48**(2): p. 16.

29. Fujikawa, S., S. Nakamura, and K. Koga, *Genipin, a new type of protein crosslinking reagent from gardenia fruits.* Agricultural and Biological Chemistry, 1988. **52**(3): p. 869-870.

30. Lima, E.G., et al., *Genipin enhances the mechanical properties of tissue-engineered cartilage and protects against inflammatory degradation when used as a medium supplement.* Journal of Biomedical Materials Research Part A: An Official Journal of The Society for Biomaterials, The Japanese Society for Biomaterials, and The Australian Society for Biomaterials and the Korean Society for Biomaterials, 2009. **91**(3): p. 692-700.

31. Haag, J., et al., *Biomechanical and angiogenic properties of tissue-engineered rat trachea using genipin cross-linked decellularized tissue.* Biomaterials, 2012. **33**(3): p. 780-9.

32. Sung, H.W., et al., *Crosslinking characteristics and mechanical properties of a bovine pericardium fixed with a naturally*

occurring crosslinking agent. Journal of biomedical materials research, 1999. **47**(2): p. 116-126.

33. Gattazzo, F., et al., *Gelatin–genipin-based biomaterials for skeletal muscle tissue engineering.* Journal of Biomedical Materials Research Part B: Applied Biomaterials, 2018.

34. Butler, M.F., Y.F. Ng, and P.D. Pudney, *Mechanism and kinetics of the crosslinking reaction between biopolymers containing primary amine groups and genipin.* Journal of Polymer Science Part A: Polymer Chemistry, 2003. **41**(24): p. 3941-3953.

35. Bi, L., et al., *Effects of different cross-linking conditions on the properties of genipin-cross-linked chitosan/collagen scaffolds for cartilage tissue engineering.* Journal of Materials Science: Materials in Medicine, 2011. **22**(1): p. 51-62.

36. Sung, H.W., et al., *Evaluation of gelatin hydrogel crosslinked with various crosslinking agents as bioadhesives: in vitro study.* Journal of Biomedical Materials Research: An Official Journal of The Society for Biomaterials, The Japanese Society for Biomaterials, and The Australian Society for Biomaterials and the Korean Society for Biomaterials, 1999. **46**(4): p. 520-530.

37. Gumbiner, B.M., *Cell adhesion: the molecular basis of tissue architecture and morphogenesis.* Cell, 1996. **84**(3): p. 345-357.

38. Yeung, T., et al., *Effects of substrate stiffness on cell morphology, cytoskeletal structure, and adhesion.* Cell motility and the cytoskeleton, 2005. **60**(1): p. 24-34.

39. Gao, L., et al., *Effects of genipin cross-linking of chitosan hydrogels on cellular adhesion and viability.* Colloids and Surfaces B: Biointerfaces, 2014. **117**: p. 398-405.

40. Wang, C., et al., *Cytocompatibility study of a natural biomaterial crosslinker—Genipin with therapeutic model cells.* Journal of Biomedical Materials Research Part B: Applied Biomaterials, 2011. **97**(1): p. 58-65.

Chapter 5

GENIPIN ATTACHMENT OF GOLD NANOPARTICLES TO AUTOGRAFT TISSUE

5.1 Abstract

The majority of ACL reconstructions in the world use autograft tissue to replace the torn ligament. While the surgery has good success in returning patients to activity, in the long term many patients develop osteoarthritis (OA). The challenge is how to prevent and/or mitigate the progression of OA. Gold nanoparticles (AuNPs) are a potential solution as they've been shown to act as an anti-inflammatory agent. Genipin was utilized and examined as a method for attaching AuNPs to freshly harvested porcine diaphragm tendon. The results demonstrated the AuNPs was successfully conjugated to the cellular tissue and the tissue appeared to be undamaged with no noticeable structural changes as noted via histology. However, the amount of gold conjugated to the cellular tissues was significantly less than on decellularized tissue. This indicates that the cells may be blocking some of the conjugation sites and that higher concentrations of AuNP or genipin may be needed to achieve a similar level of AuNP conjugation.

5.2 Introduction

Anterior cruciate ligament (ACL) tears are becoming increasingly common and surgical repair has now become routine. Every year, at least 50,000 procedures are performed in the United States alone [1]. The gold standard in ACL reconstruction has been the patellar tendon graft from the middle third of the patella tendon [2]. This surgery decreases clinical instability of the knee joint, reduces knee laxity, and decreases risk of late meniscus tear and surgery [3-5]. However, despite excellent return of function and a high rate of immediate success, patellar tendon graft reconstruction is not without faults. About 40% to 60% of patients will experience persistent morbidities in the affected knee such as tenderness, anterior knee pain, disturbance in anterior knee sensitivity, and the inability to kneel and knee-walk [6]. In addition, ACL injuries greatly increase a patient's risk of early onset osteoarthritis and ACL reconstruction surgery does not decrease the incidence [7, 8].

Gold nanoparticles (AuNPs) have the potential to improve patient outcomes following ACL reconstruction. One mechanism for this is AuNPs' well studied anti-inflammatory properties. AuNPs interfere with the transmission of inflammatory signaling and act as immunosuppressants [9, 10]. The exact mechanism for AuNPs in incompletely understood but it appears to be multifactored. One

mechanism is AuNPs' ability to scavenge free radicals and inhibit of reactive oxygen species formation. BarathManiKanth et al. [11] studied this in diabetes induced mice. AUNPs inhibited the reactive oxygen species generation at hyperglycemic conditions and the scavenging of free radicals further increased the capabilities of the body's antioxidant defense enzymes. The other major mechanism for AuNPs anti-inflammatory properties is their ability to inhibit the expression of NF-κB and subsequent inflammatory reactions. AuNPs block NF-κB activation by interacting with cys-179 of IKK-β and inhibiting the production of pro-inflammatory cytokines, such as TNF-α and IL-1β [12].

Genipin is the ideal method of the attachment of gold nanoparticles to autograft tissue. Genipin is a chemical compound extracted from the fruits of *Gardenia jasminoides*. It is a natural crosslinking agent, and it spontaneously reacts with amino-group-containing compounds such as proteins, collagens, and gelatins to form mono- to tetramer crosslinks [13]. Genipin is more biocompatible than other crosslinking agents, and the biocompatibility of genipin fixed biological tissue has been previously verified in a growing rat model [14, 15]. Because of its biocompatibility, genipin conjugated tissue do not need extensive washing unlike other chemical crosslinking agents. Thus it is feasible to conjugate AuNPs to

autografts / cellular tissue in the operating room. In addition, the genipin reaction occur almost immediately allowing it to be used in the short time period during an autograft ACL reconstruction surgery [16].

Our lab has already demonstrated the ability to attach gold nanoparticles to decellularized tissue using genipin. We hypothesize genipin will similarly attach AuNPs to non-decellularized tendon tissue. To test this hypothesis, porcine diaphragm tendon was collected and exposed to solutions containing 1) genipin and 20 nm AuNPs, or 2) 20 nm AuNPs alone for 15, 30 or 60 minutes. Gold levels were measured using neutron activation analysis (NAA), and visualized using scanning electron microscopy (SEM). The condition of the tissue and the cells was visualized using histology.

5.3 Materials and Methods

5.3.1 Tissue Harvest and Decellularization

Porcine diaphragms were harvested immediately following euthanasia after a laboratory exercise at the University of Missouri. The central tendon portion of the diaphragm was dissected from the surrounding muscle. The samples were then split into two groups. The sample allotted for the autograft group was put into phosphate-buffered saline (PBS) and 4.8 mm circular discs were cut approximately 12 hours later.

The groups allotted for the allograft was decellularized according to a previously published protocol [17]. The tissues were immersed in a tris buffer solution containing, 5 mM ethylenediaminetetraacetic acid (EDTA), 0.4 mM phenylmethylsulfonyl fluoride (PMSF), 0.2% (w/v) sodium azide and 1% (v/v) tri(n-butyl) phosphate (TnBP) (Sigma-Aldrich, St. Louis, MO) and subjected to continuous agitation on an orbital shaker at ambient temperature for 24 h. The 1% TnBP solution was removed after 24 h and exchanged with fresh solution, and the tissues were subjected to continuous agitation for an additional 24 h. This treatment was followed by a 24 h rinse with double distilled water and another 24 h rinse with 70% (v/v) ethyl alcohol, both with continuous agitation at ambient temperature. The 4.8 mm circular discs were cut from the decellularized diaphragm tendon and stored in 70% (v/v) ethanol at 4° C.

5.3.2 Conjugation of Gold

Genipin crosslinking was conducted by immersing the decellularized tissue into 1 ml of 5 mM genipin crosslinking solution. The genipin was dissolved using a minimal amount dimethyl sulfoxide and suspended in PBS. This was accompanied with 0.25 ml of 20 nm gold nanoparticles at a concentration of 7.0×10^{11} particles/ml. Nanoparticles were functionalized with amine groups by the addition of 0.001 mg/ml 2-mercaptoethyamine (MEA) to the nanoparticles. The

samples were crosslinked for timepoints ranging from 15 minutes, 30 minutes, or 1 hour and then were rinsed twice with PBS for 15 minutes.

The 20 nm AuNP tissue control samples were created using the same methodology with the exception that the genipin crosslinking solution was replaced with PBS.

5.3.3 Experimental Groups

15 minutes genipin and gold: 15 minutes of crosslinking with 0.25 ml of functionalized nanoparticles and 1 ml of 5 mM genipin.

15 minutes gold: 15 minutes of crosslinking with 0.25 ml of functionalized nanoparticles and 1 ml of PBS.

30 minutes genipin and gold: 30 minutes crosslinking with 0.25 ml of functionalized nanoparticles and 1 ml of 5 mM genipin.

30 minutes gold: 30 minutes of crosslinking with 0.25 ml of functionalized nanoparticles and 1 ml of PBS genipin.

1-hour genipin and gold: 1 hour of crosslinking with 0.25 ml of functionalized nanoparticles and 1 ml of 5 mM genipin.

1-hour gold: 1 hour of crosslinking with 0.25 ml of functionalized nanoparticles and 1 ml of PBS.

The shorter timepoints were chosen to reflect the short conjugation time available for processing an autograft tendon in the operating room.

5.3.4 Histology

Histology was conducted to visualize the autograft scaffold following genipin crosslinking. The scaffolds were examined for changes in the tissue or alterations to the cells. Following crosslinking three samples were placed in 10% neutral buffered formalin for 24 hours (N=3). The samples were embedded in paraffin and sectioned on a microtome. The slides were stained with hematoxylin and eosin.

5.3.5 Scanning Electron Microscopy

SEM was conducted to visualize the presence of gold nanoparticles on our tissue scaffolds and to look for the presence of clumping within the particles. Following crosslinking, 2 samples were prepared for fixation in 0.1M cacodylate buffer containing 2% glutaraldehyde and 2% paraformaldehyde (N=2). Samples were critically point dried and examined using a FEI Quanta 600F Environmental SEM.

5.3.6 Neutron Activation Analysis

Neutron Activation Analysis (NAA) was utilized to quantify the gold levels in the tissue scaffolds. Following crosslinking, five samples

of each treatment type (N=5) were lyophilized, weighed, and packed into high density polyethylene NAA vials. Both the autograft and allograft samples were utilized for this study in order to compare any potential differences in gold levels.

At the University of Missouri Research Reactor, the samples were loaded into a rabbit system with Au comparator standards and irradiated for 120 seconds in a thermal neutron flux of $5.0x10^{13}$ n/cm2/s. The 197Au captures a neutron to produce the radio-isotope 198Au with a 2.7 d half-life. The samples were allowed to decay for 1-7 hours and then counted for 10 minutes each using a high purity Ge detector controlled by Canberra Genie 2000 software. The detector dead-time was less than 5% for all samples.

5.3.7 Statistical Analysis

GraphPad Prism 8.0.1 (GraphPad Software, San Diego, CA) was used to analyze experimental data. One-way analysis of variance was conducted followed by a Tukey-Kramer post-test to determine significant differences between means of the experimental groups. The results were considered statistically significant where P was less than 0.05.

5.4 Results

5.4.1 Histology

Histology results show the presence of intact tendon fibers and cells for all time points with and without the addition of the genipin. However, there does appear to be minor separation of the fibers with the 1-hour conjugation times with and without the use of genipin. This is visible in Figures 4.1 and 4.2.

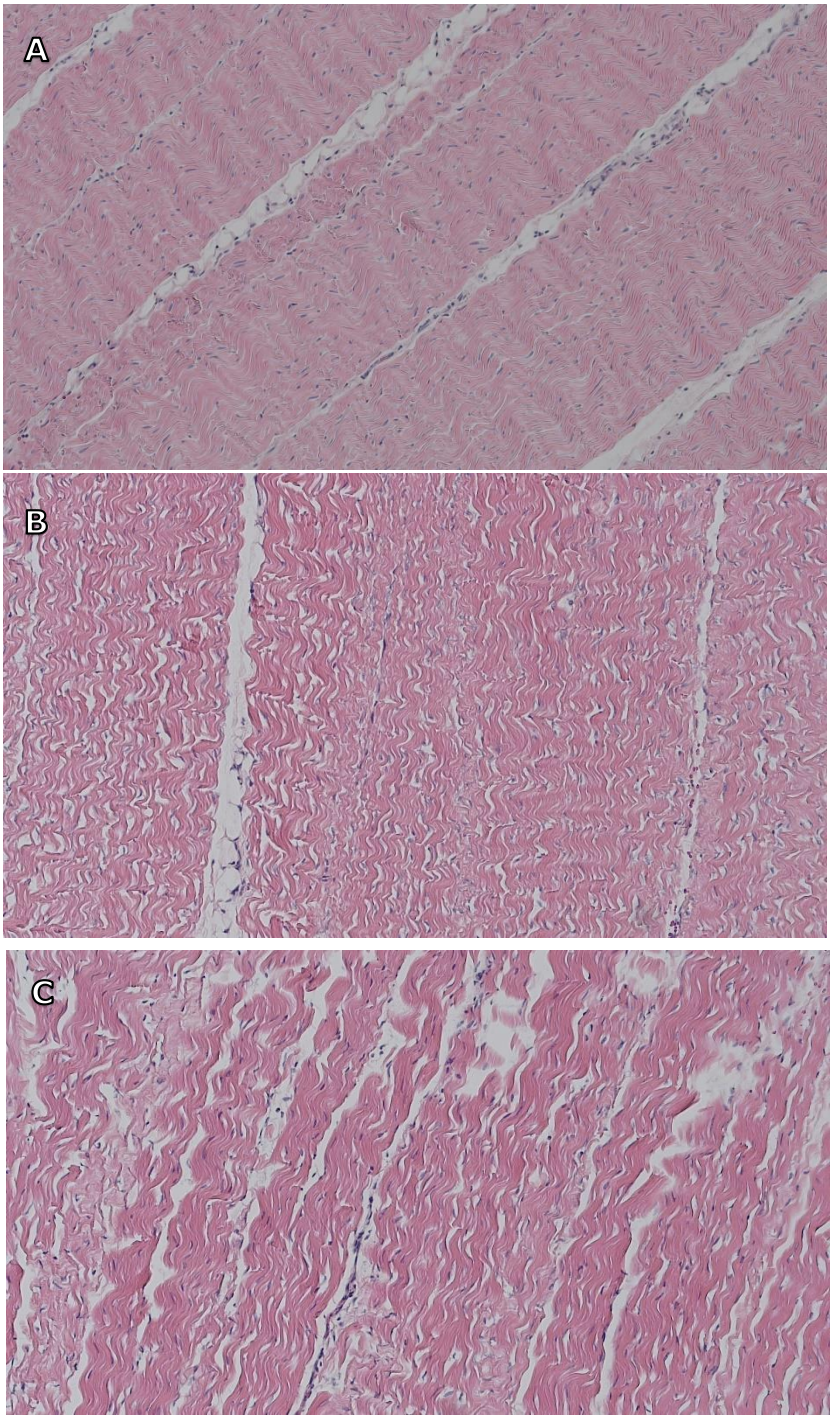

Figure 5.1 Histologic images of intact autograft scaffolds conjugated with gold nanoparticles and genipin, H&E staining at 100x.

A) 15 minutes conjugation time.

B) 30 minutes conjugation time.

C) 1-hour conjugation time.

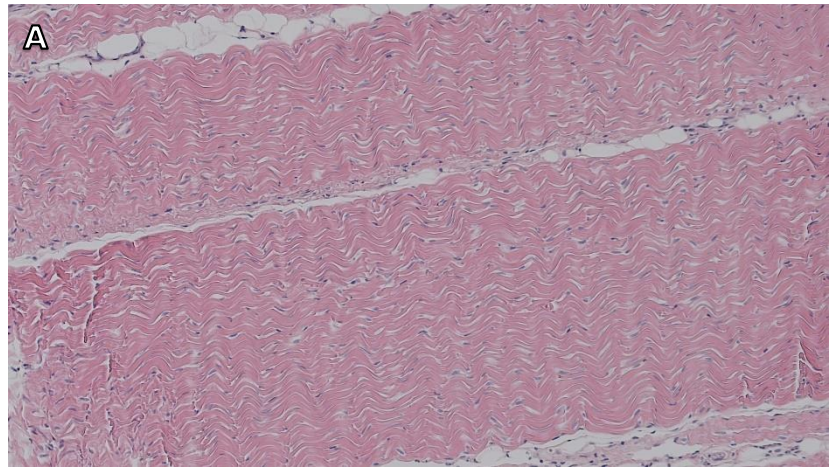

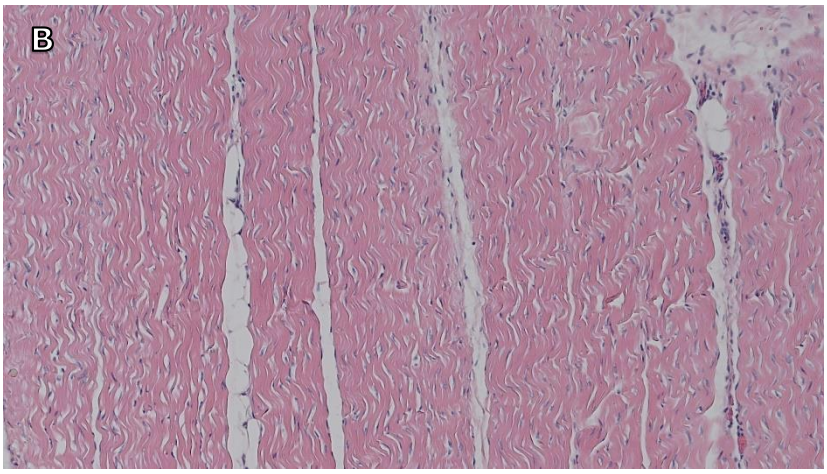

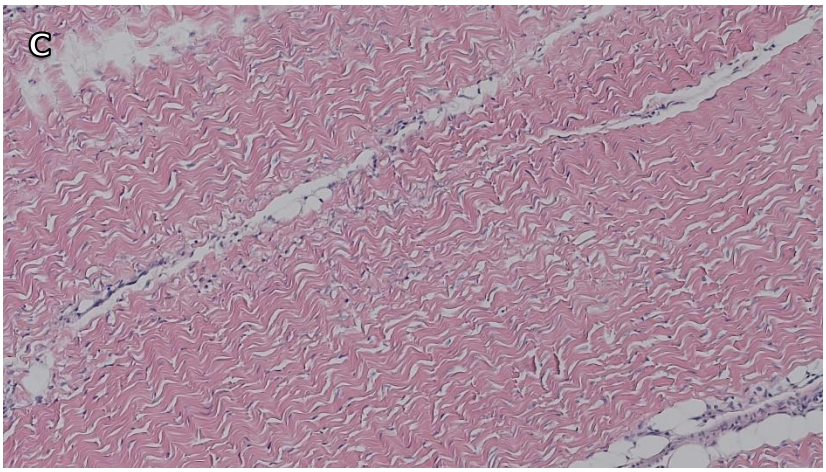

Figure 5.2 Histologic images of intact autograft scaffolds conjugated with gold nanoparticles without the use of genipin, H&E staining at 100x.

A) 15 minutes conjugation time.

B) 30 minutes conjugation time.

C) 1-hour conjugation time.

5.4.2 Scanning Electron Microscopy

Figure 5.3 and Figure 5.4 show the SEM images for the autograft scaffolds conjugated with and without the use of genipin. The SEM images clearly show the presence of gold on all of the scaffolds. There is no visible difference between the amount or distribution of gold found in the samples with or without the use of genipin. For both the scaffolds conjugated with genipin and with nanoparticles only, there are signs of the nanoparticles clumping with the 1-hour time point. This is most apparent in the samples with genipin and can be clearly seen in Figure 5.3 F.

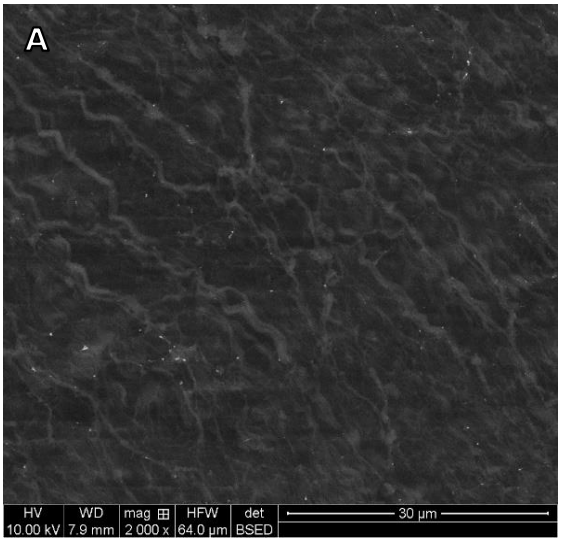
A
HV
10.00 kV
WD
7.9 mm
mag
2 000 x
HFW
64.0 µm
det
BSED
30 µm

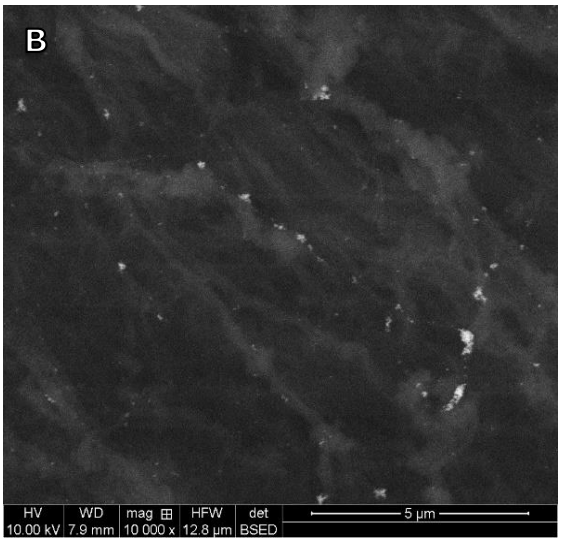
B
HV
10.00 kV
WD
7.9 mm
mag
10 000 x
HFW
12.8 µm
det
BSED
5 µm

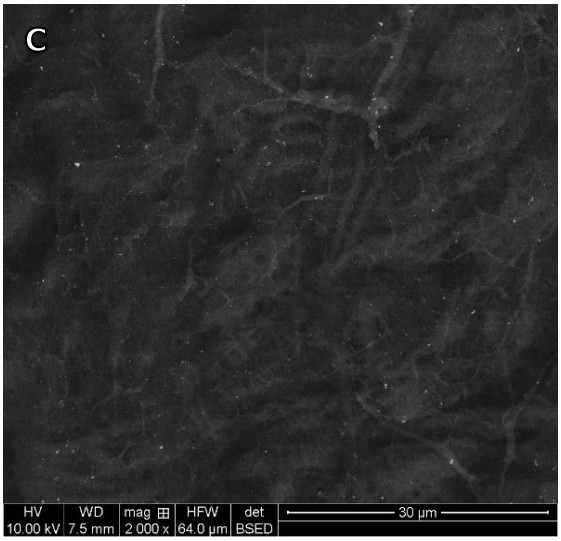
C
HV
10.00 kV
WD
7.5 mm
mag
2 000 x
HFW
64.0 µm
det
BSED
30 µm

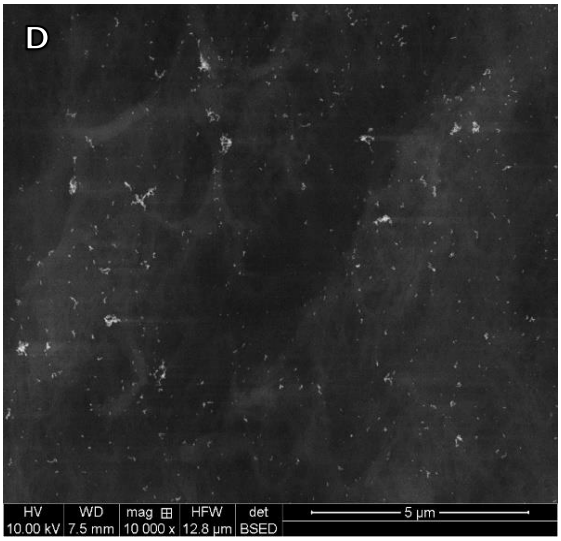
D
HV
10.00 kV
WD
7.5 mm
mag
10 000 x
HFW
12.8 µm
det
BSED
5 µm

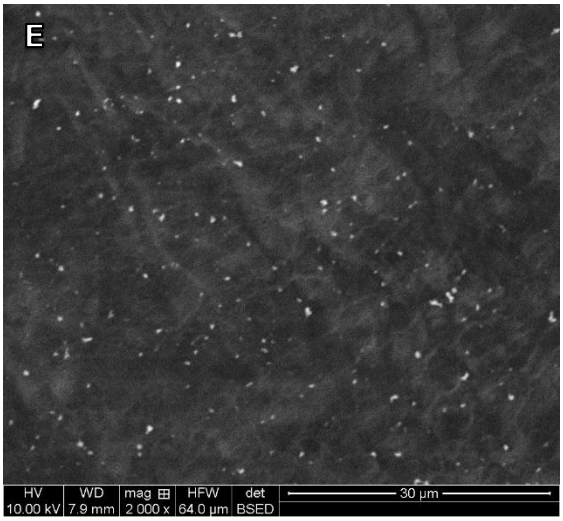
E
HV
10.00 kV
WD
7.9 mm
mag
2 000 x
HFW
64.0 µm
det
BSED
30 µm

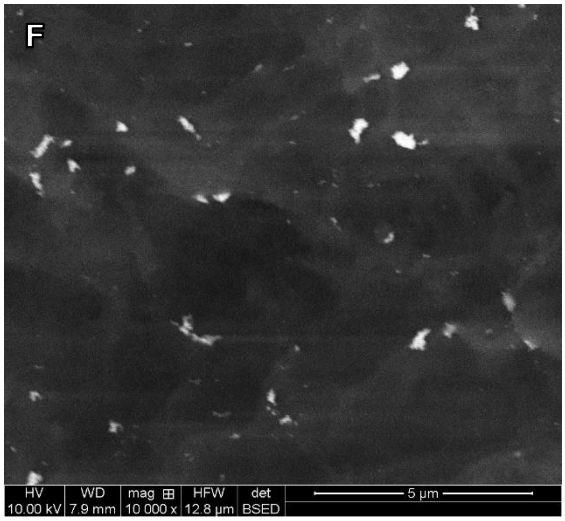
F
HV
10.00 kV
WD
7.9 mm
mag
10 000 x
HFW
12.8 µm
det
BSED
5 µm

Figure 5.3 Scanning electron micrograph imaging 20 nm AuNP crosslinked autograft scaffolds using genipin.

A, B) 15 minutes conjugation time

C, D) 30 minutes conjugation time

E, F) 1-hour conjugation time

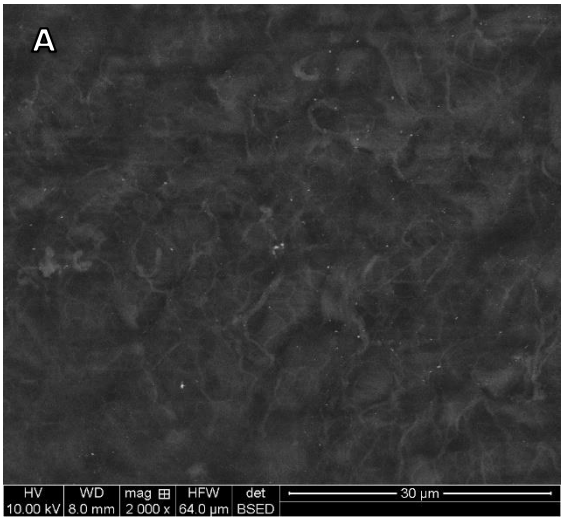
A
HV
10.00 kV
WD
8.0 mm
mag
2 000 x
HFW
64.0 µm
det
BSED
30 µm

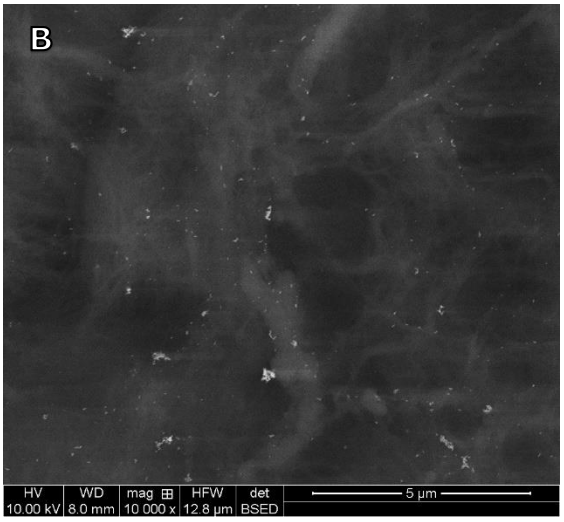
B
HV
10.00 kV
WD
8.0 mm
mag
10 000 x
HFW
12.8 µm
det
BSED
5 µm

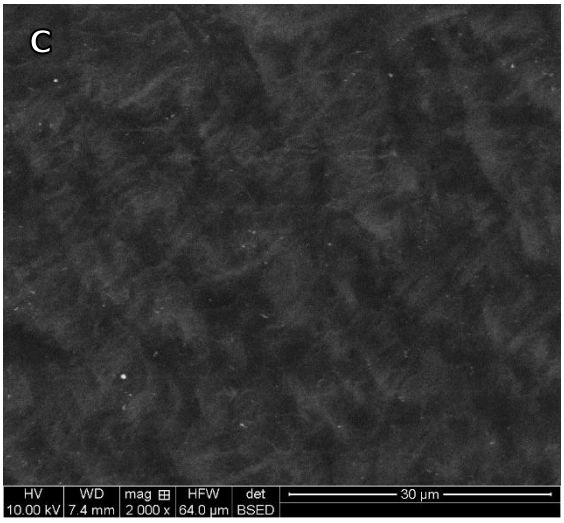
C
HV
10.00 kV
WD
7.4 mm
mag
2 000 x
HFW
64.0 µm
det
BSED
30 µm

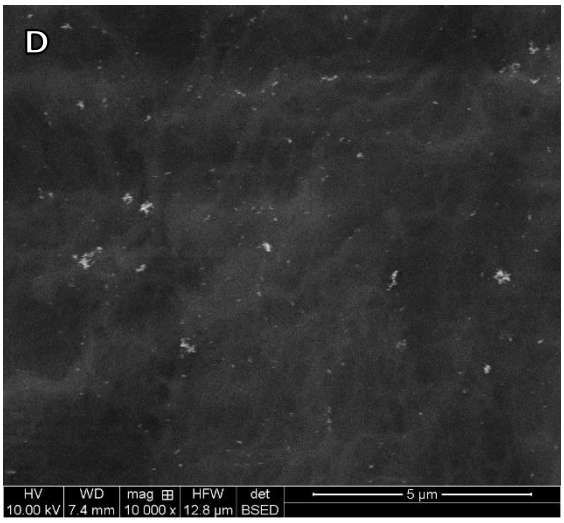
D
HV
10.00 kV
WD
7.4 mm
mag
10 000 x
HFW
12.8 µm
det
BSED
5 µm

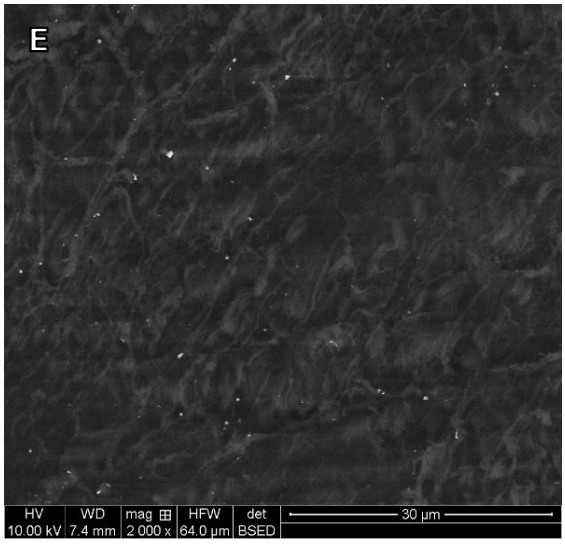
E
HV
10.00 kV
WD
7.4 mm
mag
2 000 x
HFW
64.0 µm
det
BSED
30 µm

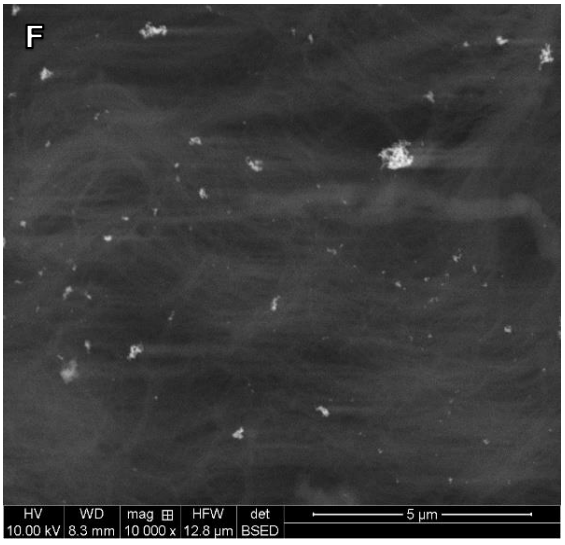
F
HV
10.00 kV
WD
8.3 mm
mag
10 000 x
HFW
12.8 µm
det
BSED
5 µm

Figure 5.4 Scanning electron micrograph imaging 20 nm AuNP crosslinked autograft scaffolds without the use of genipin.

A, B) 15 minutes conjugation

C, D) 30 minutes conjugation time

E, F) 1-hour conjugation time

5.4.3 Neutron Activation Analysis

NAA results demostrated successful attachment of the gold to all tissue types. However, the non-decellularized autograft had less gold nanoparticles attached than the decellularized allograft. This was true for samples conjugated with and without the use of genipin. The addition of genipin did not affect the level of gold concentration on the autograft tissue. The only sample with a statisical difference between tissue crosslinked with genipin versus functionalzied AuNPs alone was the 15 minute allograft sample. However, there was more gold when genipin was used in every case except 15 minute autgraft.

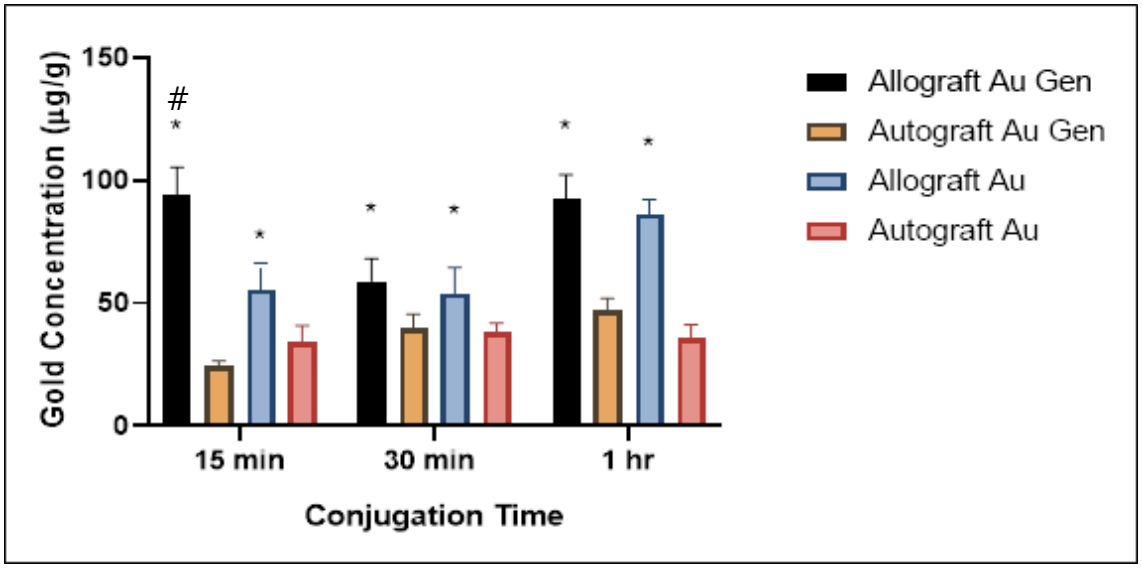

Figure 5.5 Neutron activation analysis data comparing the concentration of gold attached to decellularized tissue versus intact tissue with and without the use of genipin. * indicates significantly different from its autograft counterpart. # indicates significantly different with genipin versus with gold alone. Error bar show standard error of the mean.

5.5 Discussion

This study demonstrated the ability to attach AuNPs to intact diaphragm tendon. Both NAA and SEM images confirmed the presence of the AuNPs on the tissue scaffolds. As autografts are utilized for approximately 75% of ACL reconstructions, this study demonstrated the potential to greatly increase the number of patients that can utilize this technology [18].

The short conjugation times were chosen as a necessity to simulate the time period of an actual autograft ACL reconstruction surgery as the AuNPs will have to be conjugated to the autograft in the operating room while the patient is under. Of the time points chosen, the earlier timepoints appear to provide ideal results. The 15-minute and 30-minute timepoints did not demonstrate the clumping of the AuNPs as seen at the 60-minute timepoint. In addition, the tissue fibers may be more closely knit at the earlier timepoints, but this is difficult to conclusively stated due to the small amount of damage caused by simply punching the tissue. The tissue punchign may be the cause of the fiber separation. Further studies can be performed to determine the effects of the tissue punch. There also is not a significant difference between the concentration of AuNPs for the different time oints, so the one hour timepoint does not impart any advantages in terms of the amount of AuNPs conjugation.

There was a significant difference between the concentration of gold attached to the decellularized versus the intact tissue. This is likely the result of changes to the surface structure during decellularization. While our method for decellularization was chosen to effectively remove cellular components with minimal damage to the extracellular matrix, some minor tissue damage is probably inevitable. The damage would expose more carboxylic acid groups in the collagen

for the functionalized amine AuNPs to attach. In addition, the nanoparticles are likely able to penetrate further into the decellularized tissue without the intact cellular components inhibiting them, resulting in a higher amount of AuNPs conjugation. Future studies could include Focus Ion Beam (FIB) SEM to determine the AuNPs penetration into the tissue.

One byproduct of the genipin crosslinking reaction is the tissue samples will turn a shade of blue. The exact mechanism for this is not completely known, but when a genipin molecule interacts with an amino group a blue pigment is formed [19, 20]. This reaction has been proposed as a method of colorimetric detection of amino acids [21]. The intact tissue turned visibly bluer than the decellularized tissue. The genipin is likely reacting with the cellular components still present in the tissue. This may also contribute to the reason for the lower gold content in the intact tissue. The genipin is also reacting with the cellular component. If greater amounts of AuNPs are necessary, then a greater concentration of genipin may be utilized. It is also possible to increase the concentration of AuNPs, which we have already demonstrated can greatly increase the amount of gold attached.

5.6 Conclusion

This study demonstrated the attachment of gold nanoparticles to intact tendon tissue with or without the use of genipin. The time points 15, 30, and 60 minutes were tested with 15 and 30 minutes resulting in viable attachment without AuNPs clumping. The results did show that the amount of gold attached to intact tissue is less than that found on decellularized tissue. This could be due to a number of factors, including the less number of binding sites due to the presence of the cells. Histology demonstrated minimal damage to the tissue and cells. This method appears to be a viable method to attach AuNPs to cellular tissue. However, further studies are need in order to determine the ideal dosage of the AuNPs for achieving constructive remodeling while reducing inflammation.

5.7 References

1. Stapleton, T.R., *Complications in anterior cruciate ligament reconstructions with patellar tendon grafts.* Sports Medicine and Arthroscopy Review, 1997. **5**(2): p. 156.

2. Carmichael, J.R. and M.J. Cross, *Why bone–patella tendon–bone grafts should still be considered the gold standard for anterior cruciate ligament reconstruction.* British journal of sports medicine, 2009. **43**(5): p. 323-325.

3. Yamaguchi, S., et al., *Long term results of anterior cruciate ligament reconstruction with iliotibial tract: 6-, 13-, and 24-year longitudinal follow-up.* Knee Surgery, Sports Traumatology, Arthroscopy, 2006. **14**(11): p. 1094-1100.

4. Roe, J., et al., *A 7-year follow-up of patellar tendon and hamstring tendon grafts for arthroscopic anterior cruciate ligament reconstruction: differences and similarities.* The American journal of sports medicine, 2005. **33**(9): p. 1337-1345.

5. Spindler, K.P., et al., *Clinical outcome at a minimum of five years after reconstruction of the anterior cruciate ligament.* JBJS, 2005. **87**(8): p. 1673-1679.

6. Kartus, J., T. Movin, and J. Karlsson, *Donor-site morbidity and anterior knee problems after anterior cruciate ligament reconstruction using autografts.* Arthroscopy: The Journal of Arthroscopic & Related Surgery, 2001. **17**(9): p. 971-980.

7. Nebelung, W. and H. Wuschech, *Thirty-five years of follow-up of anterior cruciate ligament—deficient knees in high-level athletes.* Arthroscopy: The Journal of Arthroscopic & Related Surgery, 2005. **21**(6): p. 696-702.

8. Chalmers, P.N., et al., *Does ACL reconstruction alter natural history?: A systematic literature review of long-term outcomes.* JBJS, 2014. **96**(4): p. 292-300.

9. Paula, M.M., et al., *Gold nanoparticles and/or N-acetylcysteine mediate carrageenan-induced inflammation and oxidative stress in a concentration-dependent manner.* Journal of Biomedical Materials Research Part A, 2015. **103**(10): p. 3323-3330.

10. Chen, H., et al., *In Vivo Study of Spherical Gold Nanoparticles: Inflammatory Effects and Distribution in Mice.* PLoS ONE, 2013. **8**(2).

11. BarathManiKanth, S., et al., *Anti-oxidant effect of gold nanoparticles restrains hyperglycemic conditions in diabetic mice.* Journal of nanobiotechnology, 2010. **8**(1): p. 16.

12. Jeon, K.I., M.S. Byun, and D.M. Jue, *Gold compound auranofin inhibits IκB kinase (IKK) by modifying Cys-179 of IKKβ subunit.* Experimental and Molecular Medicine, 2003. **35**(2): p. 61-66.

13. Yoo, J.S., et al., *Study on genipin: a new alternative natural crosslinking agent for fixing heterograft tissue.* The Korean journal of thoracic and cardiovascular surgery, 2011. **44**(3): p. 197.

14. Sung, H.W., et al., *Feasibility study of a natural crosslinking reagent for biological tissue fixation.* Journal of Biomedical Materials Research Part A, 1998. **42**(4): p. 560-567.

15. Huang, L.L., et al., *Biocompatibility study of a biological tissue fixed with a naturally occurring crosslinking reagent.* Journal of Biomedical Materials Research Part A, 1998. **42**(4): p. 568-576.

16. Butler, M.F., Y.F. Ng, and P.D. Pudney, *Mechanism and kinetics of the crosslinking reaction between biopolymers containing primary amine groups and genipin.* Journal of Polymer Science Part A: Polymer Chemistry, 2003. **41**(24): p. 3941-3953.

17. Deeken, C., et al., *Assessment of the biocompatibility of two novel, bionanocomposite scaffolds in a rodent model.* Journal of Biomedical Materials Research Part B: Applied Biomaterials, 2011. **96**(2): p. 351-359.

18. Medicine, A.O.S.f.S., *Allografts for ACL reconstruction survey report*. 2014.

19. Park, J.E., et al., *Isolation and characterization of water-soluble intermediates of blue pigments transformed from geniposide of Gardenia jasminoides.* Journal of Agricultural and Food Chemistry, 2002. **50**(22): p. 6511-6514.

20. TOUYAMA, R., et al., *Studies on the blue pigments produced from genipin and methylamine. I. Structures of the brownish-red*

pigments, intermediates leading to the blue pigments. Chemical and Pharmaceutical Bulletin, 1994. **42**(3): p. 668-673.

21. Lee, S.-W., et al., *Colorimetric determination of amino acids using genipin from Gardenia jasminoides.* Analytica chimica acta, 2003. **480**(2): p. 267-274.

Chapter Six

THE USE OF GOLD NANOPARTICLES IN IMPROVING ACL GRAFT PERFORMANCE IN AN OVINE MODEL

6.1 Abstract

Roughly 200,000 Americans will require surgical repair of their anterior cruciate ligament (ACL) every year. There is an increased interest in allograft repairs with estimated 20% of all ACL reconstructions in the United States using cadaver tissue. Allografts are chosen to avoid donor site morbidity associated with autografts harvest, but they can also result in a prolonged inflammatory period and delayed graft remodeling when compared to autografts. Gold nanoparticles (AuNPs) are a potential solution to this problem as they interfere with the transmission of inflammatory signaling and act as immunosuppressants. Six sheep had their ACL surgically removed and replaced with a decellularized human gracilis tendon. The tendon was crosslinked with 2 mM 1-ethyl-3-[3-dimethylainopropyl]carbodiimide and 5 mM N-hydroxysuccinimide with or without the addition of 20 nm gold nanoparticles. The sheep were sacrificed 8 weeks after ACL reconstruction. Immediately following sacrifice, joint fluid was collected

for cytology. Semi-quantitative histological scoring of the bone tunnel portion and the intraarticular portion of the grafts were performed independently along with descriptive analysis of histologic changes and quantitative analysis of revascularization. The experimental grafts had better histological scores than the controls, and they exhibited decreased inflammation in the bone tunnel portion of the graft, the intraarticular portion of the graft, and in the synovial fluid cell count.

6.2 Introduction

Roughly 200,000 Americans will require surgical repair of their anterior cruciate ligament (ACL) every year [1]. A majority of ACL repairs today involve the use of an autograft, but there is an increased interest in allograft repairs with estimated 20% of all ACL reconstructions in the United States using cadaver tissue [2]. Allografts are chosen to avoid donor site morbidity associated with autografts harvest; morbidities include persistent pain at the harvest site and limited range of motion [3]. Allografts also have the advantage of being significantly more cost-effective [4]. Despite their growing popularity, there are still key factors limiting the use of allografts. Central amongst them is the prolonged graft remodeling and incorporation seen in allografts ligamentization [5].

Both allograft and autograft undergo a similar process of incorporation when implanted. There is graft necrosis with concurrent

cellular repopulation followed by revascularization and collagen remodeling [5]. However, animal studies have shown allografts have a prolonged inflammatory period, delayed graft remodeling, and fewer new collagen fibers six months after surgery [6]. This is also seen in human patients where MRI scans showed less vascularization in allografts than autografts, and human autopsy revealed allografts remained incompletely healed 3 years after surgery [7, 8]. This prolonged remodeling can lead to decreased mechanical strength of the graft and increased likelihood of graft failure [9, 10]. To alleviate some of the graft incorporation concerns, nanoparticles are currently being investigated as a new technique to enhance remodeling.

Gold nanoparticles (AuNPs) have numerous characteristics that may help reduce the challenge of graft assimilation. For example, AuNPs have long been used for their anti-inflammatory properties [11-13]. One mechanism for this is AuNPs' ability to scavenge free radicals and inhibit of reactive oxygen species formation. Haupenthal et al. [14] demonstrated gold nanoparticle injections into muscle reduced inflammation in a mouse muscular dystrophy model. The AuNPs' antioxidant potential reduced the production of reactive oxygen and reduced morphological changes induced by inflammation. Trauma from both the initial knee injury and the surgical repair have been shown to potentially cause a catabolic inflammatory cascade resulting in

abnormal tissue remodeling and damage in some patients [15]. Darabos et al. [16] demonstrated an increase in IL-beta after ACL reconstruction which is linked to bone resorption and osteolysis and can result in bone tunnel widening and greater knee laxity post-surgery. Administration of endogenous anti-inflammatory cytokines limited this effect.

AuNPs can also improve bone tunnel healing by promoting osteogenic differentiation of mesenchymal stem cells and inhibiting adipogenic differentiation [17]. Sul et al [18] demonstrated AuNPs accomplish this by activating the p38 mitogen-activated protein kinase pathway through interaction with proteins located in the cytoplasm and interfering with specific cellular signaling pathways. In addition, AuNP's antioxidant potential inhibits the formation of osteoclasts from bone marrow-derived macrophages by reducing the receptor activator of nuclear factor-kB ligand. All of these AuNPs' properties have the potential to accelerate intra-tunnel healing by supporting the necessary progressive bone ingrowth into the graft [19].

AuNPs can similarly improve graft ligamentization. Attachment of AuNPs modifies the surface structure of the graft and encouraging cellular attachment and proliferation [20, 21]. The increased surface energy of nanoparticles promotes attachment of proteins such as

fibronectin, vitronectin, laminin, and collagen which are necessary for cellular attachment [22].

This study investigated whether the presence of AuNPs conjugated to acellular human gracilis tendon will decrease inflammation and improve the graft remodeling outcomes. ACLs were reconstructed in 6 Polypay sheep using grafts conjugated with or without 20 nm AuNPs. After 8 weeks, cytology was performed on the joint fluid; the bone tunnel and intraarticular graft were each independently scored via histology for remodeling criteria and inflammation.

6.3 Materials and Methods

6.3.1 Experimental Design

The study protocol was approved by the Institutional Animal Care and Use Committee. All animals were obtained from a United States Department of Agriculture-licensed dealer and were cared for according to the standards of the National Institutes of Health. Six female skeletally 16 month old Polypay sheep were used in this study. Acellular human gracilis tendons were used to anatomically replace the ACL in the right knee of each sheep. The tendons were one of two treatment types: crosslinked and crosslinked with 20 nm AuNPs. The sheep were euthanized after 8 weeks and explanted grafts were scored by H&E histology in the bone tunnel and intraarticular space.

6.3.2 Graft Preparation

Acellular human gracilis tendon grafts were obtained frozen from MTF (Musculoskeletal Tissue Foundation, Edison, NJ). The grafts were prepared for conjugations using previously published methods with 2 mM 1-ethyl-3-[3-dimethylainopropyl]carbodiimide (EDC) and 5 mM N-hydroxysuccinimide (NHS) [23]. 100 ml of this conjugation solution was pipetted onto the tissue and submerged at room temperature for 15 minutes. In the meantime, 20 nm AuNP (7.0 x 1011 particles/mL) from Ted Pella (Redding, CA) were functionalized in 15 mM 2-mercaptoethylamine in water to prepare for conjugation with the tissue. To conjugate the AuNPs to the grafts, the grafts were removed from the first solution and placed in 100 ml of a fresh conjugation solution, which was immediately followed by pipetting 4 mL of nanoparticle solution. The grafts were incubated for 24 hours. The AuNP conjugated grafts were rinsed in PBS to remove any unreactive moieties prior to sterilization. Grafts were sterilized in a neutral solution of 0.1% (v/v) peracetic acid for 24 hours and this was followed by a rinse in sterile phosphate-buffered saline (PBS) for 24 hours. Grafts were stored in 70% ethanol and rinsed in sterile PBS prior to implantation.

6.3.3 Neutron Activation Analysis

NAA was utilized to quantify the gold levels in the tissue scaffolds. Following conjugation, five samples of each treatment type (N=5) were lyophilized, weighed, and packed into high-density polyethylene NAA vials. At the University of Missouri Research Reactor, the samples were loaded into units termed rabbits with Au comparator standards and irradiated for 120 seconds in a thermal neutron flux of 5.0x1013 n/cm2/s. The 197Au captures a neutron to produce the radio-isotope 198Au with a 2.7 d half-life. The samples were allowed to decay for 1-7 hours and then counted for 10 minutes each using a high purity Ge detector controlled by Canberra Genie 2000 software. The detector dead-time was less than 5% for all samples.

6.3.4 Cell Culture

L-929 mouse fibroblast cells were obtained from ATCC (Manassas, VA). They were cultured in EMEM (ATCC, Manassas, VA) supplemented with 10% (v/v) horse serum (Sigma-Aldrich, St. Louis, MO) and 200 U mL−1 penicillin–streptomycin (Sigma-Aldrich, St. Louis, MO) solution in an incubator at 37°C and 5% CO2. 1 ml of 3 x 104 cell/ml cell solution was plated on each scaffold and allowed to grow 24 hours.

6.3.5 Reactive Oxygen Species Assay

To analyze the ROS reducing capabilities of the scaffolds, an OxiSelectTM ROS Assay kit (Cell Biolabs) was utilized. Six scaffolds

from each treatment type were studied (n=6). Included in the assay kit were: 20x 2'–7' -dichlorodihydrofluorescin diacetate (DCFH-DA), 2'–7'-dichlorodihydrofluorescin (DCF) standard, and 2x cell lysis buffer.

Prior to the start of the ROS assay, L929 fibroblast cells were subcultured and seeded in a 96-well culture plate at a concentration of 4.42×10^4 cells cells/mL. The well plate of cells was then incubated at 37°C and 5% CO^2 for 24 h. The media was removed from the cell plates and the wells rinsed gently with Dulbecco's phosphate buffered saline (DPBS). 0.15 mL of 1x DCFH-DA/DPBS was added to the cells and incubated at 37°C and 5% CO2 for 60 min. Following the incubation, the DCFH-DA/DPBS was removed and each well was rinsed with DPBS. The scaffolds were then added to individual wells of the 96-well plate and 6 wells were left empty to be analyzed without a scaffold as controls. 0.125 mL DPBS was added to each well and the plate was incubated at 37°C and 5% CO2 for 12 h. After 12 h, the assay was terminated by adding 0.125 mL 2x cell lysis buffer to each well and incubating for 5 min. The well plate was then removed from the incubator and 0.1 mL of solution from each well was transferred to a new 96 well plate.

The fluorescence measured with a spectrofluorometer using excitation and emission wavelengths of 480 and 530 nm, respectively.

A set of DCF standards was prepared from a series dilution of the stock DCF solution in DPBS to yield concentrations ranging from 0 to 10,000 nM. Fluorescence measurements were acquired for each dilution and used to prepare the DCF standard curve which was used to correlate experimental fluorescence intensities to DCF concentration.

6.3.6 Animal model

Six Polypay sheep underwent ACL reconstruction using grafts derived from acellular human gracilis tendons. The animals were anesthetized and the surgical field shaved and prepped. The skin and subcutaneous tissue were dissected to expose the joint capsule. The knee was then hyperflexed and the ACL removed at the osteoligamentous junction. Bone tunnels were created using a stainless-steel drill bit. Once the tunnels were created, the graft was passed tightly through the tibial bone tunnel, intra-articular space, and pulled through the femoral bone tunnel. The end of implant graft was fixed to the bone using spiked washers. (Figure 1).

During surgery, one of the control animals had a prolonged procedure due to equipment difficulties. This animal later developed a bacterial infection and bacterial culture showed *Staphylococcus aureus*, *Leclercia adecarboxylata*, and *Acinetobacter calcoaceticus*

lwoffii present in the joint. The data from this animal was not included in the results.

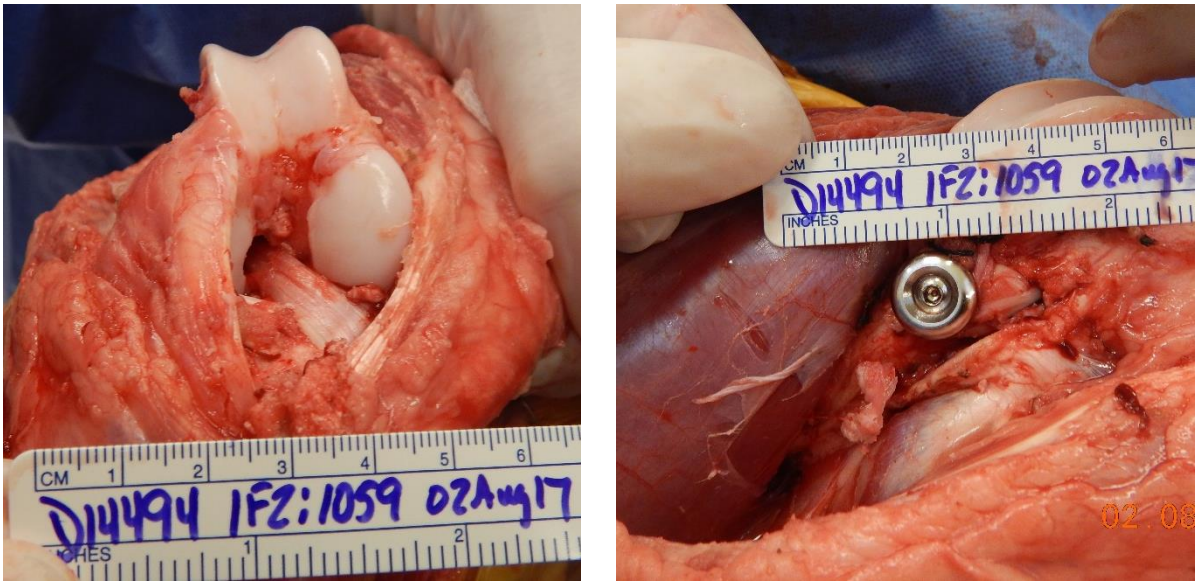

Figure 6.1 The ACL reconstruction with human gracilis tendon in a sheep. The tendon graft was inserted and routed through the bone tunnels, which was subsequently fixed on the femoral and tibial tunnel exits.

6.3.7 Cytology

After 8 weeks, the sheep were sacrificed, the synovial fluid was immediately aspirated from both the surgical and intact knee. The fluid was analyzed via direct smear and 100 cell differential count was performed via a cytocentrifuge concentrated slide preparation.

6.3.8 Histopathology

6.3.8.1 Intraarticular Graft

The knee was removed and placed in 10% neutral buffered formalin for at a minimum of two weeks. The medial tibial and lateral femoral insertion sites of the graft were incised and the intraarticular graft removed. After harvest, the graft was split longitudinally and embedded in paraffin and sectioned on a microtome. The slides were stained with hematoxylin and eosin and probed with antibodies to Factor VIII to label vascular endothelium. Grafts were scored by two blinded pathologists using the scale featured in Table 6.1.

Table 6.1 Grading scale for histological evaluation of the intra-articular graft per high power field (×100).

Characteristic features	*Definition*	*Score*
Inflammation	Marked	*0*
	Moderate	*1*
	Mild	*2*
	Very Mild	*3*
	None	*4*
Peripheral Vessel Number	<30	*0*
	30 - 44	*1*
	45 - 59	*2*
	60 - 74	*3*
	>75	*4*
Fibroblast Rich Connective Tissue	none	*0*
	CT < 10% of graft	*1*
	CT 10-39% of graft	*2*
	CT 40-60% of graft	*3*
	CT > 60% of graft	*4*
Collagen Fiber Organization	Disorder	*0*
	Irregular	*1*
	Regular	*2*
Collagen Fiber Density	<25%	*0*
	26 -50%	*1*
	51 - 75%	*2*
	76 - 100%	*3*

6.3.8.2 Bone Tunnel Pathology

The bone tunnel samples were cut into six transverse slices, three from the tibia and three from the femur, representative of both ends and the center of the bone tunnel. The samples were

demineralized in 10% ethylenediaminetetraacetic acid (EDTA) solution for 10 weeks. Bone blocks were embedded in paraffin and sectioned on a microtome in transverse slices. Slides were stained with hematoxylin and eosin and picrosirius red and graded by two blinded pathologists using the tendon-bone tunnel healing (TBTH) validated by Lui et al. and featured in Table 6.2 and Table 6.3.

Table 6.2 TBTH Scoring for evaluation of tendon graft to bone tunnel healing in ACL reconstruction.

Characteristic features	*Definition*	*Score*
Graft degeneration	Severe (≥75% of graft remnant)	*0*
	Substantial (<75% of graft remnant)	*1*
	Moderate (<50% of graft remnant)	*2*
	Slight (<25% of graft remnant)	*3*
	None (0% of graft remnant)	*4*
Graft remodeling	None (0% of graft remnant)	*0*
	Slight (<25% of graft remnant)	*1*
	Moderate (<50% of graft remnant)	*2*
	Substantial (<75% of graft remnant)	*3*
	Intense (≥75% of graft remnant) or any remodeling of tendon graft to bone	*4*
Percentage of fibrous tissue	Empty space between graft remnant and bone	*0*
	Massive (≥75% of healing interface)	*1*
	Substantial (<75% of healing interface)	*2*
	Moderate (<50% of healing interface)	*3*
	Slight (<25% of healing interface)	*4*
	None (0% healing interface)	*5*
Collateral connection	None (0% of healing interface)	*0*
	Fair (<25% of healing interface)	*1*
	Moderate (<50% of healing interface)	*2*
	High (<75% of healing interface)	*3*
	Very High (≥75% of healing interface)	*4*
Head-to-head connection	None (0% of healing interface)	*0*
	Fair (<10% of healing interface)	*1*
	Moderate (<25% of healing interface)	*2*
	High (<50% of healing interface)	*3*
	Very High (≥50% of healing interface)	*4*
Inflammation	Marked Inflammation	*0*
	Moderate Inflammation	*1*
	Mild Inflammation	*2*
	Very Mild Inflammation	*3*
	No Inflammation	*4*

Table 6.3 Other histologic assessments evaluated but not included in the TBTH score for the bone tunnel portion of the graft.

Characteristic features	*Definition*	*Score*
Graft collagen fiber organization	Poor fiber arrangement	*0*
	Fair with some fiber organization	*1*
	Moderately organized	*2*
	Highly organized	*3*
	Graft remodeling coupled with bone replacement	*4*
Fibrous tissue organization	Empty space between graft and bone	*0*
	Loose and poorly organized	*1*
	Fairly organized	*2*
	Moderately organized	*3*
	None with 100% bone graft connection	*4*
Chondrocyte-like cells	No	*0*
	Yes	*1*
Graft cellularity	None	*0*
	Small amount of cellularity	*1*
	Moderate levels of cellularity	*2*
	High levels of cellularity	*3*

6.3.9 Statistical Analysis

GraphPad Prism 8.0.1 (GraphPad Software, San Diego, CA) was utilized to analyze experimental data. Results were individually compared using paired student's t-test. The results were considered statistically significant where P was less than 0.05.

6.4 Results

6.4.1 Neutron Activation Analysis

NAA was performed to measure the concentration of gold attached to the tissue scaffold. As shown in Table 6.4, the experimental grafts had 15 μg/g per gold. A trivial amount of gold seen in the controls is likely the result of contamination from shared equipment.

Table 6.4 Neutron Activation Analysis Results for ACL Graft. Concentration of gold on lyophilized human gracilis tendon. * represents a statistical difference from the control.

Control	Experimental
2 μg/g	15 μg/g*

6.4.2 Reactive Oxygen Species

The reactive oxygen species assay showed no difference between the control graft and the gold conjugated graft. Both grafts showed more ROS than the cells alone control.

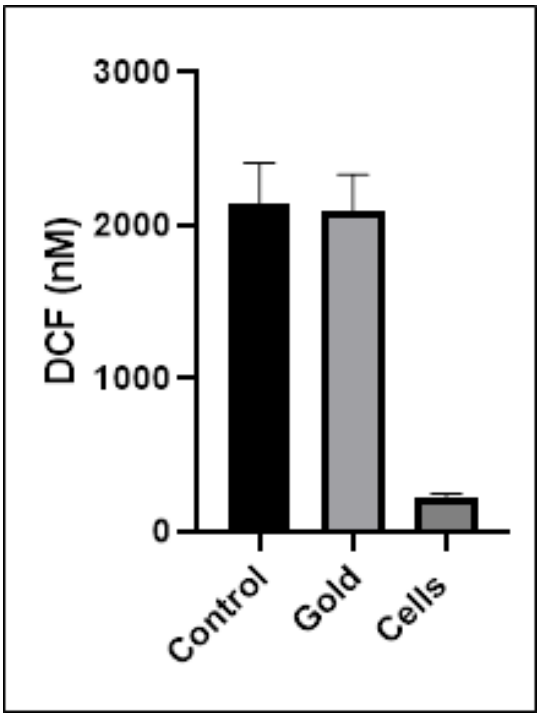

Figure 6.2 Reactive oxygen species assay showing DCF fluorescence concentrations for each of the experimental ACL groups. A cell plate with cells only and no scaffolds was used for the control.

6.4.3 Cytology

Figure 6.3 displays the percentage of synovial cells present in a 100 cell differential count from both the intact knee and the reconstructed knees 8 weeks after surgery. The intact knees (normal) had the highest percentage of synovial cells followed by the experimental animals. The other cells present were neutrophils and lymphocytes. The primary difference between the experimental and control knees is the controls had a greater number of neutrophils. This

may indicate that the control knees had a higher inflammatory, and prolonged inflammatory response.

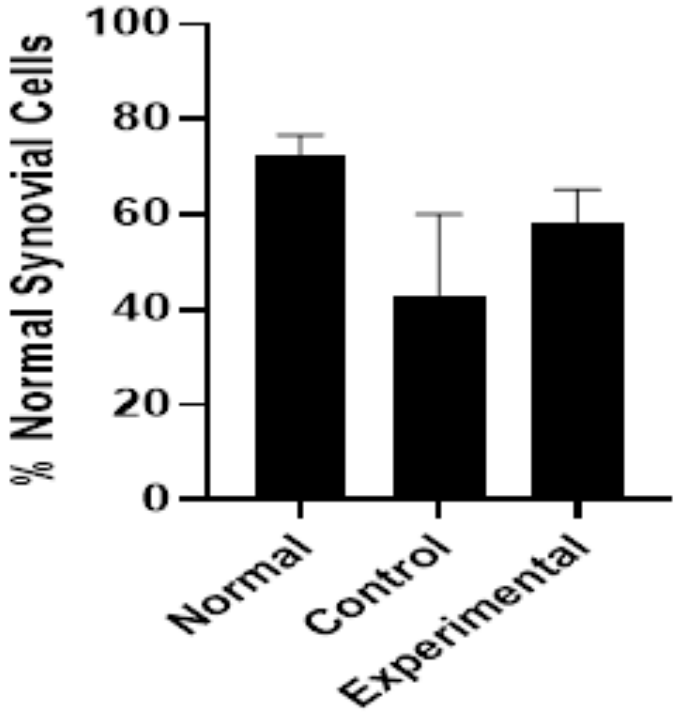

Figure 6.3 The number of synovial lining cells present in 100 cell differential count performed on a cytocentrifuge concentrated slide preparation of synovial fluid from both the intact and surgically repaired stifle 8 weeks after surgery. The other cells present in the sample consist of lymphocytes and neutrophils. Error bar displays standard error of the mean.

6.4.4 Intraarticular Histology

The intraarticular score was created based on 5 different criteria, totaling 17 points where a higher score indicates a better graft quality

(Table 1). Figure 3 displays the individual scores alongside a graph of the averages. Although not statistically significant, the intraarticular score for the experimental group is trending higher. Out of a total score of 17, the experimental grafts received a mean score of 11±1.5 and controls received an 8±0.3. The experimental grafts had an equal or greater than the control in all categories with the biggest difference occurring in the inflammation score. The exact values are show in Table 6.5.

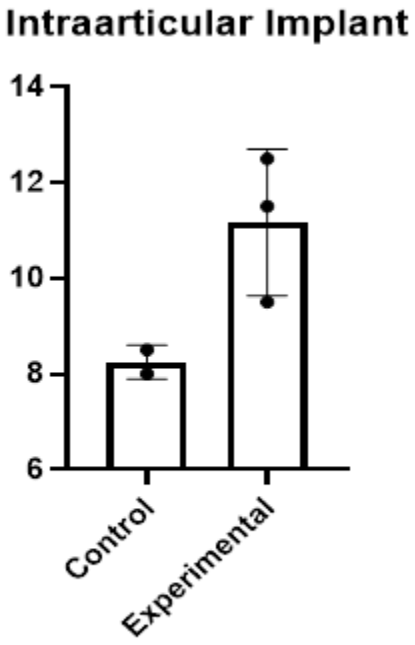

Figure 6.4: Histological score of the intraarticular graft. Error bar displays standard error of the mean.

Table 6.5 Average histological score of the intraarticular grafts as evaluated by two blinded pathologists

	Control	Gold
Inflammation	0	1.5
Peripheral Vessel Number	2.25	2.83
Fibroblast Rich Connective Tissue	2.5	2.5
Collagen Fiber Organization	1.25	1.83
Collagen Fiber Density	2.25	2.5
Sum of Scores	**8.25**	**11.16**

6.4.5 Bone Tunnel Histology

The bone tunnel portion of the graph was scored according to the tendon-bone tunnel healing score (Table 6.2). The maximum score is 25 points where a higher score indicates a better bone tunnel graft healing. The tibia and femur were scored separately with 3 representative transverse slides made for each and the mean of 6 scores for each animal is shown in Figure 6.5. The total score shows a trend of the experimental graft scoring better than the control. The experimental grafts received a total score of 12±1.5 on average while the controls received a total score of 10±0.6 out of a total possible score of 25. The complete TBTH scoring is featured in Table 6.6. Table 6.7 shows all other values appraised by the pathologists that are not included in the TBTH score. There are no major differences found in the other values.

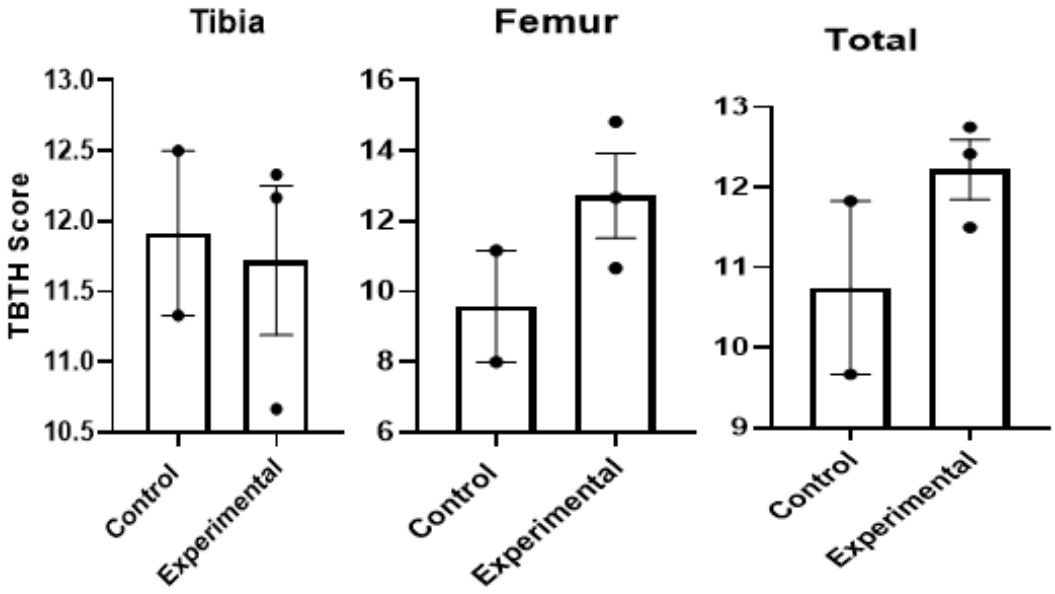

Figure 6.5 Tendon-bone tunnel healing score for the tibia, femur, and a summation of them both. Error bar displays standard error of the mean.

Table 6.6 Average TBTH score of the bone tunnel grafts as evaluated by two blinded pathologists.

	Control	Gold
Graft Degeneration	2.08	1.97
Graft Remodeling	2.50	2.61
Percentage of Fibrous Tissue	1.46	1.75
Collateral Connection	2.25	2.22
Head-to-head Connection	1.08	1.39
Inflammation	1.37	2.27
Sum	**10.74**	**12.21**

Table 6.7 Average score for other assessments not included in the TBTH score for the bone tunnel portion of the graft as evaluated by two blinded pathologists.

	Control	Gold
Graft Collagen Fiber Organization	1.62	1.58
Fibrous Tissue Organization	2.58	2.5
Chondrocyte-like Cells	0.08	0.28
Graft Cellularity	1.96	1.89

6.4.6 Inflammation

Figure 6.6 demonstrates the inflammation score for both the bone tunnel and the intraarticular portion of the graph. A score of 0 is representative of marked inflammation, 1 moderate, 2 mild, 3 very mild, and 4 equals no inflammation. Both the portions of the graph trended toward less severe inflammation when AuNPs were attached. This can also be seen in the histology images of the bone tunnel graft (Figure 6.7) and intraarticular graft (Figure 6.8). The control grafts show a marked to moderate lymphoplasmacytic infiltration while the experimental grafts have a milder inflammatory response with less mononuclear cells and, in the intraarticular graft, more fibroblasts present.

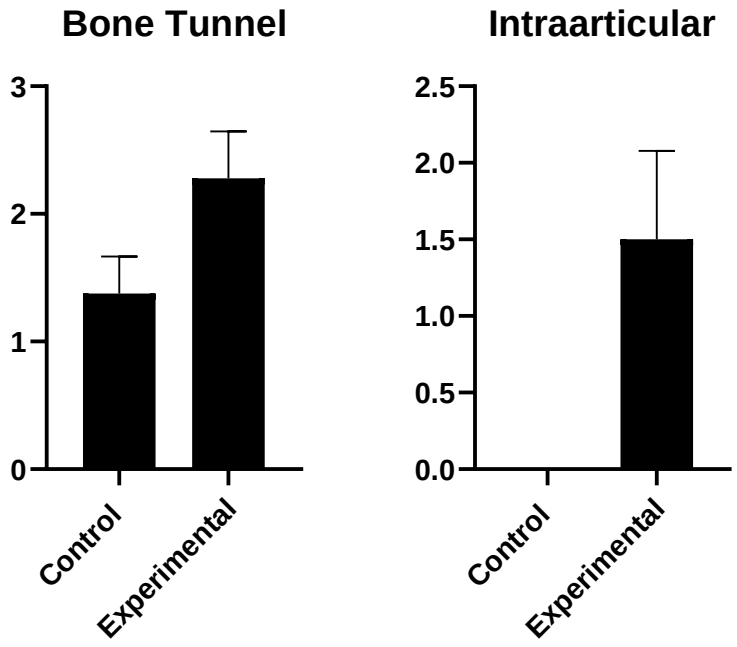

Figure 6.6: Inflammation scores for the bone tunnel and intraarticular graft. 0 equals marked inflammation, 1 moderate, 2 mild, 3 very mild, and 4 equals no inflammation.

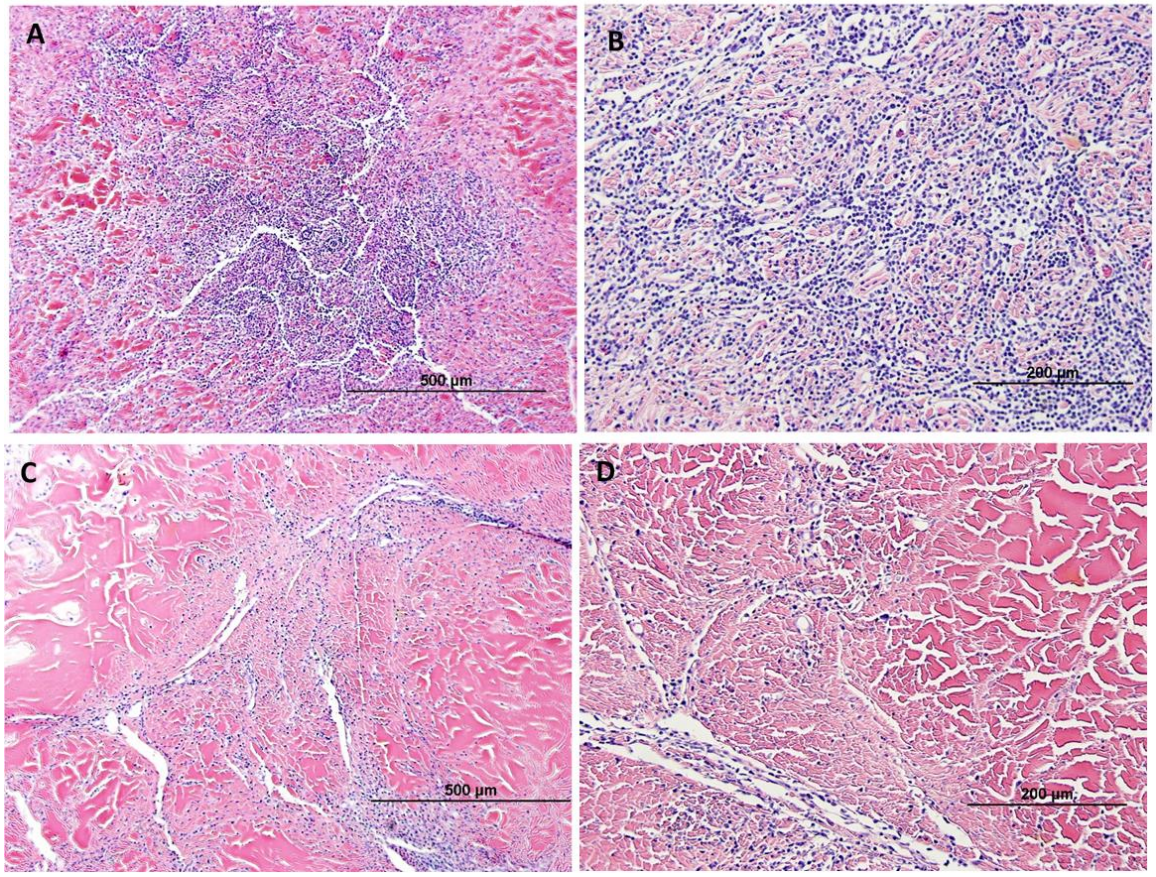

Figure 6.7 Representative histological findings of the bone tunnel portion of the graft at eight weeks. Slides were stained using hematoxylin and eosin. Figures A and B feature control grafts and C and D are experimental.

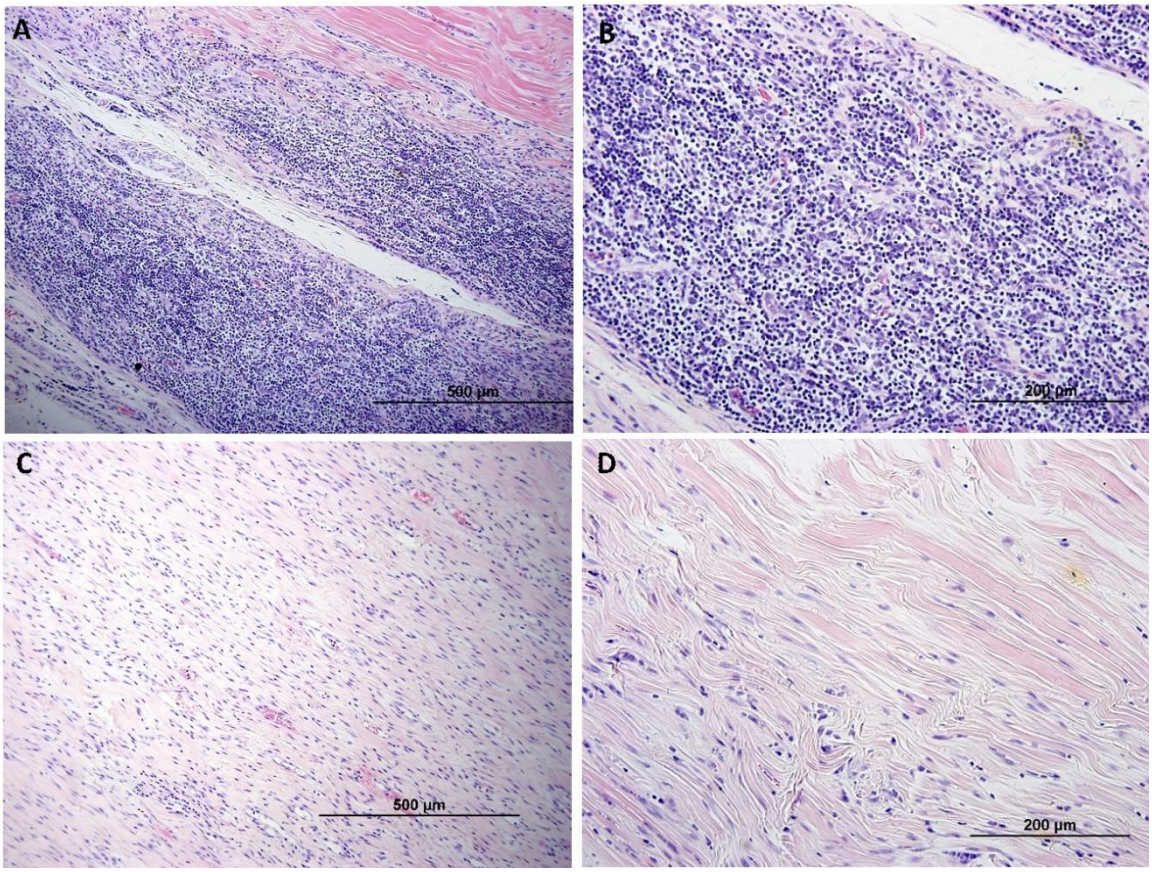

Figure 6.8 Representative histological findings of the intraarticular graft at eight weeks. Slides were stained using hematoxylin and eosin. Figures A and B feature control grafts and C and D are experimental

6.5 Discussion

In the past, allografts were utilized for chiefly revision surgery. However, there is a growing trend to use allografts in primary ACL reconstruction. Therefore, it is imperative to ensure allografts can be used safely without the increased inflammation and prolonged remodeling often associated with allograft repairs. The present study demonstrated the biocompatibility of a AuNP tissue scaffold in a large

animal model. The sheep all recovered and were fully weight bearing 5 weeks after surgery. The results of the study builds upon a previous study conducted using AuNPs scaffolds in a rabbit model. In that study, AuNPs were attached to tissue scaffold and used in ACL reconstruction in rabbits. After 14 weeks, all the grafts were intact with new, organized host fibrous connective tissue present in all graft types [24].

As a result of the small sample size, there were no statistically significant differences between the control and experimental grafts. However, several promising trends were observed. The AuNP conjugated grafts scored better histologically than the control for both the bone tunnel portion of the graft and the intraarticular portion. The biggest contributor to this was inflammation. The control grafts exhibited marked to moderate inflammation on every slide. This can be seen both in the bone tunnel (Figure 6.7) and intraarticular graft (Figure 6.8). The control grafts feature multifocal aggregates of predominantly mononuclear cells with rare neutrophils. The experimental grafts, on the other hand, were typically scored as either mild to moderate inflammation and features less inflammatory cell infiltration. These results were also mirrored by the joint cytology results (Figure 6.3). The synovial cytology results from the AuNP graft knees had a greater percentage of normal synovial cells and more

closely resembled the intact knees. The control grafts had more inflammatory cells present specifically neutrophils. While inflammation is a normal part of ACL reconstruction healing, excess inflammation can result in tissue damage and long-term degenerative changes in some patient [15]. This is part of the reason why ACL reconstruction patients have a high risk of developing osteoarthritis [25]. Inflammatory mechanisms are being increasingly recognized for their role in post-traumatic osteoarthritis (PTOA) [26-28]. Key inflammatory cytokines are consistently increased following joint injury, and data from animal studies and early clinical trials have suggested that early inhibition of these cytokines improves long-term clinical outcomes [29].

Several other researchers have shown AuNPs ability to suppress inflammation. The mechanism of AuNPs anti-inflammatory properties is multifactored, and not yet fully understood but it's clear AuNPs interfere with the transmission of inflammatory signaling and act as immunosuppressants [30-33]. In vivo studies have shown intraarticular application of AuNP can decrease pathomorphological joint changes associated with arthritis [34, 35]. In 2012 Leonavičienė et al. found continuous intraarticular AuNP treatment decreased joint swelling in rats. The rats also had a decrease in the histological changes associated with arthritis [32]. Continuous injections come

with their owns risks and morbidities, however. The ability to attach the nanoparticles directly to the healing surface may allow us to forgo repeated injections but still reap the benefits. Without the repeated injections, we also avoid the bioaccumulation and potentially adverse effect on the liver and lungs others have reported [36].

6.6 Conclusion

Acellular human gracilis tendons conjugated with AuNPs were used to reconstruct the ACL in sheep. All AuNP grafts were intact after 8 weeks and were not significantly different from the control grafts. Several promising trends were present nevertheless. The experimental grafts showed signs of decreased inflammation in the bone tunnel portion of the graft, the intraarticular portion of the graft, and in the synovial fluid cell count. Overall, grafts conjugated with nanoparticles appear to be good candidates for use as grafts in ACL reconstruction.

6.7 References

1. Sanders, T.L., et al., *Incidence of anterior cruciate ligament tears and reconstruction: a 21-year population-based study.* The American journal of sports medicine, 2016. **44**(6): p. 1502-1507.

2. Cohen, S.B. and J.K. Sekiya, *Allograft safety in anterior cruciate ligament reconstruction.* Clinics in sports medicine, 2007. **26**(4): p. 597-605.

3. Kartus, J., T. Movin, and J. Karlsson, *Donor-site morbidity and anterior knee problems after anterior cruciate ligament reconstruction using autografts.* Arthroscopy: The Journal of Arthroscopic & Related Surgery, 2001. **17**(9): p. 971-980.

4. Cole, D.W., et al., *Cost comparison of anterior cruciate ligament reconstruction: autograft versus allograft.* Arthroscopy: The Journal of Arthroscopic & Related Surgery, 2005. **21**(7): p. 786-790.

5. Jackson, D.W., J. Corsetti, and T.M. Simon, *Biologic Incorporation of Allograft Anterior Cruciate Ligament Replacements.* Clinical Orthopaedics and Related Research, 1996. **324**: p. 126-133.

6. Jackson, D.W., et al., *A comparison of patellar tendon autograft and allograft used for anterior cruciate ligament reconstruction in the goat model.* The American Journal of Sports Medicine, 1993. **21**(2): p. 176-185.

7. Muramatsu, K., Y. Hachiya, and H. Izawa, *Serial Evaluation of Human Anterior Cruciate Ligament Grafts by Contrast-Enhanced Magnetic Resonance Imaging: Comparison of Allografts and Autografts.* Arthroscopy: The Journal of Arthroscopic & Related Surgery, 2008. **24**(9): p. 1038-1044.

8. Malinin, T.I., et al., *A study of retrieved allografts used to replace anterior cruciate ligaments.* Arthroscopy: The Journal of Arthroscopic & Related Surgery, 2002. **18**(2): p. 163-170.

9. Kirkpatrick, J., et al., *Cryopreserved anterior cruciate ligament allografts in a canine model.* Journal of the Southern Orthopaedic Association, 1996. **5**(1): p. 20-29.

10. Csintalan, R.P., et al., *Risk factors of subsequent operations after primary anterior cruciate ligament reconstruction.* The American journal of sports medicine, 2014. **42**(3): p. 619-625.

11. Norton, S., *A brief history of potable gold.* Molecular interventions, 2008. **8**(3): p. 120.

12. Ionita, P., F. Spafiu, and C. Ghica, *Dual behavior of gold nanoparticles, as generators and scavengers for free radicals.* Journal of materials science, 2008. **43**(19): p. 6571-6574.

13. BarathManiKanth, S., et al., *Anti-oxidant effect of gold nanoparticles restrains hyperglycemic conditions in diabetic mice.* Journal of nanobiotechnology, 2010. **8**(1): p. 16.

14. Haupenthal, D.P.d.S., et al., *Effects of chronic treatment with gold nanoparticles on inflammatory responses and oxidative stress in Mdx mice.* Journal of drug targeting, 2019(just-accepted): p. 1-27.

15. Lieberthal, J., N. Sambamurthy, and C.R. Scanzello, *Inflammation in joint injury and post-traumatic osteoarthritis.* Osteoarthritis and cartilage, 2015. **23**(11): p. 1825-1834.

16. Darabos, N., et al., *Intraarticular application of autologous conditioned serum (ACS) reduces bone tunnel widening after ACL reconstructive surgery in a randomized controlled trial.* Knee Surgery, Sports Traumatology, Arthroscopy, 2011. **19**(1): p. 36-46.

17. Yi, C., et al., *Gold nanoparticles promote osteogenic differentiation of mesenchymal stem cells through p38 MAPK pathway.* Acs Nano, 2010. **4**(11): p. 6439-6448.

18. Sul, O.-J., et al., *Gold nanoparticles inhibited the receptor activator of nuclear factor-κb ligand (RANKL)-induced osteoclast formation by acting as an antioxidant.* Bioscience, biotechnology, and biochemistry, 2010. **74**(11): p. 2209-2213.

19. Rodeo, S.A., et al., *Tendon-healing in a bone tunnel. A biomechanical and histological study in the dog.* The Journal of bone and joint surgery. American volume, 1993. **75**(12): p. 1795-1803.

20. Hsu, S.-h., C.-M. Tang, and H.-J. Tseng, *Gold nanoparticles induce surface morphological transformation in polyurethane and*

affect the cellular response. Biomacromolecules, 2007. **9**(1): p. 241-248.

21. Grant, S.A., et al., *Assessment of the biocompatibility and stability of a gold nanoparticle collagen bioscaffold.* Journal of Biomedical Materials Research Part A, 2014. **102**(2): p. 332-339.

22. Christenson, E.M., et al., *Nanobiomaterial applications in orthopedics.* Journal of Orthopaedic Research, 2007. **25**(1): p. 11-22.

23. Deeken, C., et al., *Method of preparing a decellularized porcine tendon using tributyl phosphate.* Journal of Biomedical Materials Research Part B: Applied Biomaterials, 2011. **96**(2): p. 199-206.

24. Grant, S.A., et al., *In vivo bone tunnel evaluation of nanoparticle-grafts using an ACL reconstruction rabbit model.* Journal of Biomedical Materials Research Part A, 2017. **105**(4): p. 1071-1082.

25. Lohmander, L.S., et al., *The long-term consequence of anterior cruciate ligament and meniscus injuries: osteoarthritis.* The American journal of sports medicine, 2007. **35**(10): p. 1756-1769.

26. Heard, B., et al., *Analysis of change in gait in the ovine stifle: normal, injured, and anterior cruciate ligament reconstructed.* BMC musculoskeletal disorders, 2017. **18**(1): p. 212.

27. Cuellar, V.G., et al., *Cytokine profiling in acute anterior cruciate ligament injury.* Arthroscopy: The Journal of Arthroscopic & Related Surgery, 2010. **26**(10): p. 1296-1301.

28. Friel, N.A. and C.R. Chu, *The role of ACL injury in the development of posttraumatic knee osteoarthritis.* Clinics in sports medicine, 2013. **32**(1): p. 1-12.

29. Olson, S.A., et al., *The role of cytokines in posttraumatic arthritis.* JAAOS-Journal of the American Academy of Orthopaedic Surgeons, 2014. **22**(1): p. 29-37.

30. Uchiyama, M.K., et al., *In vivo and in vitro toxicity and anti-inflammatory properties of gold nanoparticle bioconjugates to the vascular system.* Toxicological Sciences, 2014. **142**(2): p. 497-507.

31. Sumbayev, V.V., et al., *Gold nanoparticles downregulate interleukin-1β-induced pro-inflammatory responses.* Small, 2013. **9**(3): p. 472-477.

32. Leonavičienė, L., et al., *Effect of gold nanoparticles in the treatment of established collagen arthritis in rats.* Medicina, 2012. **48**(2): p. 16.

33. Paula, M.M., et al., *Gold nanoparticles and/or N-acetylcysteine mediate carrageenan-induced inflammation and oxidative stress in a concentration-dependent manner.* Journal of Biomedical Materials Research Part A, 2015. **103**(10): p. 3323-3330.

34. Tsai, C.Y., et al., *Amelioration of collagen-induced arthritis in rats by nanogold.* Arthritis & Rheumatism: Official Journal of the American College of Rheumatology, 2007. **56**(2): p. 544-554.

35. Huang, Y.-J., et al., *Multivalent structure of galectin-1-nanogold complex serves as potential therapeutics for rheumatoid arthritis by enhancing receptor clustering.* Eur Cell Mater, 2012. **23**: p. 170-181.

36. Sonavane, G., K. Tomoda, and K. Makino, *Biodistribution of colloidal gold nanoparticles after intravenous administration: effect of particle size.* Colloids and Surfaces B: Biointerfaces, 2008. **66**(2): p. 274-280.

Chapter 7

FUTURE WORK

7.1 Future Studies

Anterior cruciate ligament (ACL) reconstruction is one of the most common orthopedic operations performed in the world [1]. Improvements in surgical technique and rehabilitation have led to significantly reduced morbidity following surgery. However, thousands of patients still suffer long-term consequences as a result of their injury [2-4]. The research in this dissertation demonstrates the viability of using genipin and AuNPs as a supplement to ligament and tendon grafts. The long-term goal of the project is to develop a bath containing AuNPs and genipin that can be used in the surgical site for either allograft or autograft surgery. However, there are still numerous questions that need to be answered before this can make its way into human patients.

The first question that needs to be answered is what quantity of AuNPs is ideal for cellular proliferation and inflammation suppression. Our studies demonstrated we can vary the amount of gold by changing the conjugation time or modifying the gold concentration, but it is not yet clear what concentration is ideal for our goals. In a study by Lu et al.[5], they found a gold concentration of 5.0 ppm supported cell growth in keratinocytes. However, at concentration greater than 10.0

ppm, the AuNPs slowed cell growth. In our own studies, we found high gold concentrations led to clumping of the AuNPs, and decreased cell attachment when compared to the use of genipin alone. To find the ideal quantity of AuNPs, scaffolds would be created varying the concentration of AuNPs and cell studies performed using both fibroblasts and osteoblasts to examine cell attachment and proliferation. Reactive oxygen species assay can be performed to examine this aspect of AuNPs anti-inflammatory properties, but to measure the full complexity of the immune reaction of the nanoparticles, animal studies will need to be performed.

Another question to be answered pertains to the use of genipin. Our cell studies showed the most positive results when crosslinking was allowed to progress for 24 hours [6]. However, this extended crosslinking time is not possible in the operating room. The question that needs to be is answered is whether or not the genipin will continue to crosslinking the scaffold from within the joint capsule if the graft is not washed following conjugation. The genipin crosslinking reaction is known to be affected by factors such as pH value, temperature, and genipin concentration [7, 8]. To test the effect implantation would have on the crosslinking reaction, tissue scaffolds would be submerged in crosslinking solution for 30 minutes. The tissue would be moved into 6 ml of artificial synovial fluid at 37 °C overnight

to complete the crosslinking reaction. After, crosslinking differential scanning calorimetry could be run to measure the degree of crosslinking and cell studies conducted.

For the gold and genipin dipcoating method to become a viable product, a major in vivo study will need to be conducted. While we have conducted a small pilot study using sheep, there are many questions yet to address. Our previous analysis was a small study that did not have sufficient number to show statistical differences. Additionally, the study was only examining a single timepoint. To properly conduct this study a range of timepoints are needed including long-term to properly view how the body responds over time. Lastly, our previous study was only investigating the effects of the AuNPs. Genipin was not used to attach the particles. In order to study the possible synergy and overlapping effects of gold and genipin, they not only need to be studied independently, but also in combination.

One of the reasons AuNPs are used in such a wide variety of applications is due to their easy surface modification for attaching a ligand, drug or other targeting molecules [9]. AuNPs form a protein corona across their surface when they’re introduced into a biological medium [10]. By attaching different proteins to the surface of the AuNPs, cell behavior and interactions between the graft and the body can be manipulated for the benefit of the patient. Immunosuppressing

cytokines can supplement the already present anti-inflammatory properties of the gold and genipin. Glycoproteins can be used to further accelerate cell attachment to the cell scaffold. By further manipulating the size and shape of the AuNPs the drug targeting and delivery capabilities become even greater allowing the AuNPs to bind with specific biomolecules located either on the cell surface or inside the cell cytoplasm [11].

The potentially greatest advantage of our technology is its use is not limited to ligaments and tendons. Genipin will crosslink any amine groups present, as a result our product potentially works with any autograft, allograft, or xenograft on the market. Decellularized tissue is currently used for cardiology, dentistry, ophthalmology, and wound repair for array of a soft tissues [12]. Despite its wide use, there still remains many problems to be solved. High immunogenicity, weakening tissue, rapid biodegradation, and slow integration are a constant problem for all fields using allograft tissue and our genipin gold dip coating could potentially be useful for all of them [13, 14]. This dissertation has begun the extensive research needed to characterize, optimize, and discover the capabilities of this technology. The further development of this work has the potential to advance a whole class of biomaterials.

7.2 References

1. Lyman, S., et al., *Epidemiology of anterior cruciate ligament reconstruction: trends, readmissions, and subsequent knee surgery.* JBJS, 2009. **91**(10): p. 2321-2328.

2. Lohmander, L.S., et al., *The long-term consequence of anterior cruciate ligament and meniscus injuries: osteoarthritis.* The American journal of sports medicine, 2007. **35**(10): p. 1756-1769.

3. Gillquist, J. and K. Messner, *Anterior cruciate ligament reconstruction and the long term incidence of gonarthrosis.* Sports Medicine, 1999. **27**(3): p. 143-156.

4. Paschos, N.K. and S.M. Howell, *Anterior cruciate ligament reconstruction: principles of treatment.* EFORT open reviews, 2016. **1**(11): p. 398-408.

5. Lu, S., et al., *Concentration effect of gold nanoparticles on proliferation of keratinocytes.* Colloids and Surfaces B: Biointerfaces, 2010. **81**(2): p. 406-411.

6. Bellrichard, M., et al., *Genipin Attachment of Conjugated Gold Nanoparticles to a Decellularized Tissue Scaffold.* Applied Sciences, 2019. **9**(23): p. 5231.

7. Mi, F.L., S.S. Shyu, and C.K. Peng, *Characterization of ring-opening polymerization of genipin and pH-dependent cross-linking reactions between chitosan and genipin.* Journal of Polymer Science Part A: Polymer Chemistry, 2005. **43**(10): p. 1985-2000.

8. Butler, M.F., Y.F. Ng, and P.D. Pudney, *Mechanism and kinetics of the crosslinking reaction between biopolymers containing primary amine groups and genipin.* Journal of Polymer Science Part A: Polymer Chemistry, 2003. **41**(24): p. 3941-3953.

9. Zhang, X., *Gold nanoparticles: recent advances in the biomedical applications.* Cell biochemistry and biophysics, 2015. **72**(3): p. 771-775.

10. Lynch, I. and K.A. Dawson, *Protein-nanoparticle interactions.* Nano today, 2008. **3**(1-2): p. 40-47.

11. Lin, M., et al., *Applications of gold nanoparticles in the detection and identification of infectious diseases and biothreats.* Advanced Materials, 2013. **25**(25): p. 3490-3496.

12. Crapo, P.M., T.W. Gilbert, and S.F. Badylak, *An overview of tissue and whole organ decellularization processes.* Biomaterials, 2011. **32**(12): p. 3233-3243.

13. Partington, L., et al., *Biochemical changes caused by decellularization may compromise mechanical integrity of tracheal scaffolds.* Acta biomaterialia, 2013. **9**(2): p. 5251-5261.

14. Wang, Y., et al., *Genipin crosslinking reduced the immunogenicity of xenogeneic decellularized porcine whole-liver matrices through regulation of immune cell proliferation and polarization.* Scientific reports, 2016. **6**: p. 24779.

VITA

Mitchell A. Bellrichard was born in Rochester, Minnesota to Tod and Margaret Bellrichard. He attended the University of Minnesota obtaining a bachelor's degree in Ecology, Evolution and Animal Behavior with a minor in Animal Science in the spring of 2011. He then continued his education at the University of Minnesota where he graduated with his Doctorate in Veterinary Medicine.

In 2015, Mitch entered the comparative medicine residency and Ph.D. program at the University of Missouri. He pursued his Doctorate of Philosophy in Veterinary Pathobiology in the lab of Dr. Sheila Grant developing and optimizing methods of nanoparticle attachment to improve tendon and ligament grafts. In addition to his research and laboratory animal responsibilities, he also completed a graduate certificate in Life Science Innovation and Entrepreneurship and was elected to the position of city alderman in Jonesburg, MO.